TRACK GEOMETRY SURVEY DEVICE FOR LIM RESEARCH VEHICLE TEST TRACK

REPORT NO.
FRA-ORD&D-74-36

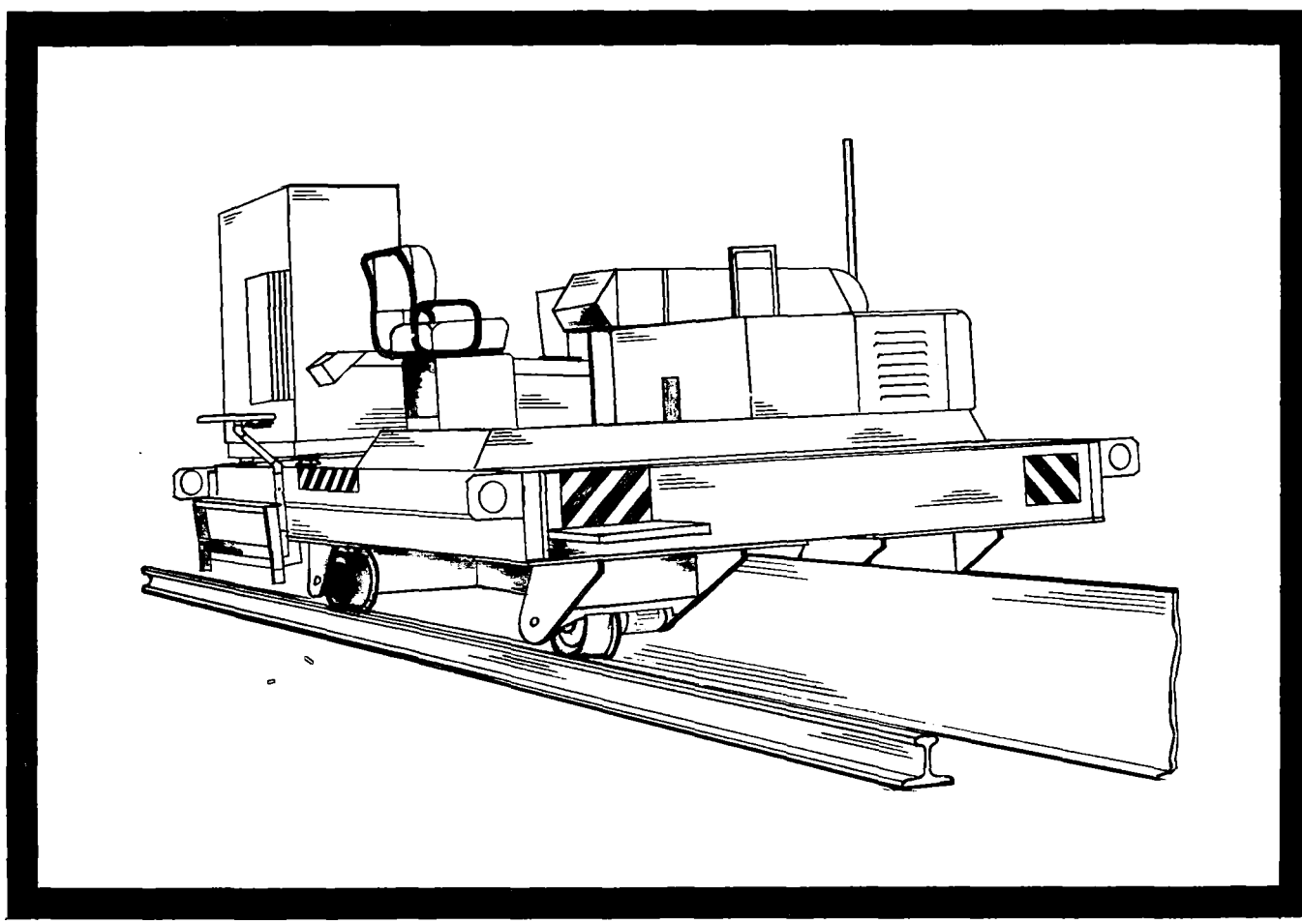

DEPARTMENT OF TRANSPORTATION/Federal Railroad Administration
Office of Research, Development and Demonstrations

October 1973

TECHNICAL REPORT STANDARD TITLE PAGE

1. Report No.	2. Government Accession No.	3. Recipient's Catalog No.
FRA-ORD&D-74-36		

4. Title and Subtitle	5. Report Date
TRACK GEOMETRY SURVEY DEVICE FOR LIM RESEARCH VEHICLE TEST TRACK	October 1973
	6. Performing Organization Code

7. Author(s)	8. Performing Organization Report No.
HECTOR MEDECKI, and SERGIO PANUNZIO	GASL TR-776

9. Performing Organization Name and Address	10. Work Unit No.
General Applied Science Laboratories, Inc. Merrick & Stewart Avenues Westbury, New York 11590	11. Contract or Grant No. DOT-FR-10016

12. Sponsoring Agency Name and Address	13. Type of Report and Period Covered
Department of Transportation Federal Railroad Administration Washington, D. C.	Final Report Period: June 1971- August 1972
	14. Sponsoring Agency Code

15. Supplementary Notes

16. Abstract

A track survey device was designed, built and operated to measure the geometry of the FRA Linear Induction Motor Test Track at Pueblo, Colorado.

A laser beam is used for the measurement of profile and alignment; an electronic level for the measurement of super-relation and mechanical sensors for both support rail and reaction rail gages. The measurement is stored in magnetic tape for processing.

17. Key Words	18. Distribution Statement
Track Geometry Survey Device (TGSD) Linear Induction Motor (LIM) Data Acquisition System (DAS) laser beam — track measurement tie counter — gage bench marker — rail support rail — electronic level odometer	Unlimited

19. Security Classif. (of this report)	20. Security Classif. (of this page)	21. No. of Pages	22. Price
Unclassified	Unclassified	110	

Form DOT F 1700.7 (8-69)

TABLE OF CONTENTS

TABLE OF CONTENTS (concluded)

LIST OF ILLUSTRATIONS

LIST OF ILLUSTRATIONS (concluded)

ACKNOWLEDGMENT

A special acknowledgment is given to Mr.Thomas P. Woll of the Federal Railroad Administration for his valuable assistance in the design and testing portions of this program.

1. INTRODUCTION

This report describes a unique track survey device developed by General Applied Science Laboratories, Inc. (GASL), for the Federal Railroad Administration (FRA) under Contract DOT-FR-10016, to be used to survey the FRA Linear Induction Motor Test Track in Pueblo, Colorado.

Conventional track survey techniques were not applicable due to the extreme accuracy requirements. In addition, the presence of the LIM reaction rail requires specially designed vehicles. To satisfy these unique requirements, GASL developed an approach which had both a high degree of sophistication in the sensor design as well as in overall design of the survey device.

The GASL track survey device makes use of optical as well as electromechanical techniques to perform the desired measurements. The survey device is mounted on two independent vehicles which ride the support rails. Included in one of the vehicles is a data acquisition system which stores the measured information on magnetic tape. This stored information is subsequently processed to provide the desired track geometry information.

A detailed discussion of the GASL approach is presented in Section 2. Section 3 describes the various components of the survey device. Then, Section 4 describes the two vehicles which make up the survey device and, finally, Section 5 presents the calibration, validation, and demonstration of the track survey device and some results from the initial survey of the LIM track.

2. TECHNICAL APPROACH TO THE PROBLEM

2.1 Description of LIM Test Track and Measuring Requirements

The Track Geometry Survey Device (TGSD) described in this report is designed to survey the experimental test track for the Linear Induction Motor (LIM) propelled vehicle at the DOT Test Center at Pueblo, Colorado.

Basically, the test track is of conventional railroad construction. However, the quality of the track will be very carefully controlled and consequently requires a precision on the measurement of the pertinent track parameters far in excess of that which is required for conventional track. A third rail is fastened to the ties along the center line of the track. This third rail is the aluminum reaction rail for the linear induction motor. The test track which is presently 6.2 miles long is approximately half tangent and half curved. The radius of the curved portion is two and a half miles.

The range and tolerances required for the track measurements are presented in Table I. A cross section of the experimental LIM track is shown in Figure 2-1. Figure 2-2 is a cross section of the support rail which is the conventional 119 CF&I section. This rail is mounted on a shim-rail anchor-tie plate with an inward cant whose slope is 1 in 40. Figure 2-3 shows a cross section of the type C LIM reaction rail and its tie plate.

The Track Geometry Survey Device developed at GASL is an absolute measuring system designed to determine the following LIM track parameters:

Profile
Alignment
Cross Level
Gage
LIM Reaction Rail Position

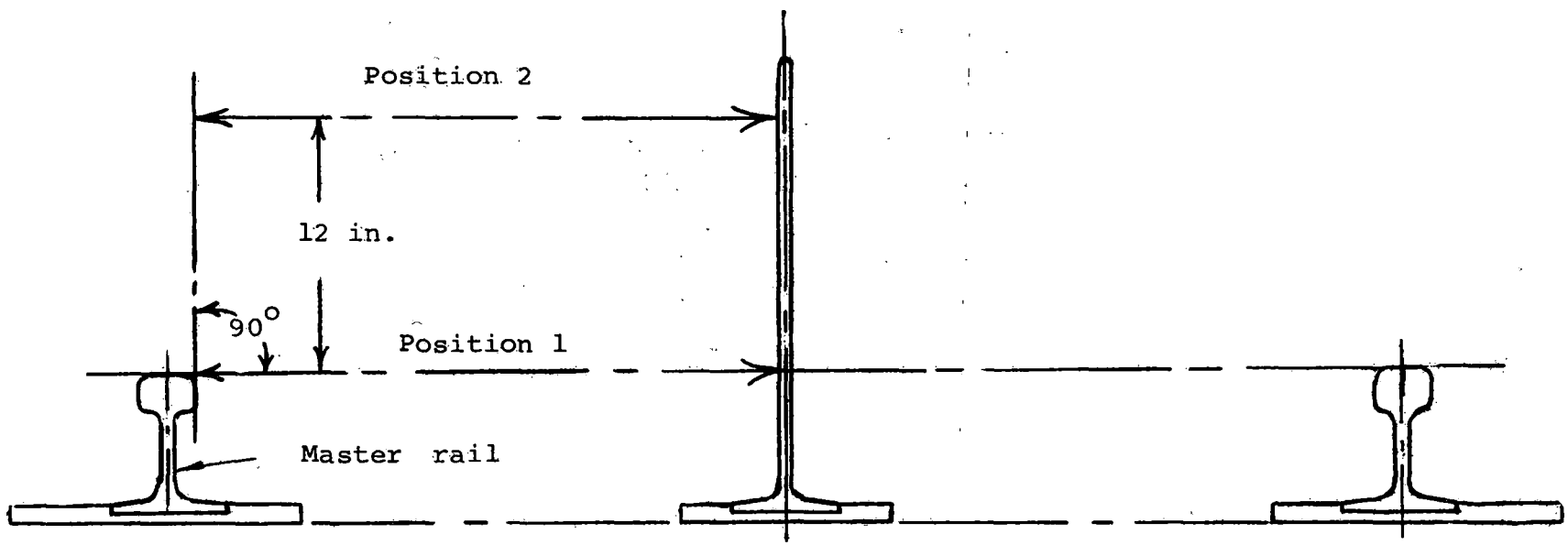

Figure 2-1. Cross Section of the LIM Test Track

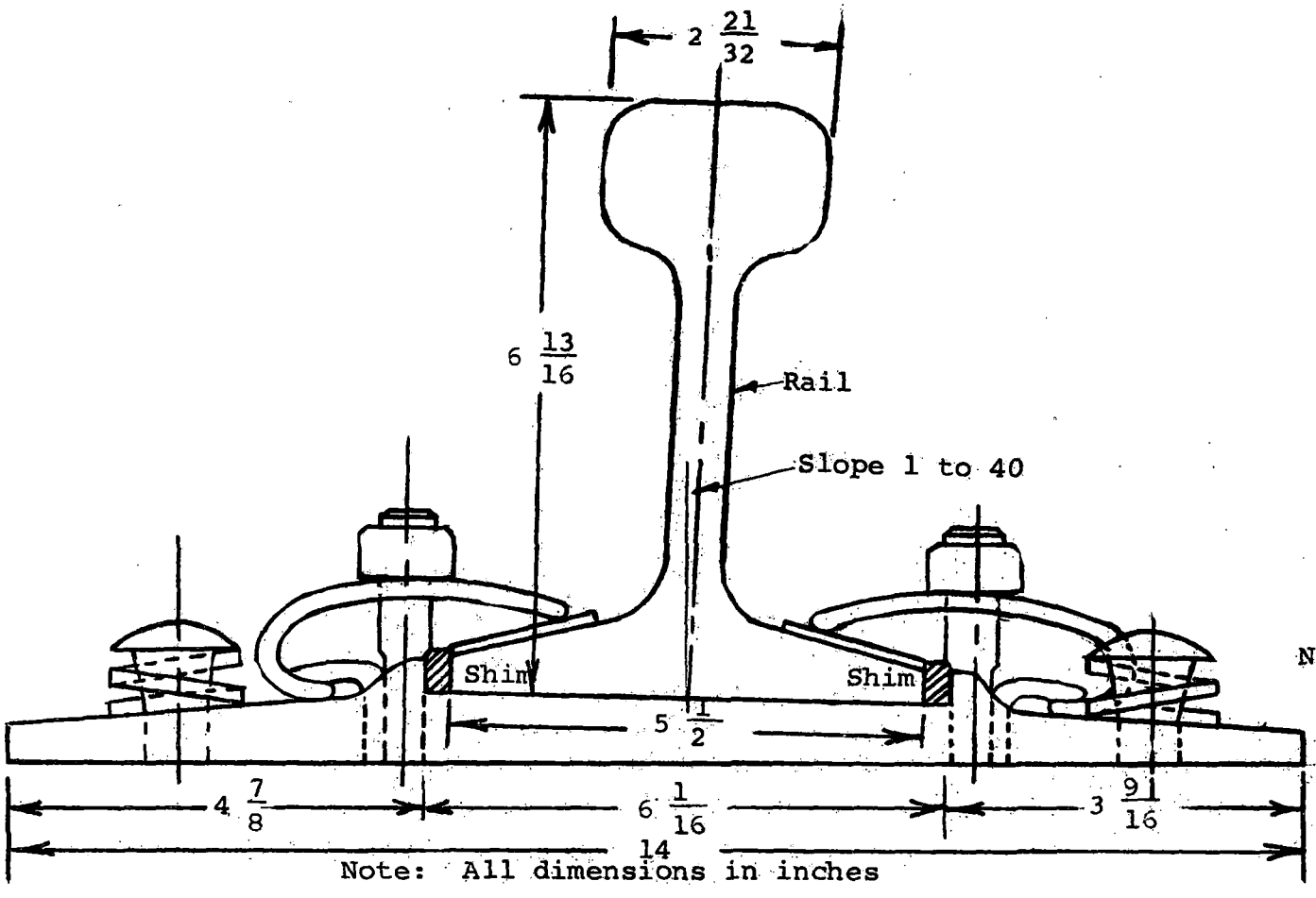

Figure 2-2. Cross Section of Support Rail and Tie Plate

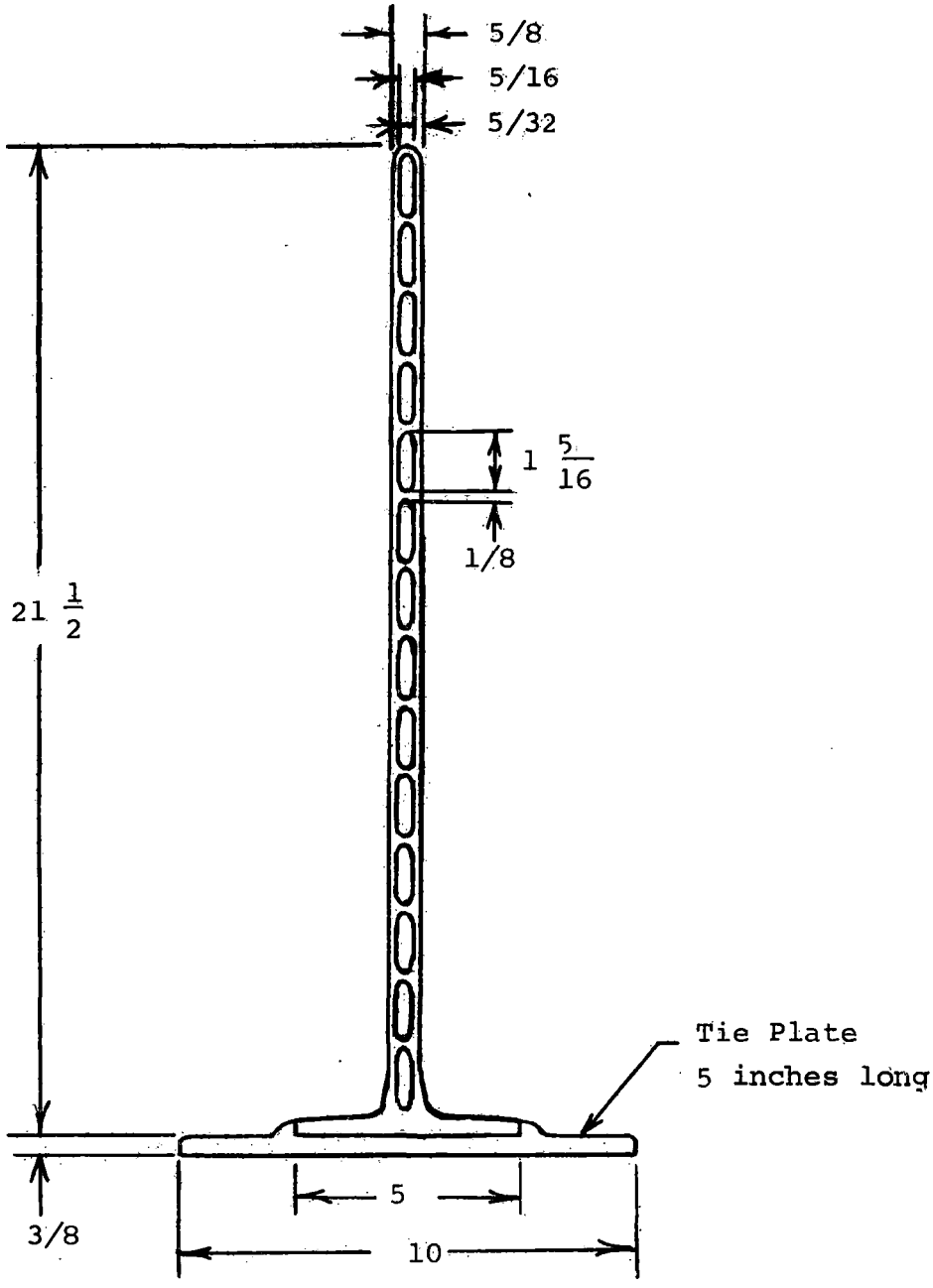

Figure 2-3. Cross Section to Type C Reaction Rail

TABLE 1-1

Measured Parameter	Tolerance	Range
Profile (for each rail)	± 1/64 in.	± 2 in. + x
Alignment (for each rail)	± 1/64 in.	± 2 in. + y
Cross-Level (and superelevation)	± 1/32 in.	± 10 in.
Gage (support rail)	± 1/32 in.	55½ to 57 ½ in.
Gage (reaction rail)	± 1/32 in.	26 to 30 in.
Distance Measurement	.1%	

where x is the offset resulting from vertical curvature
y is the midchord offset

These quantities, together with the selection of the reference system and the measuring technique will be discussed in the following section.

2.2 Definition of the Reference System and Measurements

The TGSD was designed to measure the track parameters specified in the previous section. These measurements are to be performed using the following defintion of the reference system.

(1) Absolute reference points are selected along the track by means of bench markers B_m whose known coordinates are x_m, y_m, z_m, as shown in Figure 2-4.

(2) A reference line P_ℓ, P'_ℓ, is established by means of a laser beam oriented along the track.

(3) One of the two rails R_1 is defined as the master rail, and the rail R_2 is called the secondary rail. R_1 is chosen as the inner rail of the LIM test track.

(4) At each position along the track a plane surface A is defined which is perpendicular to the master rail. This plane will contain the measuring sensors mounted on a special frame.

(5) An orthogonal system of reference x, y, z, is selected in a sensor's frame with the axis x perpendicular to the plane A and the axis y parallel to a straight line which connects the top centers of the two rails, R_1, R_2. Thus, the axis x is tangent to the master rail at the position of the plane A.

(6) An angle θ is defined in the plane A as the angle between the axis y and the intersection between A and a horizontal plane.

(7) The initial setting of the measuring procedure is obtained by locating the surface A at a position along the track which contains the point x_m, y_m, z_m, of a bench marker.

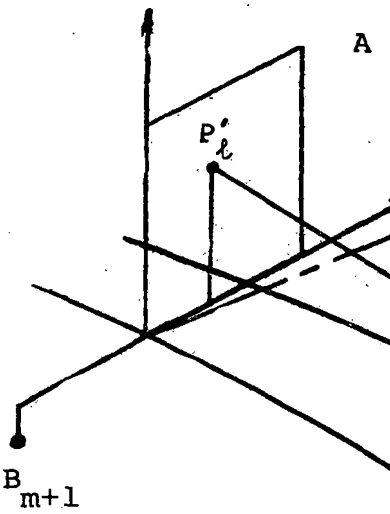

∞

Figure 2-4.

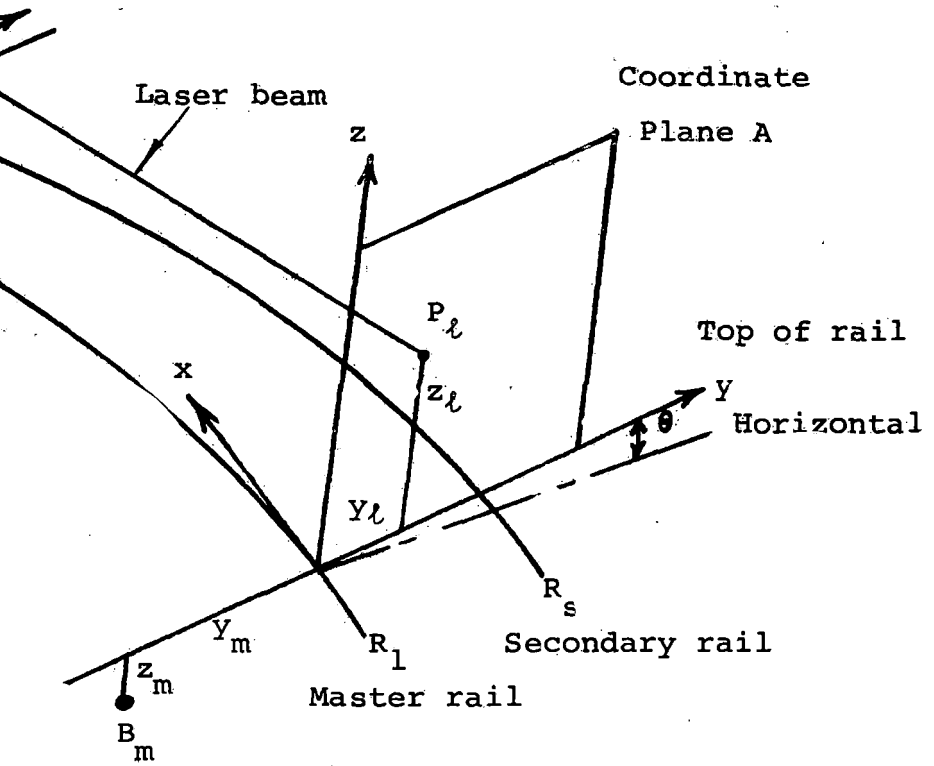

Reference System

(8) In the frame of reference x, y, z, the measurements are made of the coordinates of the bench marker and of the point P_ℓ which is defined by the intersection of the laser reference line with the plane surface A.

(9) In the cross section of the track in the plane A, each rail is identified by two points: the gage point P_g and the top point P_t, as shown in Figure 2-5. The gage point is located on the inner side of the rail at 5/8 in. below the axis y.

(10) In the plane A the position of the LIM reaction rail is identified by two gage points, P_1, P_2, at two positions along the axis. P_1 is located on the axis y and P_2 above the axis y at z = 12 in.

(11) As the sensor frame is moved along the track, the following quantities are measured as a function of the frame position:

g gage between master rail and secondary rail measured along the axis y

g_1, g_2 gages between master rail and LIM reaction rail measured at P_1, P_2, along the axis y

θ cross level

y_ℓ coordinate of P_ℓ along the axis y relative to the gage point master rail

z_ℓ coordinate of P_ℓ along the axis z relative to the top of the master rail relative to P_t

(12) As the sensor frame moves along the track, the two coordinates y'_ℓ, z'_ℓ, and the cross level θ determine the points of a curve which defines the profile and alignment of the track.

The measuring phase, in the particular section of track under survey, proceeds by moving the measuring frame towards the laser beam source until reaching a separation distance of

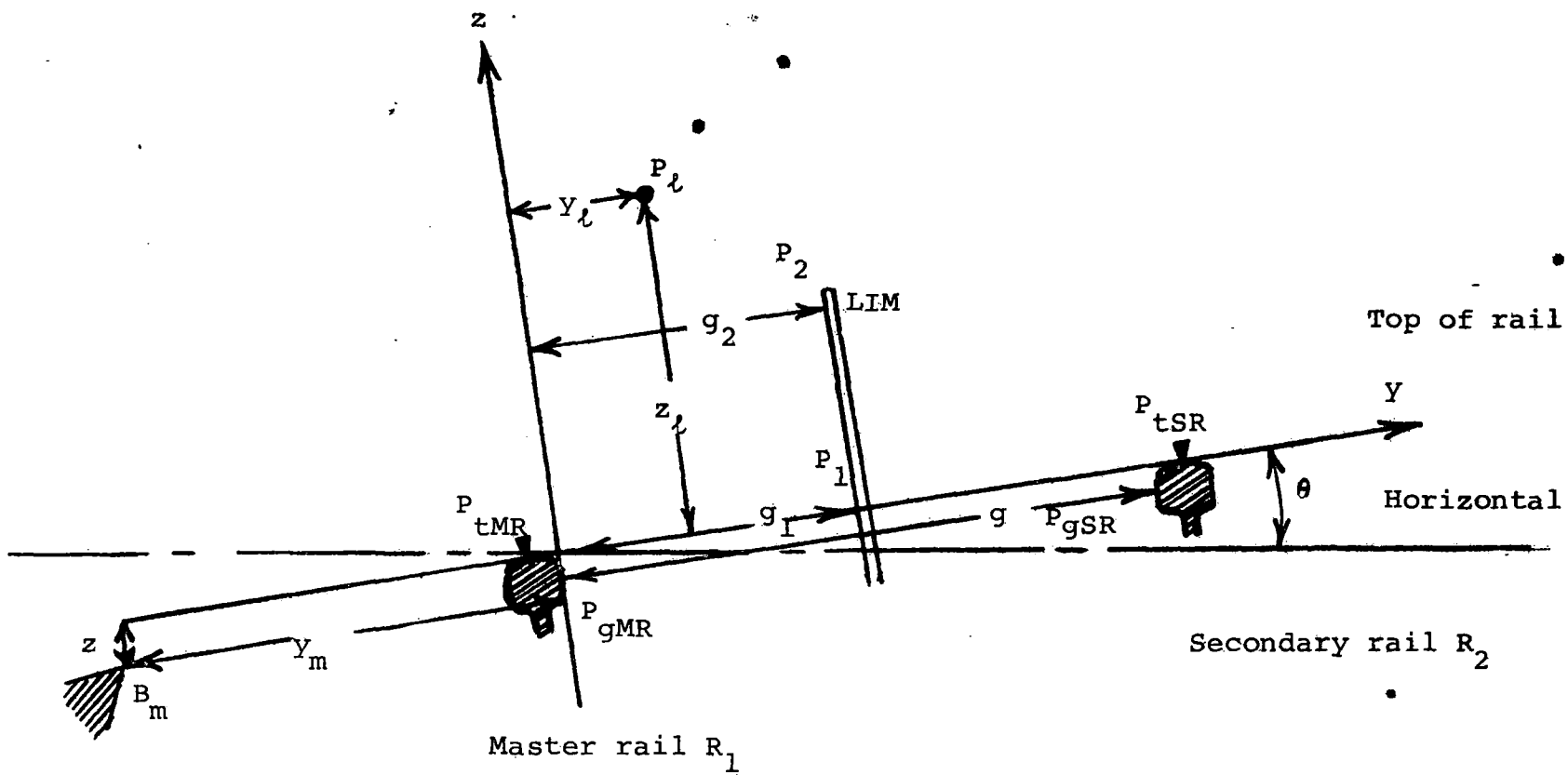

Figure 2-5. Track Cross Section Reference System

approximately 15 to 20 feet. This separation distance is considered adequate to eliminate interaction of the laser source due to the presence of the measuring frame and its carrier. This minimum separation distance, which has been estimated by GASL for an assumed track design, could probably be reduced depending on the actual elastic modulus of the rail and roadbed configuration (see Appendix I).

2.3 Principle of Operation of the Survey Device

To perform the measurement of the required track parameters according to the concept outlined in the previous section, the design of the Track Geometry Survey Device was undertaken using the following approach:

(1) Bench markers are periodically deployed in the ground along the track at a prescribed distance from the master rail (inner rail).

(2) A laser beam is used to provide the reference line basically oriented along the track itself, and the laser beam is generated by a laser transmitter located at a given position on the track.

(3) All of the sensors are mounted on a frame which is positioned in the plane surface A defined in Section 2.2.

(4) Sensors consisting of one optical sensor which measures the intersection of the laser beam with plane A and a series of electromechanical sensors which measure all of the other parameters defined in the previous section.

(5) The measurement of the track parameters in a position of the track between two bench markers, B_m, B_{m+1}, proceeds in the following way:

(a) The laser transmitter is positioned a short distance beyond the bench marker B_{m+1}. The laser is oriented roughly along the position of the track under measurement.

(b) The frame containing all of the sensors (measuring frame) is positioned along the track in plane A which contains the bench marker B_m.

(c) At this position, the location of the intersection of the laser beam with plane A is measured in addition to the bench marker position and all of the other parameters.

(d) Upon completion of the measurement at the position of bench marker B_m the measuring frame is moved along the tracks towards bench marker B_{m+1} by a predetermined distance. This distance is of the order of one foot. At this new position all of the measurements are repeated except the bench marker reading.

(e) The measurements are repeated at intervals of the order of one foot up to the final position of the measuring frame corresponding to the position of plane A which contains the bench marker B_{m+1}.

(f) At the final position the coordinates of the laser beam as well as the coordinates of the bench marker and the other track parameters are measured.

(g) Upon completion of the measurement on the position of the track between bench markers B_m and B_{m+1} the laser transmitter is moved beyond the position of the bench marker B_{m+2} so as to generate a new reference line over a position of track between the bench marker B_{m+1} and B_{m+2} and the measurement procedure is repeated.

(h) The output of the electromechanical sensors mounted on the measuring frame provides the local values of the track parameters defined in the previous section. As the measuring frame is moved along the track, the output of the optical sensor provides the alignment and profile.

The above described procedure of the track measurement can be classified as an absolute measurement technique in the sense that all of the track perameters are referred to the fixed bench markers whose positions have been previously determined.

A second measuring procedure may be followed without the use of bench markers wherever the position of the track is not required with respect to the ground. This second procedure still makes use of the reference line generated by the laser transmitter positioned at discrete intervals along the track; however, instead of determining the position of each reference line with respect to the bench marker the relative positions of the reference lines corresponding to adjacent sections of track are determined by means of the same sensors mounted on the measuring frame. It is apparent that to establish the relative position of two adjacent reference lines an overlapping of the measurements is required.

Finally, if profile and alignment are not required, the laser reference line can be eliminated and the system of electromechanical sensors can be used to measure the cross sectional properties, gage, and LIM reaction rail position.

In conclusion, the basic concept of the design of the TGSD permits the following three modes of operation:

Mode I Absolute track measurement system.

Mode II Relative track measurement system.

Mode III Track cross-sectional properties.

2.4 System Components

The schematic of TGSD is shown in Figure 2-6. The system consists of two vehicles, V_1 and V_2. V_1, which is manually operated, supports the laser transmitter and its power supply, and will be referred to as the Laser Support Vehicle (LSV). The other vehicle, V_2, referred to as the transfer vehicle (TV), contains the following major components:

(1) measuring frame

(2) odometer

(3) data acquisition system

(4) control panel

(5) electrical power plant

(6) propulsion plant

Vehicle V_2 is a self propelled four wheeled vehicle, having a total weight of 26,300 lbs which simulates the track load of each truck of the LIM Test Vehicle.

The measuring frame F shown in Figure 2-6 is attached to the transfer vehicle by means of a special linkage which makes it possible to maintain the frame perpendicular to the master rail as the measuring frame moves along the track. The measuring frame is shown schematically in Figure 2-7. The frame structure, an inverted U-shape, rides on the two support rails by means of rollers R_1 and R_2. The two rollers are conical with 1 in 40 conicity to insure that the contact between the rollers and rails are established at the rail head of the two support rails.

W_1 and W_2 are the two gage wheels which rotate about inclined axes to maintain contact with the support rails at the gage point. The angle of inclination of the axes of rotation of the two wheels W_1 and W_2 was selected to minimize the effect of any angular misalignment of the plane of the frame with respect to the master rail. The gage wheel W_2 which rides against the secondary rail is hydraulically loaded. With this arrangement the position of the measuring frame is uniquely defined with

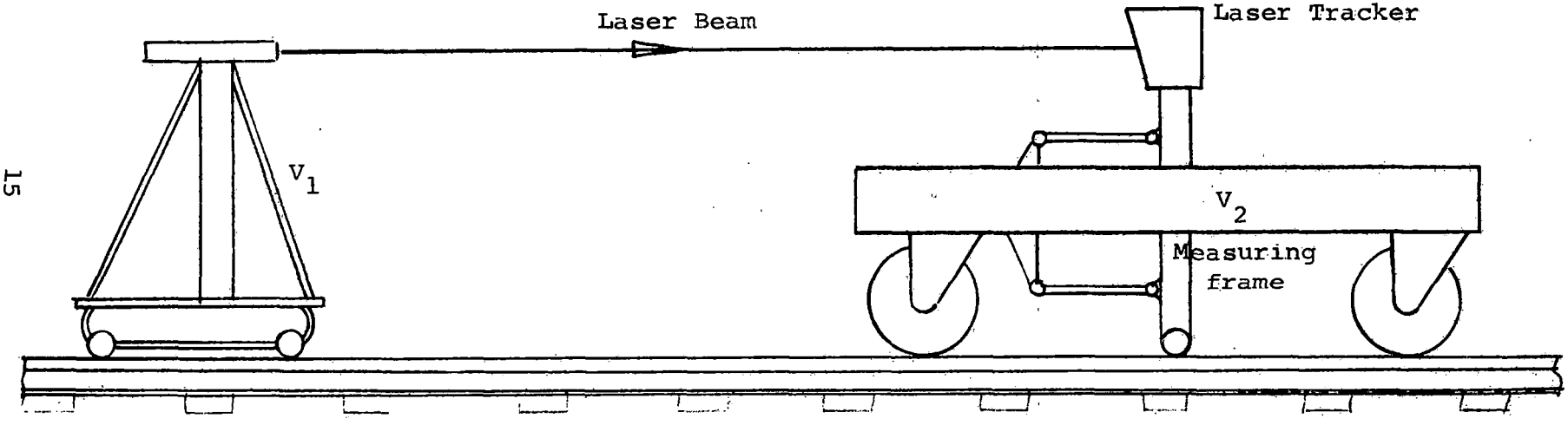

Figure 2-6. Schematic of the Track Geometry Survey Device

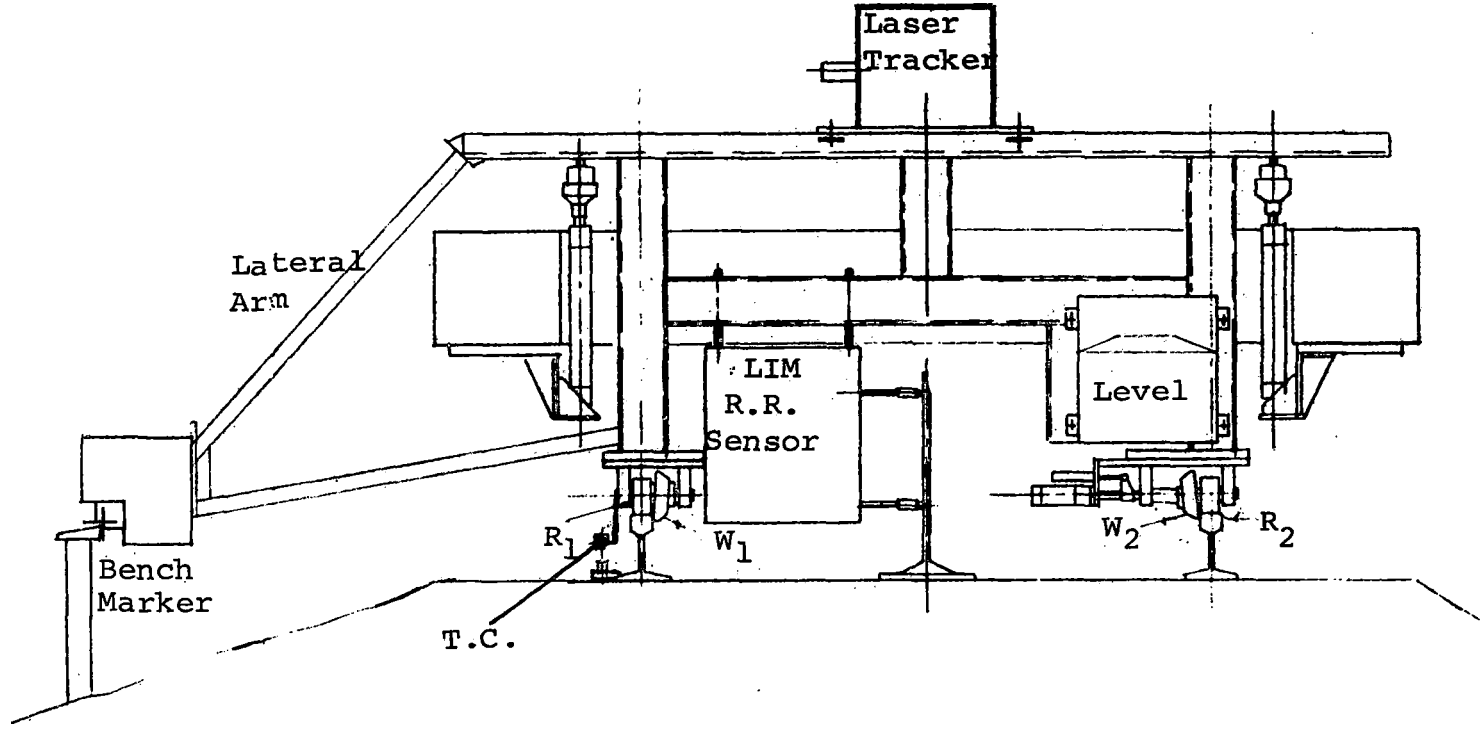

Figure 2-7. Schematic of the Measuring Frame

respect to the track. The distance between W_1 and W_2 provides the measurement of the gage.

Attached to the measuring frame is a lateral arm with two mechanical sensors which measure the position of the wayside bench marker in the frame of reference x, y, z, of the measuring frame.

The two mechanical sensors which measure the position of the LIM reaction rail are shown in Figure 2-7 at the two points previously defined (see Figure 2-5).

The cross level is measured by means of an electronic level also shown schematically in Figure 2-7.

The position of the point of intersection of the laser beam with the measuring frame (plane A defined in Section 2.2) is performed by means of a photodetector which automatically follows the laser beam along the two coordinates y and z. The photodetector system, which will be referred to as the laser tracker, is mounted in a chassis on top of the measuring frame. As the measuring frame moves along the track, the change of the two coordinates y and z of the photodetector provide the data which define both alignment and profile of the support rails.

Finally, the measuring frame holds a tie counter which is triggered by the nuts of the bolts holding the rails to the ties shown in Figure 2-2.

Odometer: The front wheel of the transfer vehicle which is unpowered and without brakes and rides the master rail contains an odometer with a 44 pulse per revolution encoder. This transfer vehicle odometer wheel has been accurately machined to a diameter so that the distance between the two pulses of the encoder corresponds to one inch of travel along the master rail.

Data Acquisition System: The DAS collects the output from the sensors and stores them in a digital form on magnetic tape. The schematic of the DAS is shown in Figure 2-8. The system accepts a total of 22 input signals consisting of eight analog signals generated by:

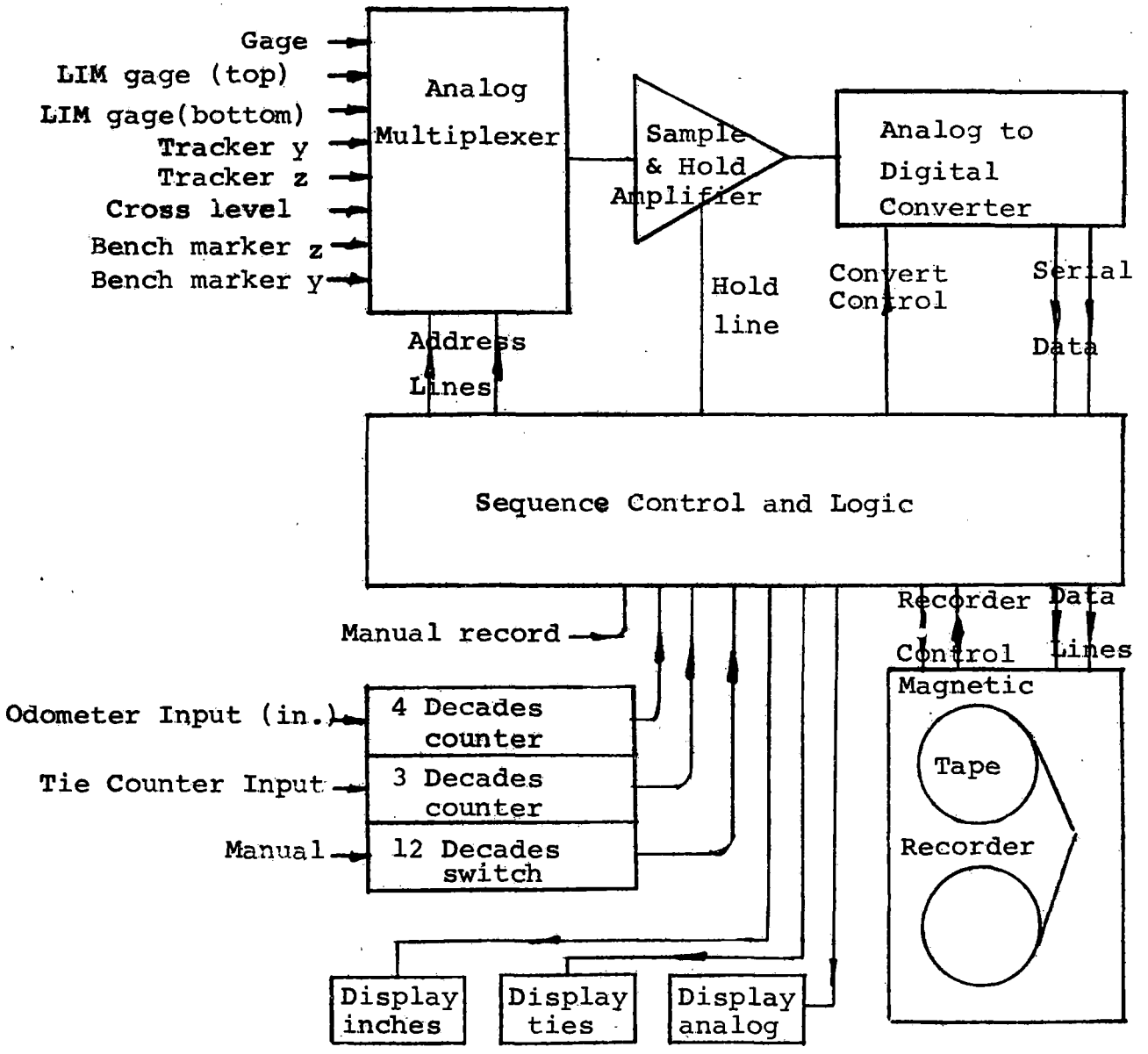

Figure 2-8. Data Acquisition System Schematic

1 gage sensor,

2 LIM reaction rail gage sensors,

1 level sensor,

2 laser tracker sensors,

2 bench marker sensors, and the following

digital signals generated by

12 fixed data channels,

1 tie counter and

1 odometer sensor.

The 12 fixed data channels are used to record data, run, sequence and all information which is pertinent for each particular measurement. The 8 analog channels are digitized in an analog to digital converter shown in Figure 2-8.

All of the digital information is then recorded on magnetic tape. The data recorder can be triggered either automatically or manually. The automatic trigger can be provided either by the tie counter or the odometer at twelve inches intervals. The manual trigger is normally used at the bench marker location or at the operator's option.

Control Panel: The control panel contains the following:

(1) Switches for activation of the sensors

(2) Instrumentation for the on-board electrical power plant

(3) Laser tracker controls

(4) Instrumentation of the electronic level

(5) Tie counter circuit

A schematic of the control panel is presented in Figure 2-9.

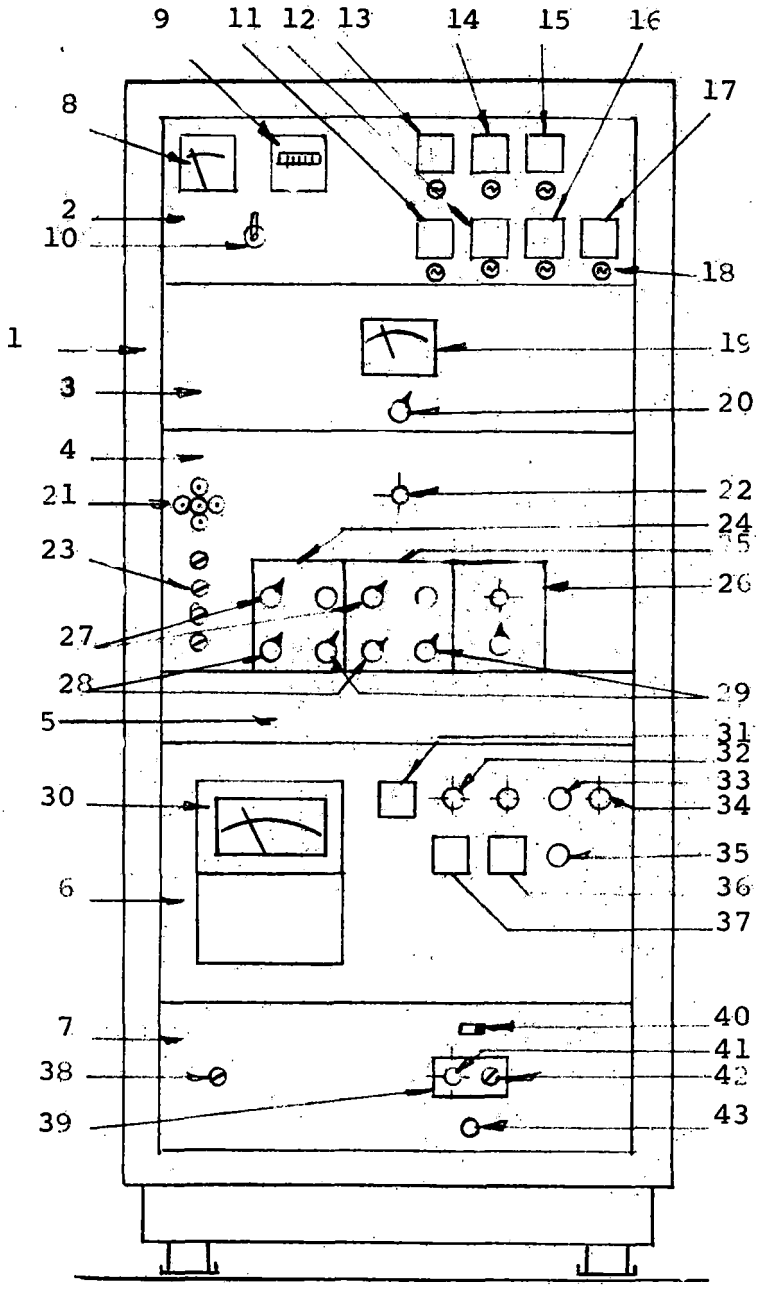

1. Control rack
2. A.C. power control panel
3. Reference and 12 VDC power supply panel
4. Laser tracker control panel
5. Drawer
6. Level and bench marker sensor control panel
7. Tracker alarm and tie counter control panel
8. AC power plant voltmeter
9. AC power frequency meter
10. Master switch
11. Level power switch
12. Laser tracker power switch
13. 12 VDC power supply switch
14. ± 10 VDC power supply (reference) switch
15. Data acquisition power switch
16. Auxiliary outlets power switch
17. Panel light switch
18. Fuses
19. Voltmeter for 12V and reference power supply
20. Selector switch for 12V; ± 10V and -10V to voltmeter 19
21. Test points for laser tracker photodetector
22. Laser tracker alarm
23. Laser tracker servo response adjustment
24. Laser tracker servo amplifier (vertical)
25. Laser tracker servo amplifier (horizontal)
26. Laser tracker power conditioner
27. Laser tracker offset control
28. Laser tracker servo gain adjustment (coarse)
29. Laser tracker servo gain adjustment (fine)
30. Level amplifier and sensor display
31. Bench marker power switch
32. Bench marker location light
33. Bench marker sensor extension
34. Bench marker sensor extended light
35. Bench marker sensor retraction and manual recording button
36. Horizontal bench marker or + 10V selector switch
37. Vertical bench marker or -10V selector switch
38. Laser tracker alarm sensitivity switch
39. Tie counter amplifier
40. Forward or reverse tie counting
41. Tie-on light indicator
42. Tie counter sensitivity adjustment
43. Tie simulator switch

Figure 2-9. Control Panel.

Electrical Power Plant: The on-board electrical power plant supplies the 115 volts, 60 cps power for the instrumentation. The power is produced by a gasoline powered generator having a maximum output of 2.5 KW.

Propulsion Plant: The propulsion plant which propels the transfer vehicle is a conventional four cylinder internal combustion engine. In addition, the vehicle can be manually moved by means of a hand crank for accurate positioning in the vicinity of the bench markers.

3. MEASURING SYSTEM

3.1 Measuring Frame

This section presents a detailed description of the various sensors which make up the measuring system. The sensors are mounted on the measuring frame which is linked to the transfer vehicle. A cross-section of the measuring frame, shown in Figure 3-1, is of rigid construction to minimize distortions which would affect the track parameter measurements.

Figure 3-1 shows the arrangement of the various sensors which follows the description given in Section 2.4.

LT is the laser tracker

EL is the electronic level

LB is the box holding the two LIM reaction rail sensors

GS is the gage sensor which is connected to wheel W_2, which makes contact with the gage point on the side of the secondary rail

MB is the box containing the two mechanical sensors for the wayside bench marker

The drawing of the roller wheel R_1 and gage wheel W_1 which rides on the master rail are shown in Figure 3-2, together with the tie counter TC.

Figure 3-3 shows the drawing of roller wheel R_2 and gage wheel W_2. Also included in this figure is the gage sensor GS. To maintain the gage wheels in contact with the two support rails, an hydraulic system H is attached to the assembly as shown in Figure 3-2 which generates a force of approximately 200 lbs.

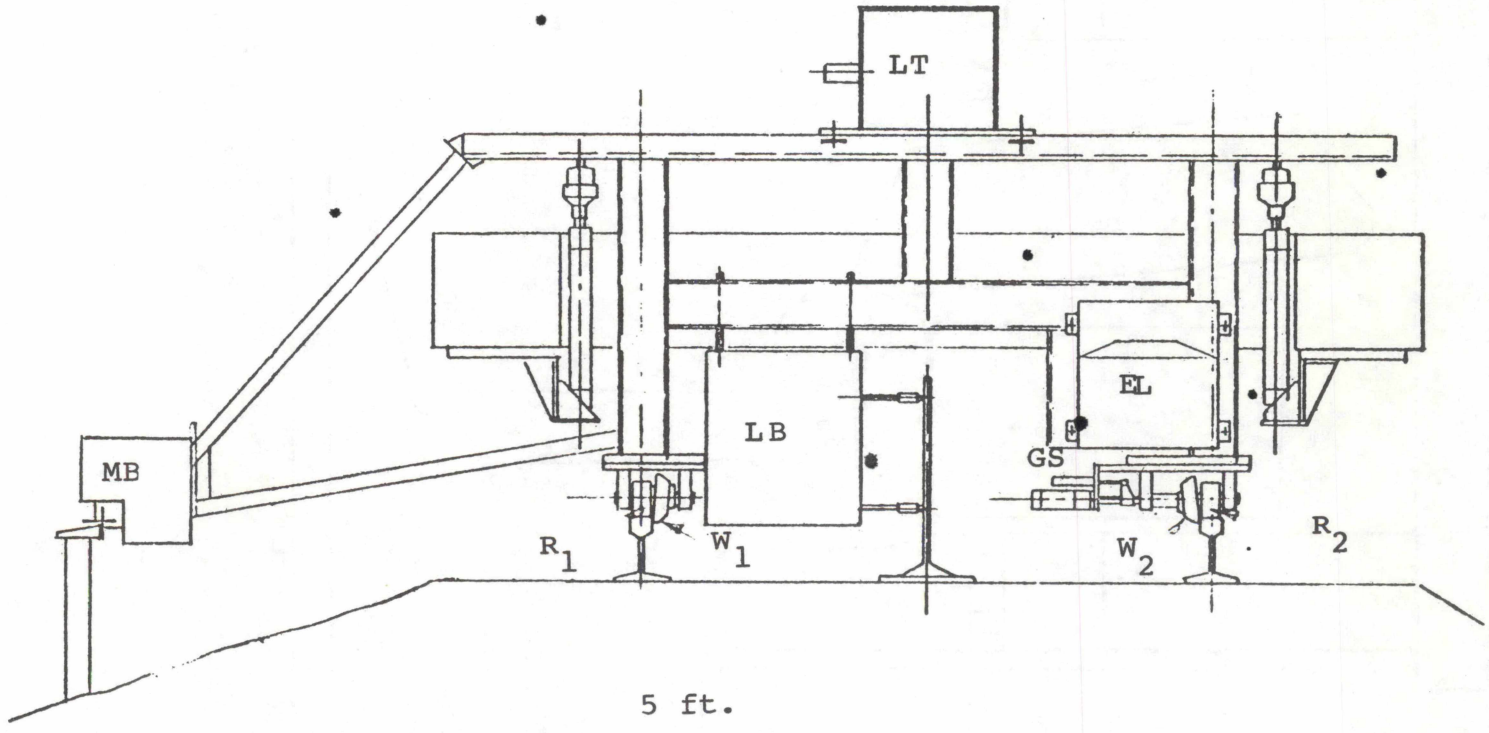

Figure 3-1. Schematic of Measuring Frame and Sensors

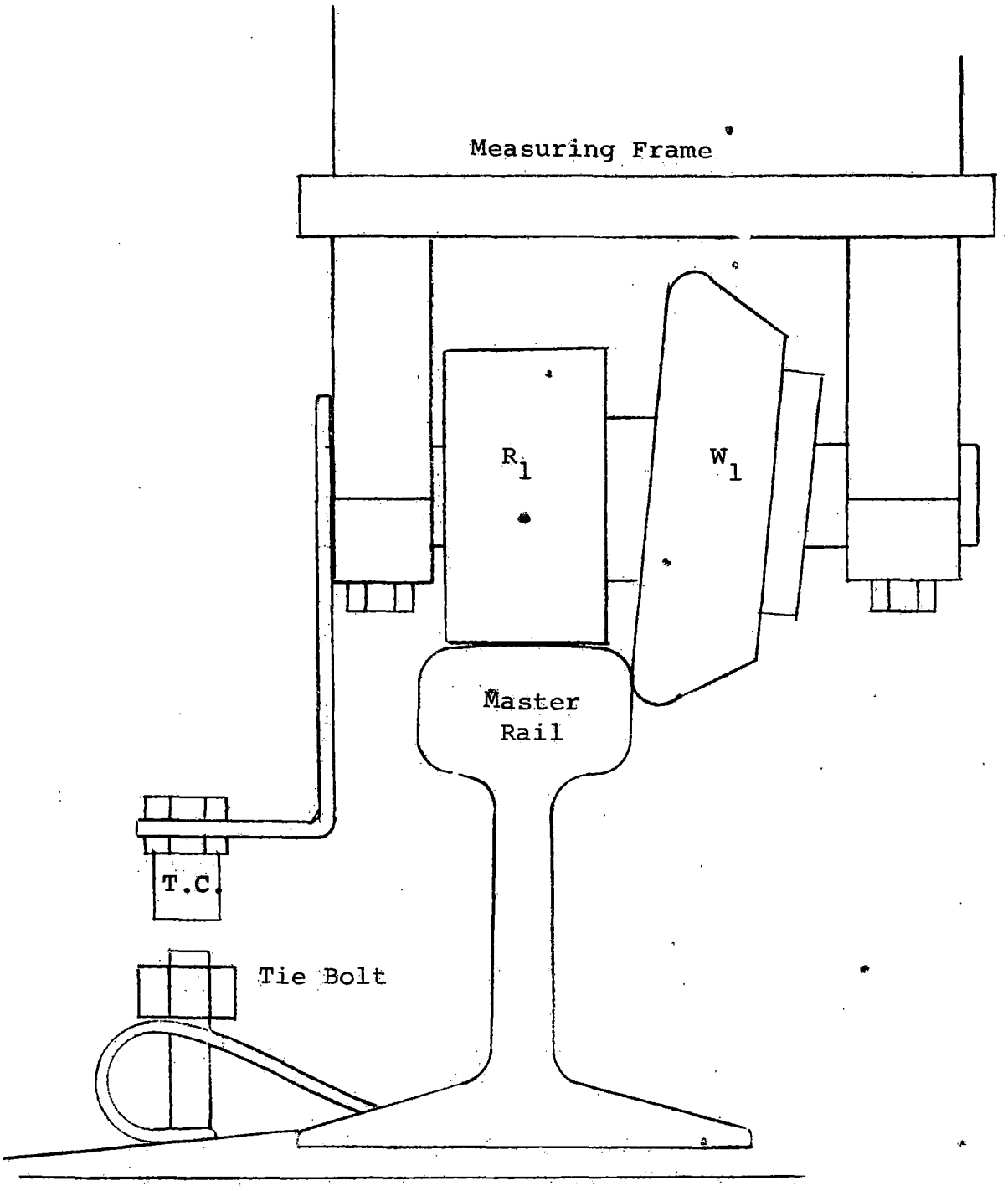

Figure 3.2 Measuring Frame to Master Rail Contact

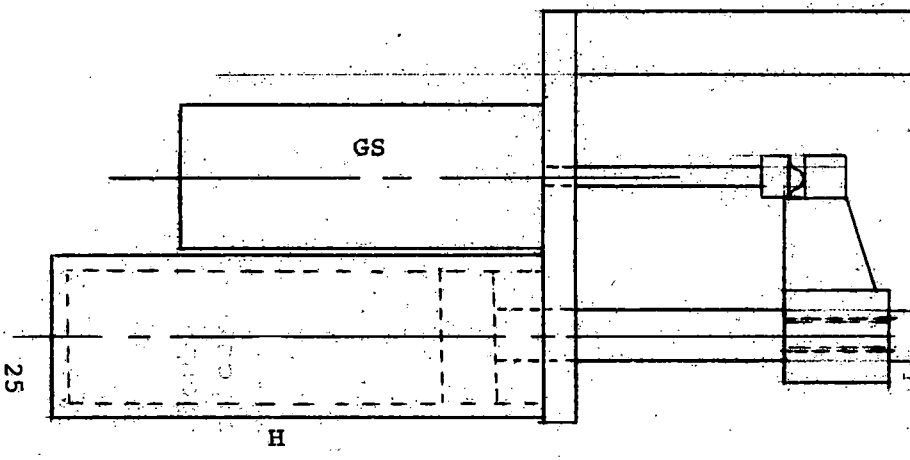

Figure 3-3.

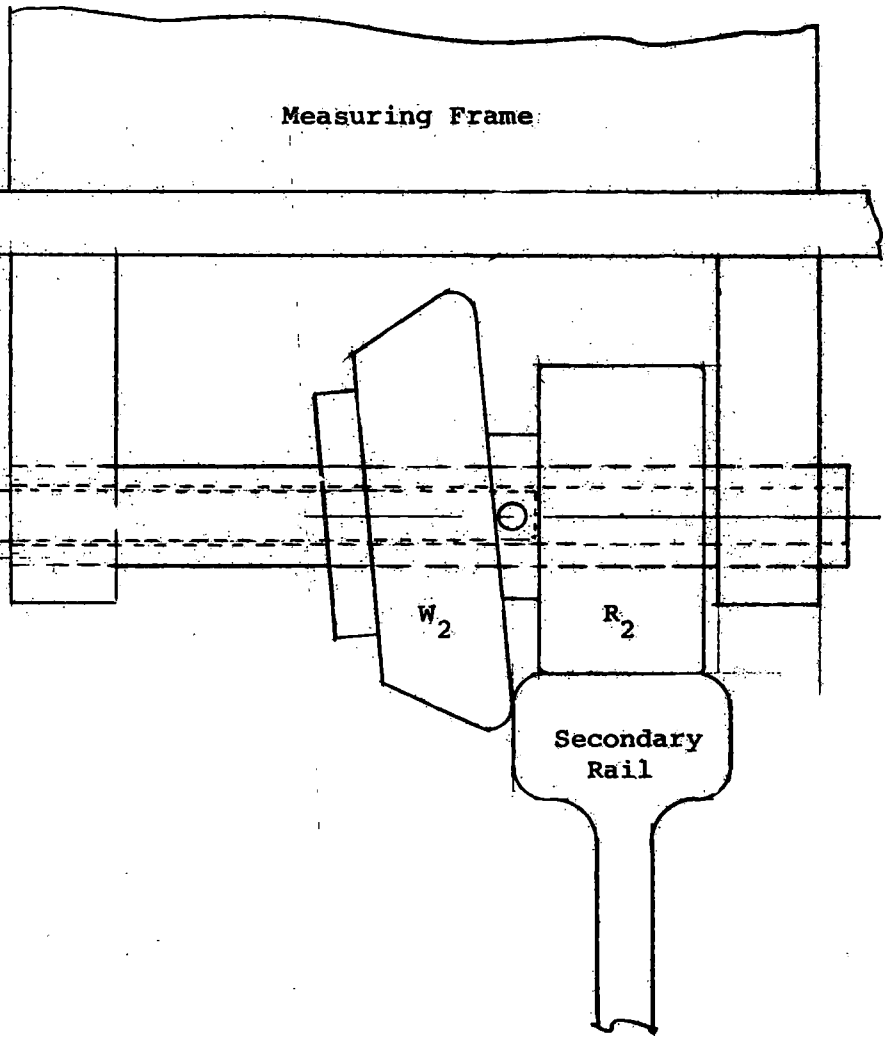

Gage Sensor Assembly

3.2 Laser Tracker

The laser tracker consists of photodetector units which automatically follow the position of the laser beam. A schematic of the laser tracker is shown in Figure 3-4. The photodetector head is divided into four quadrants oriented along the axis y and z in the plane of the sensor frame as shown. The photodetector itself is a silicon energy converter. The diameter of the detector head is 1 1/8 in. with a separation between sectors of approximately .006 in. The pair of quadrants aligned along axis y is connected to a differential amplifier, A_1, and the pair of quadrants along the axis z is connected to a differential amplifier A_2. The photodetector head can move along a support bar oriented along the axis z. This support bar, in turn, can translate in the y direction. The motion in these two directions is controlled by means of two servos which are powered by the output of the two differential amplifiers. The stationary position of the photodetector is reached when the image of the laser beam is centered with respect to the four sectors of the photodetector head in which case no signals are applied from the differential amplifiers. A displacement of the beam image with respect to the center of the photodetector head unbalances the system and energizes the sensors which bring the photodetector head back to the null position.

Two linear potentiometers P_y and P_z provide the analog signal corresponding to the two coordinates of the photodetector head to the data acquisition system. The maximum travel of the detector is 8 inches along the z axis and 10 inches along the y axis. The linearity of the two linear potentiometers is within .05% and the mechanical system is designed to have a backlash smaller than the minimum increment of the potentiometer position. A balanced power supply having an output of $\pm$ 9.95 volts provides the signal for the two potentiometers.

An extensive test program was conducted to determine the operating characteristics of the laser tracker. The output of the tracker was measured by moving the laser beam in the y direction at three positions, z = 2 in., 0 in., and -2 in., and in the z direction at three positions; y = 3 in., 0 in., and -3 in. These positions correspond to the two center lines

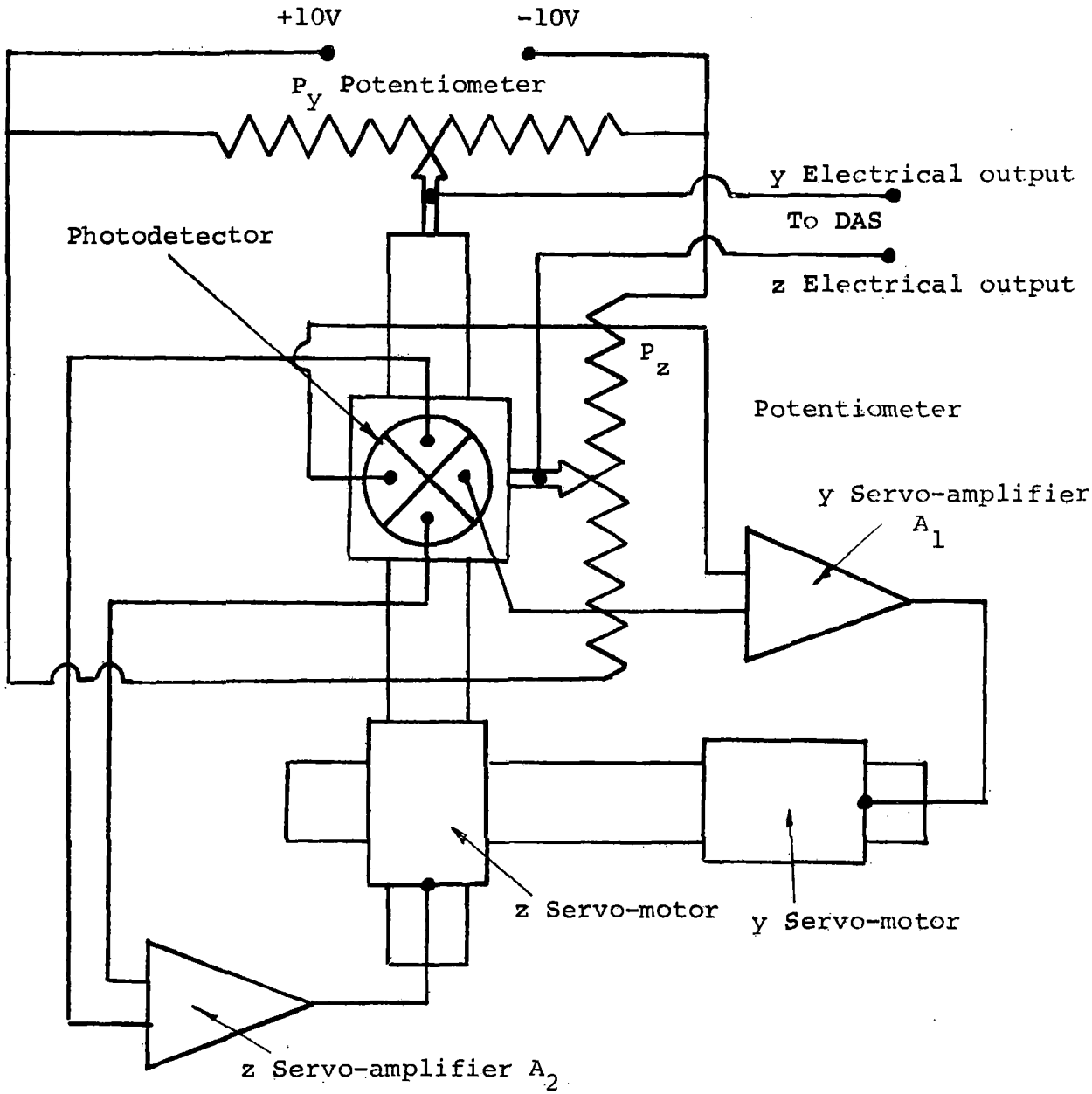

Figure 3-4. Schematic of the Laser Tracker

and the vicinity of the perimeter of the tracking surface. The result of these measurements performed along the two center lines (along the y axis and z axis) allows for the determination of the calibration constant as the straight line best fit. The difference between actual measurements and the straight line best fit is given in Figure 3-5, which shows the result of a typical measurement.

The values of the calibration constant are:

$$1.796 \frac{\text{volt}}{\text{inch}} \text{ in the horizontal (y) direction}$$

$$2.428 \frac{\text{volt}}{\text{inch}} \text{ in the vertical (z) direction}$$

One observes in Figure 3-5 that the actual measurements differ from the linear approximation $\pm$ .005 in. in the y direction and $\pm$ .002 in. in the z direction. The scattering of values among various measurements is $\pm$ .003 inches along y and $\pm$ .001 inches along z. A photograph of the laser tracker assembly is given in Figure 3-6.

3.3 Electronic Level

A schematic drawing of the electronic level is given in Figure 3-7. The level sensor itself is a Federal Level Model 232 P-68 having a total range of $\pm$ 50 arc seconds. The level sensor output is connected to an amplifier unit A which also contains a display instrument. The output from this amplifier goes into a servo amplifier, SA, which controls a servo motor, SM, which keeps the pendulum oriented along the vertical. The casing of the level sensor is free to rotate about an axis which is perpendicular to the plane of the measuring frame. The angular orientation of the sensor casing relative to the plane of the measuring frame is measured by means of a potentiometer. Also shown in Figure 3-7 is a tachometer connected to the servo motor which provides the servo system damping.

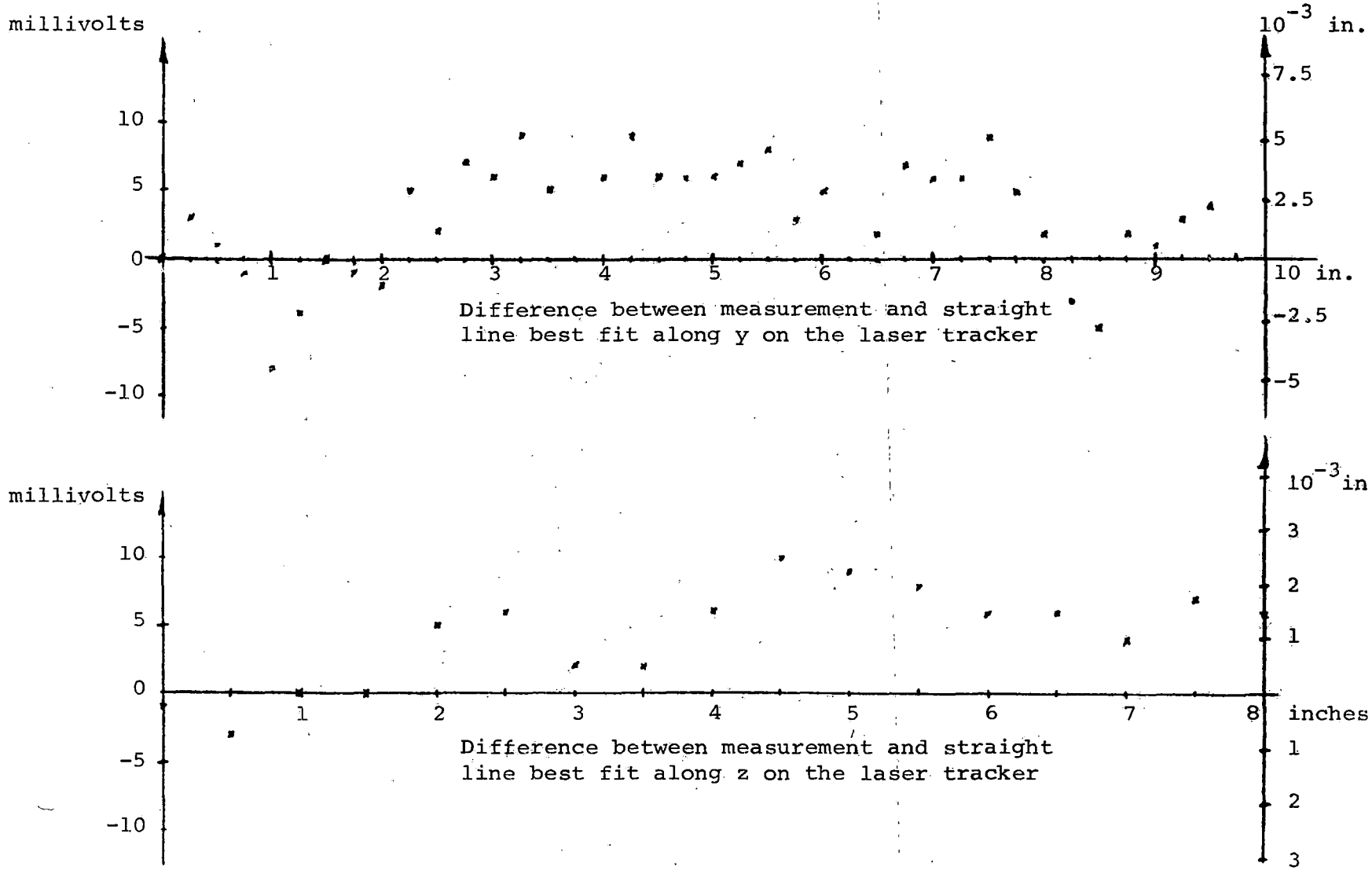

Figure 3-5. Calibration of the Laser Tracker

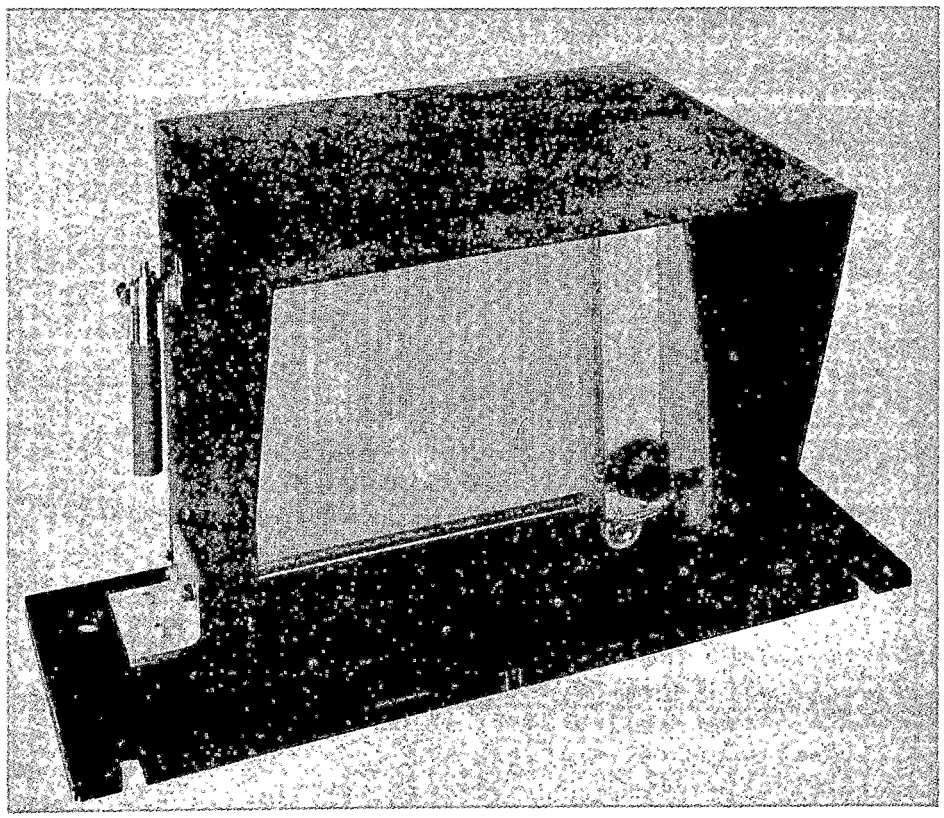

Figure 3-6. View of Laser Tracker

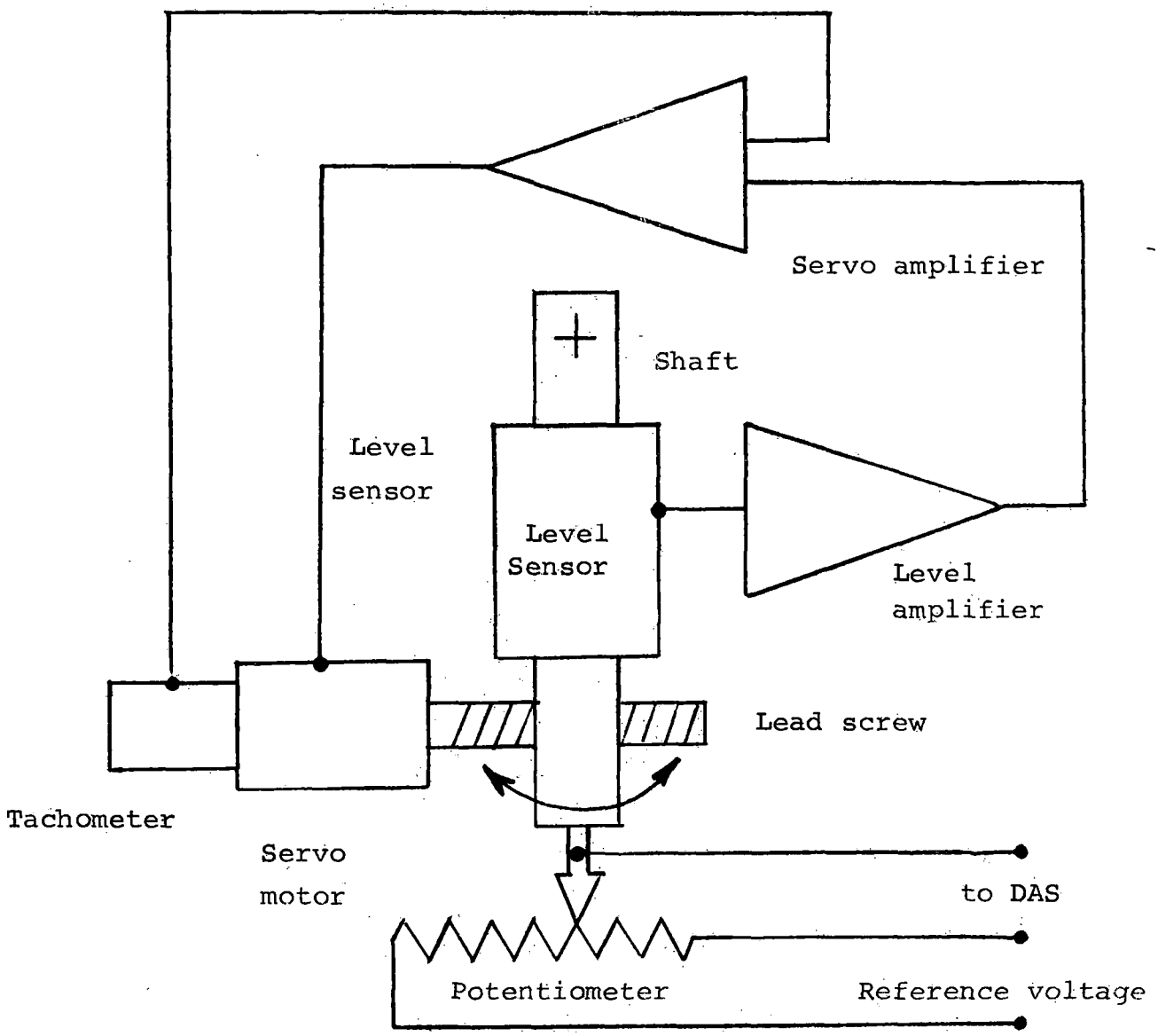

Figure 3-7. Simplified Circuit of the Electronic Level

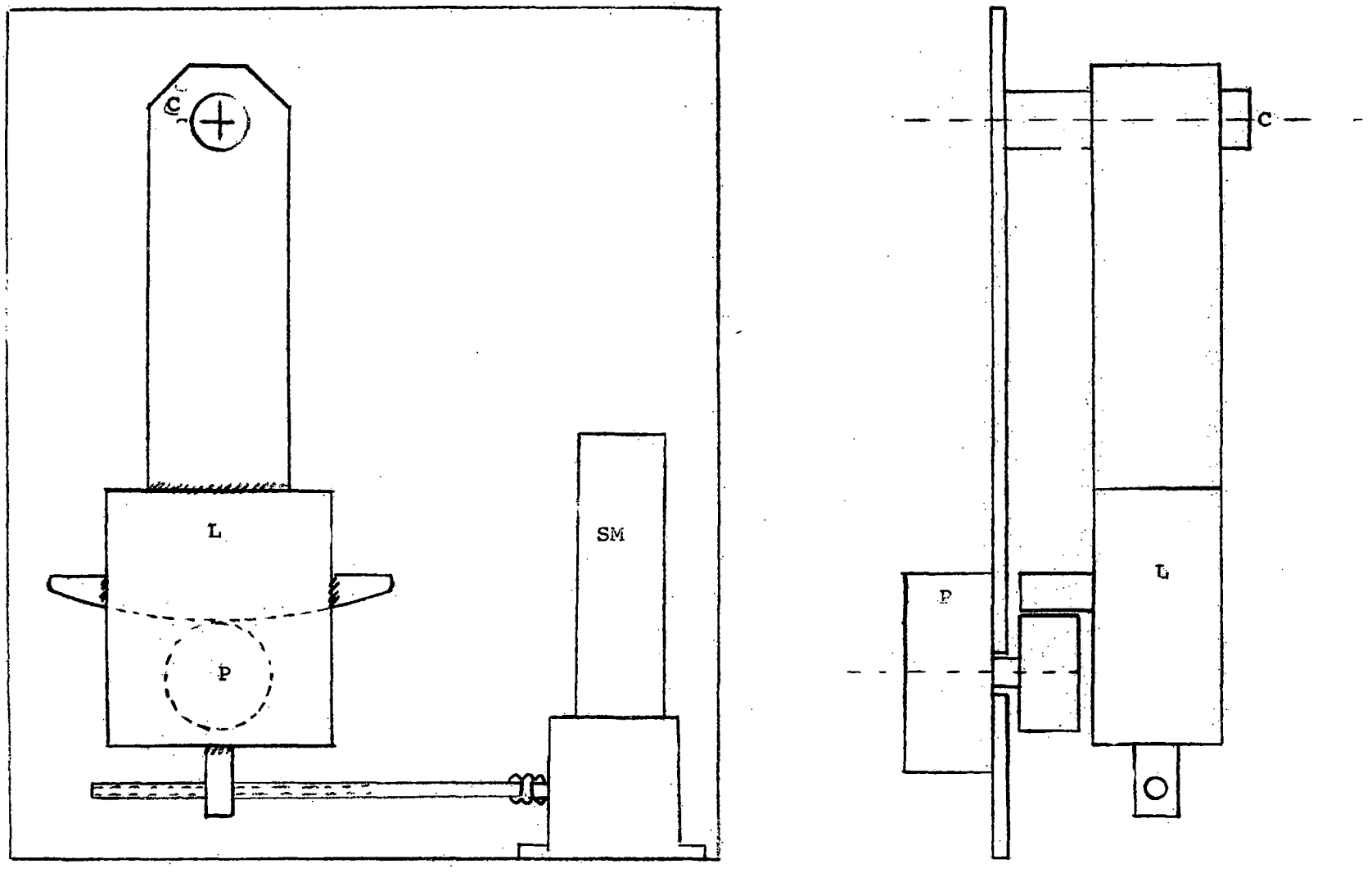

Figur3 3-8. Schematic of the Electronic Level

A schematic of the level sensor assembly is shown in Figure 3-8. L is the level sensor which is rigidly attached to an arm which rotates around an axis C; P is the precision potentiometer whose rotor is driven by the rotation of the sensor casing through a drum-belt linkage. The servo motor, SM, drives a right angle worm-nut mechanical linkage with a spring loaded arm to eliminate backlash effects.

The characteristic of the electronic level was measured in the laboratory. The output of the sensor was measured by rotating the casing known increments between -10^{o} and $+10^{o}$. The result of these measurements indicate a slight nonlinearity of the instrument output. The slope of the experimental curve at $\theta = 0$ determined the calibration constant of the instrument which is .854 volts/degree.

Figure 3-9 shows the difference between the experimental points and the straight line which corresponds to the calibration constant. The scattering of the experimental points results in an instrument error of $\pm 6 \cdot 10^{-3}$ degrees. The linearity of the sensor output leads to a departure of approximately 4×10^{-2} degrees over the total range of the instrument.

An external view of the electronic level assembly is shown in Figure 3-10. One observes three precision bubble levels which are preset at -2^{o}, 0^{o} and 5^{o}, to provide the reference points for the field checking of the instrument.

3.4 Mechanical Sensors

The mechanical sensors are grouped in the following three sub assemblies:

a) support-rail gage sensors

b) LIM-rail gage sensors

c) bench marker sensors

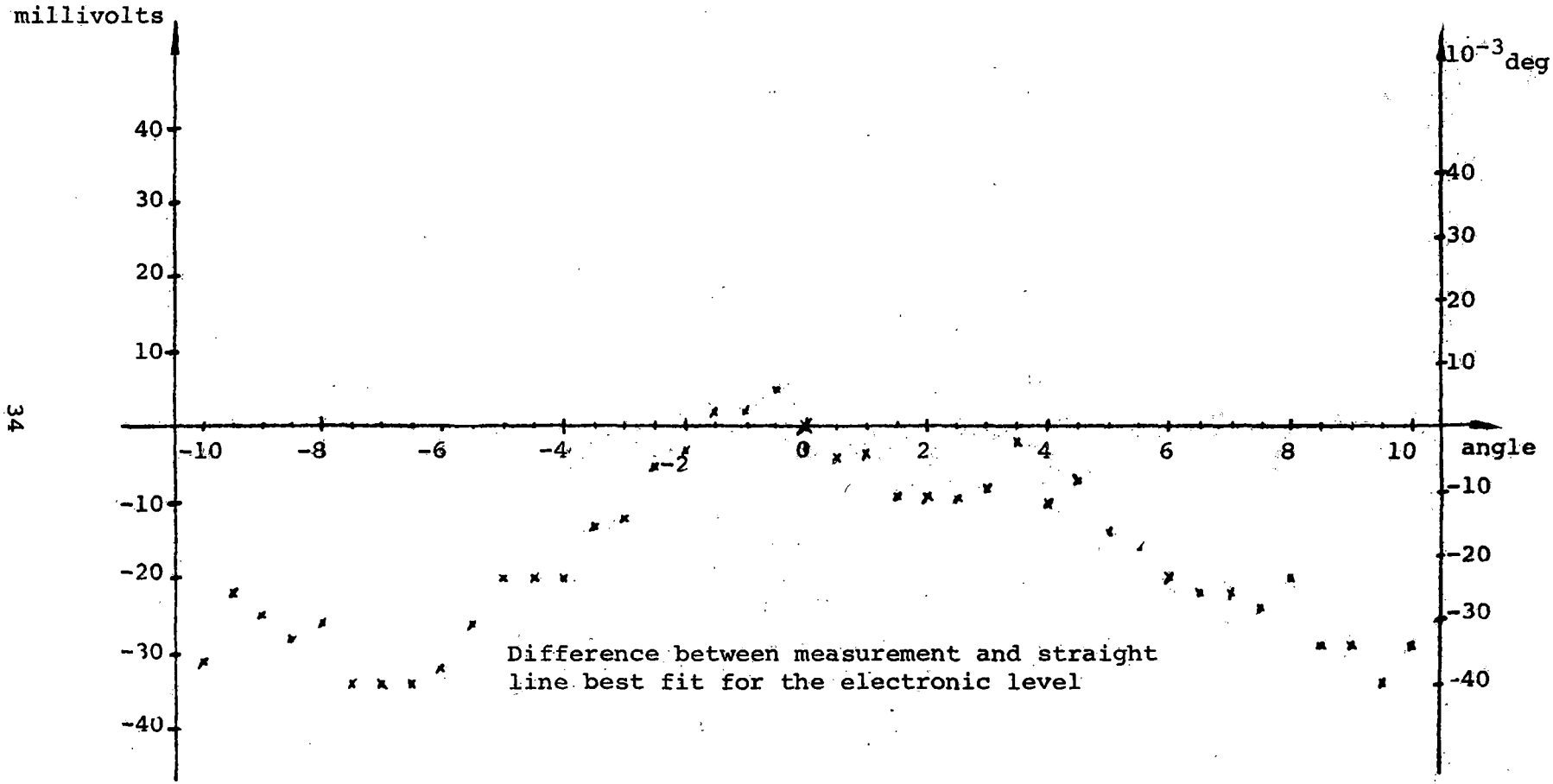

Figure 3-9. Calibration of Electronic Level

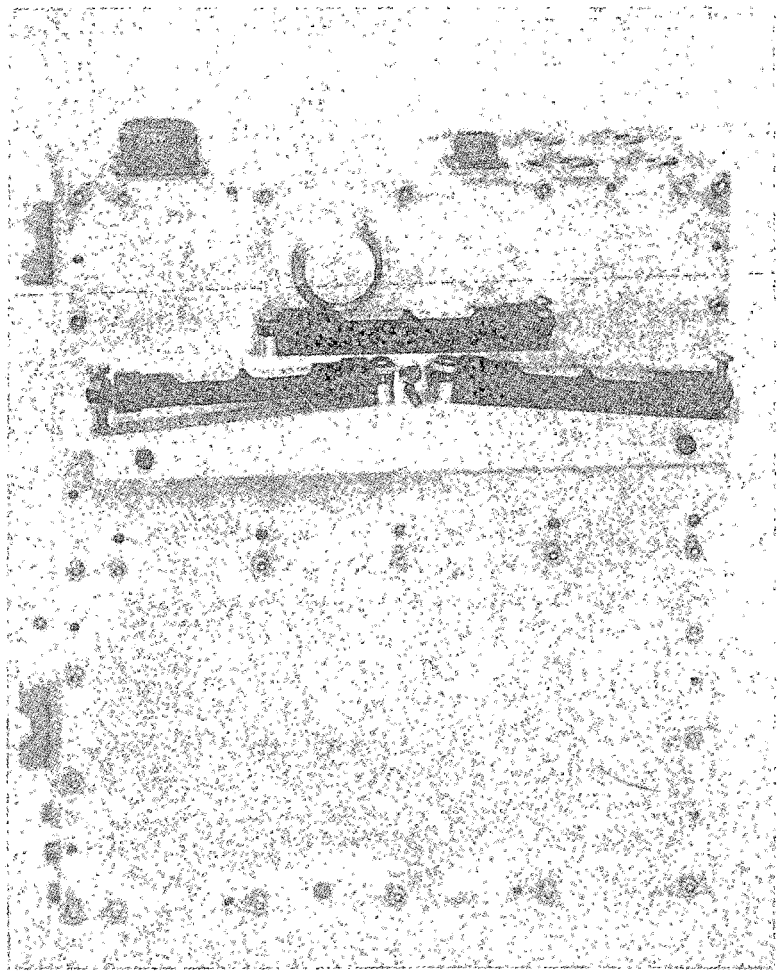

Figure 3-10. View of the Electronic Level

All of these sensors use mechanical contact against the element whose position has to be measured and the mechanical contact positions a precision rectilinear potentiometer which provides the analog output.

3.4.1 Support-Rail Gage Sensor. This sensor uses the gage wheel, W_2, which is kept in contact with the gage point of the secondary rail as shown in Figure 3-3. The linear potentiometer whose arm is connected to the gage wheel is a Bourns 108-0-2.25-103. The range of total travel of the gage wheel is two inches. One observes that the sensor is mounted on a platform P which can be mounted in two positions to measure gages from 55 1/2 to 57 1/2 inches or from 56 to 58 inches, respectively.

A photograph of the support rail gage sensor mounted on the measuring frame is shown in Figure 3-11.

3.4.2 LIM Rail Gage Sensors. As described in Section 2.4, two mechanical sensors are used to measure position and orientation of the LIM reaction rail. The two mechanical sensors are kept in contact with the reaction rail at the two positions z = 0 and z = 12 in. The two sensors which measure the displacement along the y axis use small metal wheels which roll against the reaction rail. Contact with the reaction rail is maintained with a spring loading of 5 pounds. Each sensor actuates a Helipot 1422-28-0 high precision rectilinear potentiometer. The total range of travel of the sensor is 4 inches. The best fit linear characteristics are: top sensor 4.008 volts/inches , bottom sensor 4.000 volts/inches. The discrepancy between measurements and straight line best fit is shown in Figure 3-12. The two sensors are mounted in a single box as shown in Figure 3-11.

3.4.3 Bench Marker Sensor. The bench markers are located on the axis y of the reference system connected to plane A at a distance of 60 inches for the center top of the master rail. The bench marker is in the form of a wedge as shown in Figure 3-13. The wedge is machined to have an angle of five degrees with respect to both y and z axes. The bench marker sensors use two contact pads as shown in Figure 3-14, to make contact with the edge of the bench marker wedge. The two contact pads are attached to two shafts oriented along the axes y

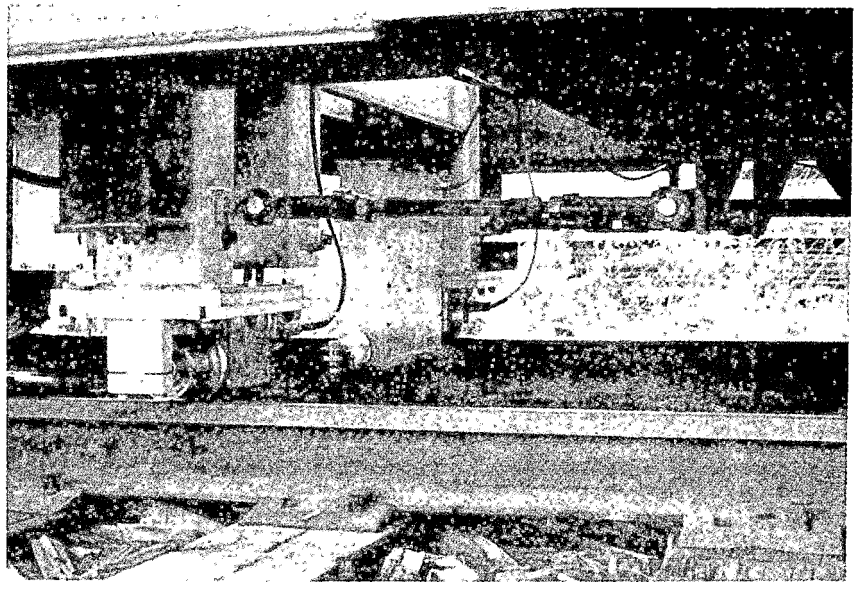

Figure 3-11. View of the Gage Sensor

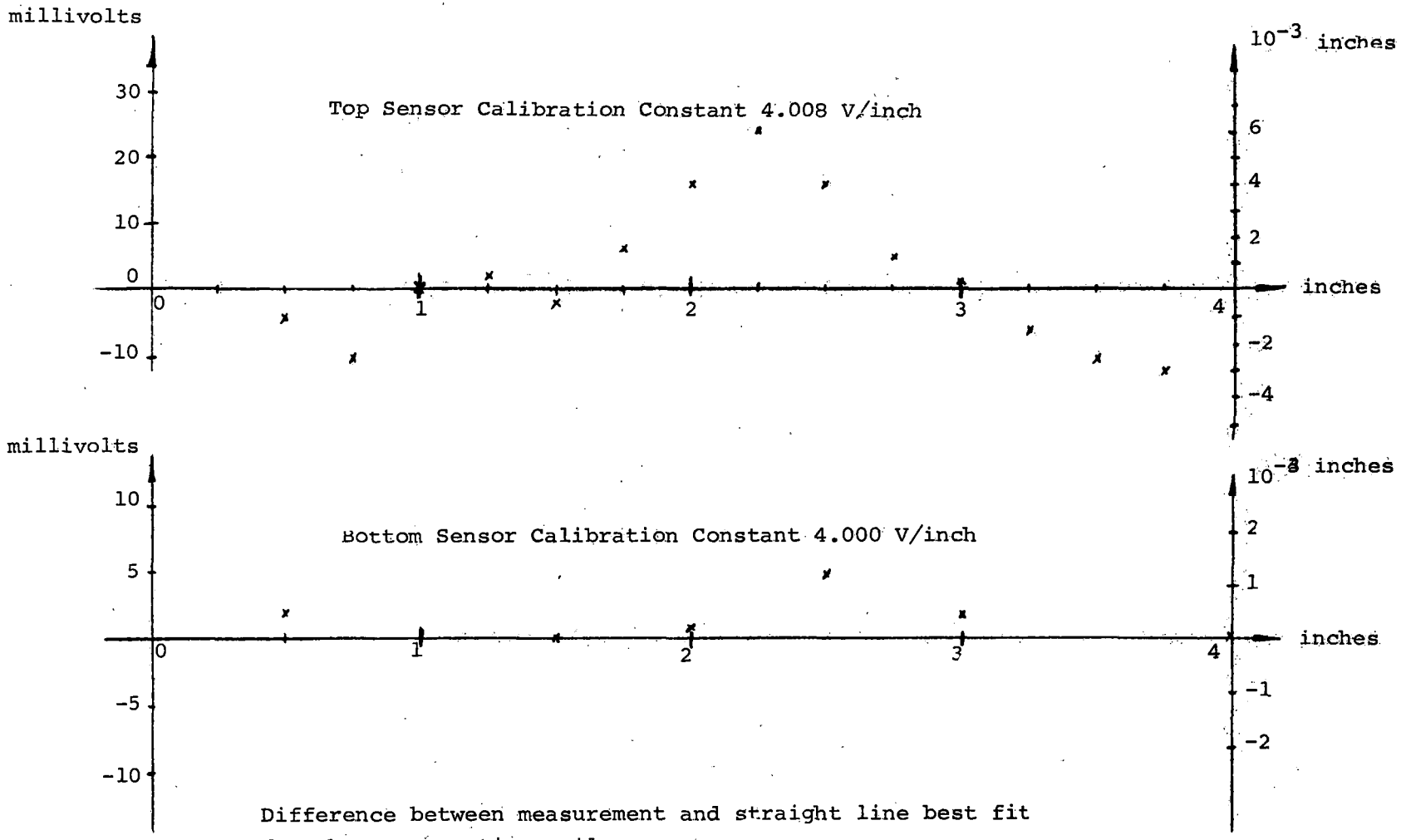

Difference between measurement and straight line best fit for the two reaction rail sensors.

Figure 3-12. Reaction Rail Gages Calibration

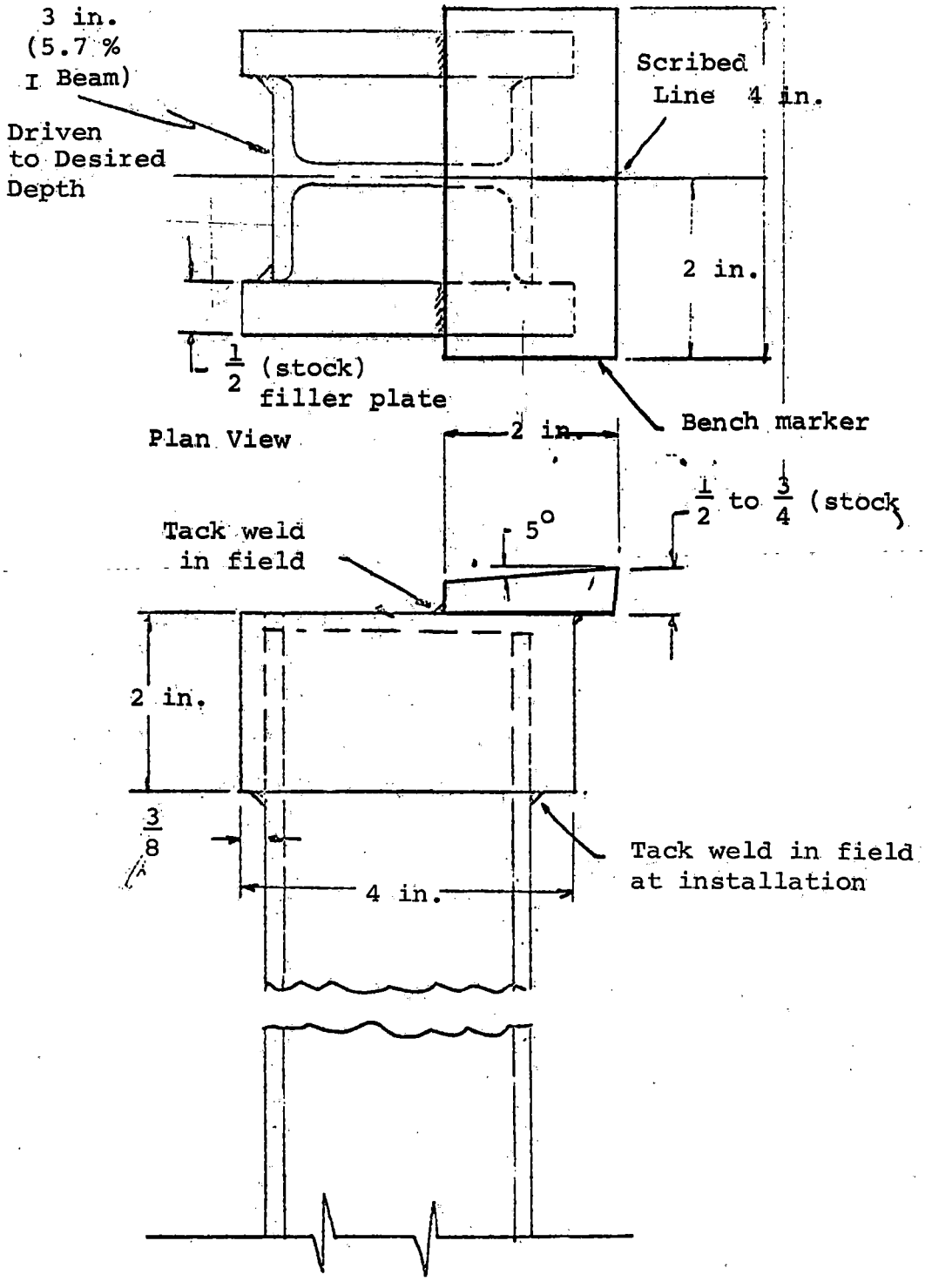

Figure 3-13. Typical Bench Marker Head.

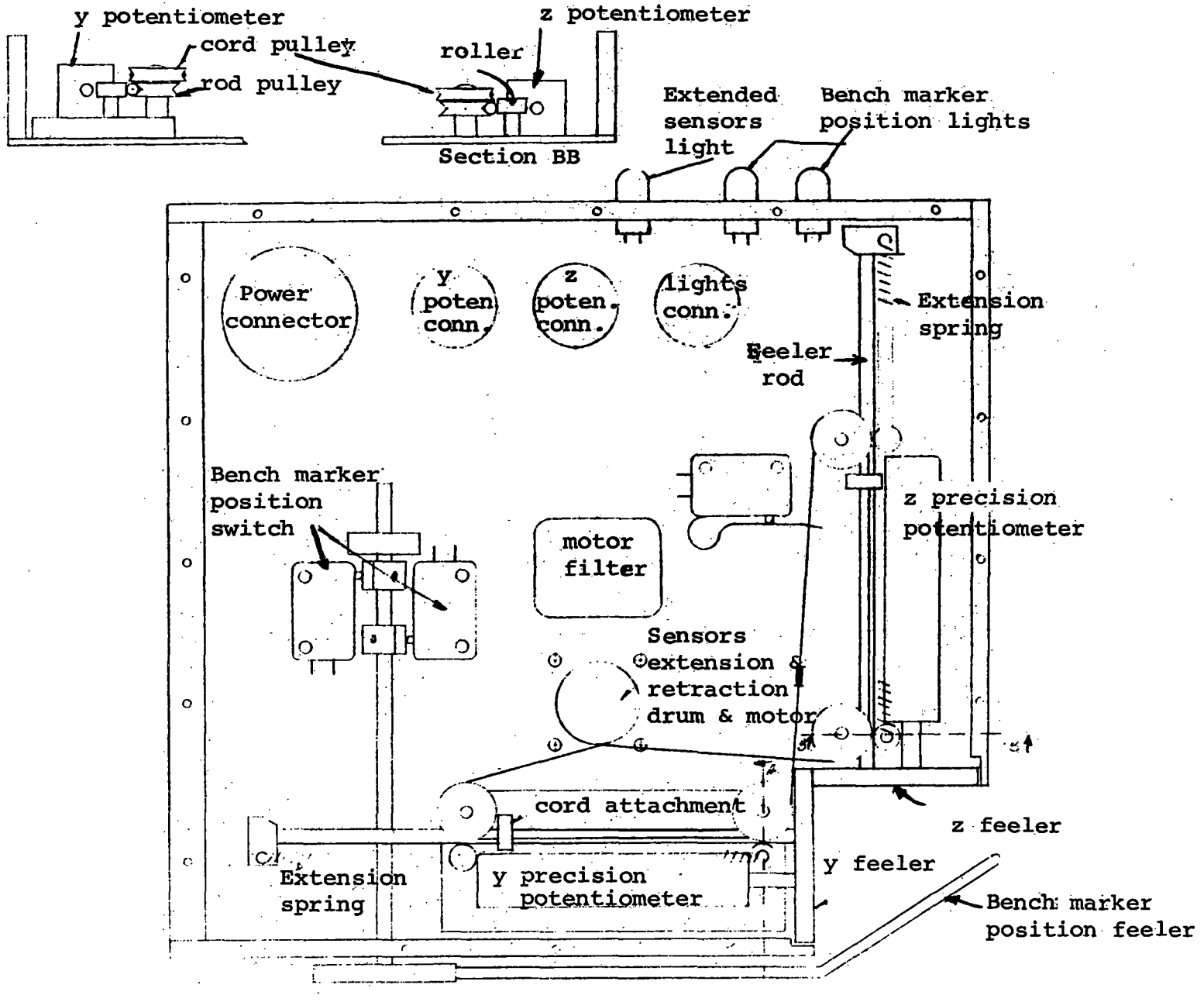

Figure 3-14. Bench Marker Sensors Construction

and z. These shafts are connected to precision potentiometers which provide the electrical analog signal. The total range of both contact pads is two inches. The potentiometers used were similar to that used for the gage sensor. The best fit of the linear characteristic gives:

$$y_{direction}\ 8.506 \text{ volt/inch}$$

$$z_{direction}\ 8.544 \text{ volt/inch}$$

The discrepancy between the linear fit and the actual measurement is shown in Figure 3-15, with a maximum difference of $\pm$ .003 inches; the scattering among measurements is approximately $\pm$.001 inches. The bench marker sensor box is rigidly attached to the measuring frame by means of three beams. A close-up of the bench marker sensor box is shown in Figure 3-16.

3.4.4 Calibration Jig. For field calibration and checking mechanical sensors mounted on the measuring frame, a jig was built which provides the reference points for the measuring system. This calibration jig, shown in Figure 3-17, is a rigid frame approximately twelve feet long. One block, A, attached to the frame, simulates the master rail and provides the reference gage point and the reference center top of the rail. Three interchangeable blocks can be attached to the jig at the position of the secondary rail to provide the calibration point for three different gages: 56.00 in., 56.50 in. and 57.00 in. Two additional mechanical pads are attached to the vertical member which provides the two calibration points for the LIM reaction rail. The two LIM reaction rail calibration pads are positioned at the extreme position of the measuring range away from the master rail and calibrated spacer blocks are inserted to calibrate the LIM reaction rail sensors at 1/8 in. intervals. Finally, a bench marker wedge identical to those used for the bench marker is attached to the jig as shown in Figure 3-17.

3.5 Positioning and Retracting System

To avoid damage and unnecessary wear of the sensor system the transfer vehicle is designed so that the measuring frame can be lifted when not being used. A special hydraulic system was

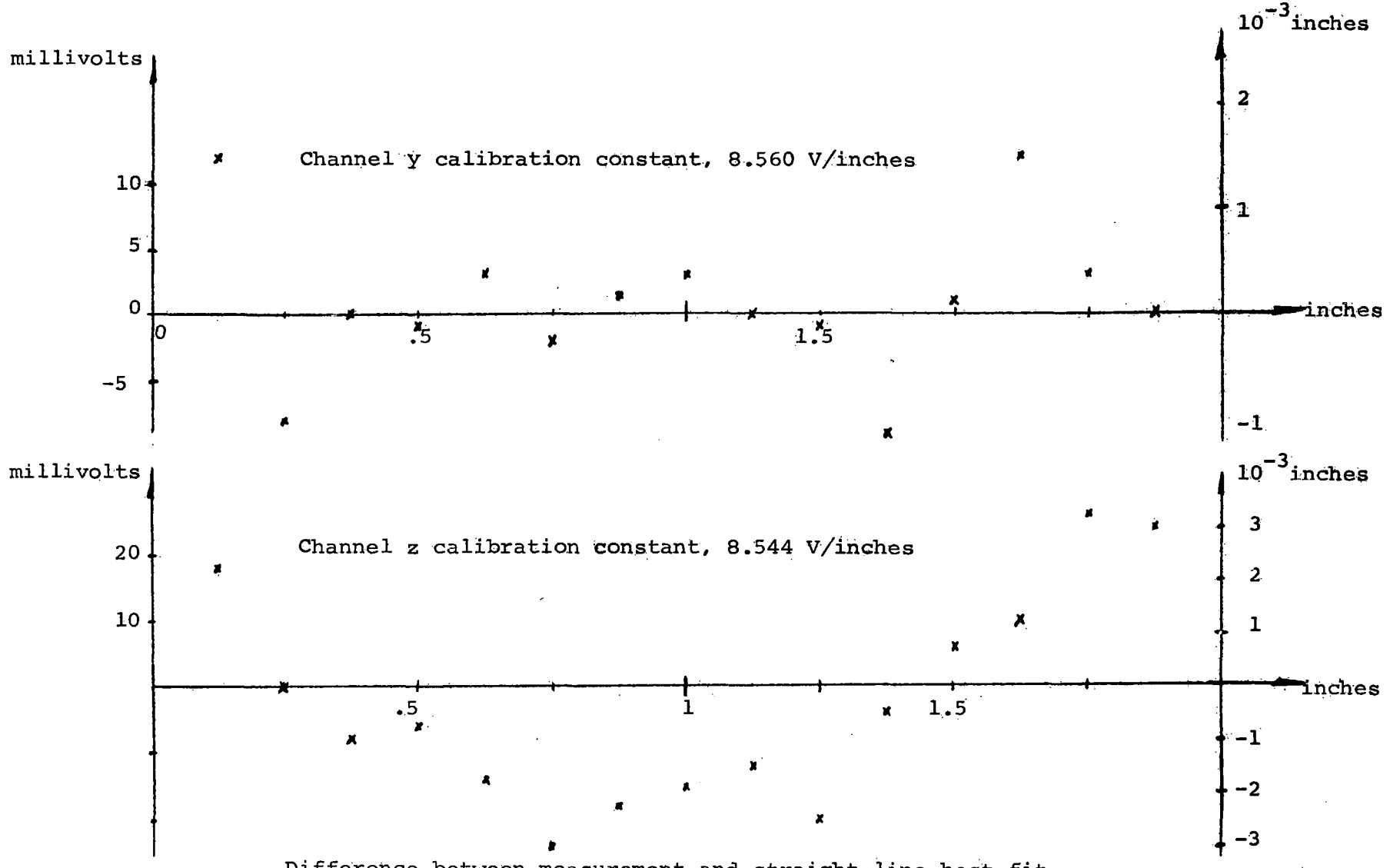

Figure 3-15. Bench Marker Sensors Calibration

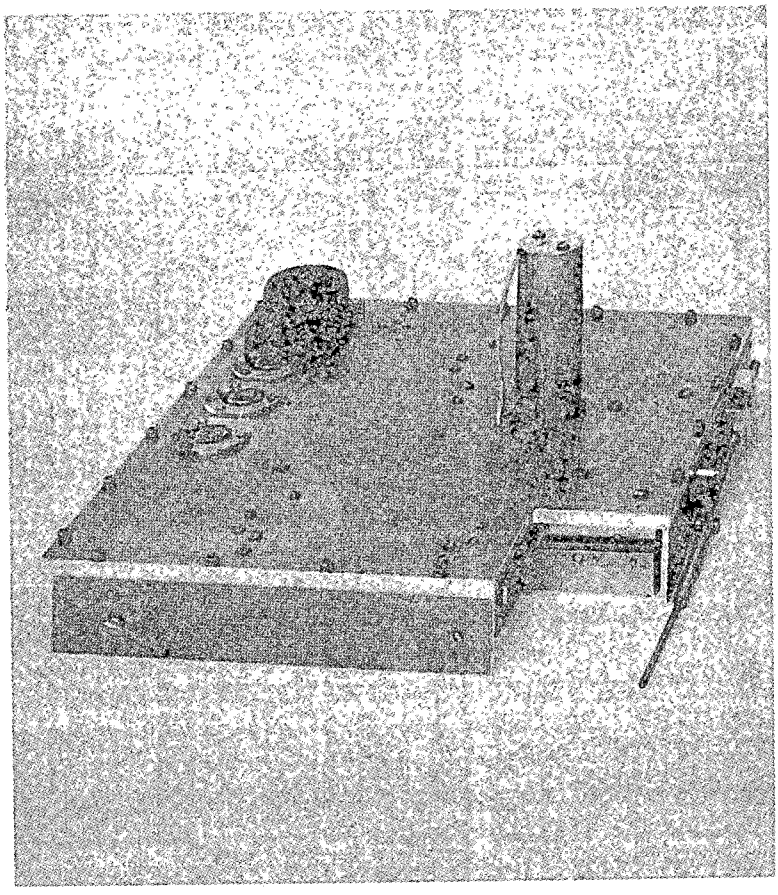

Figure 3-16. View of Bench Marker Sensor

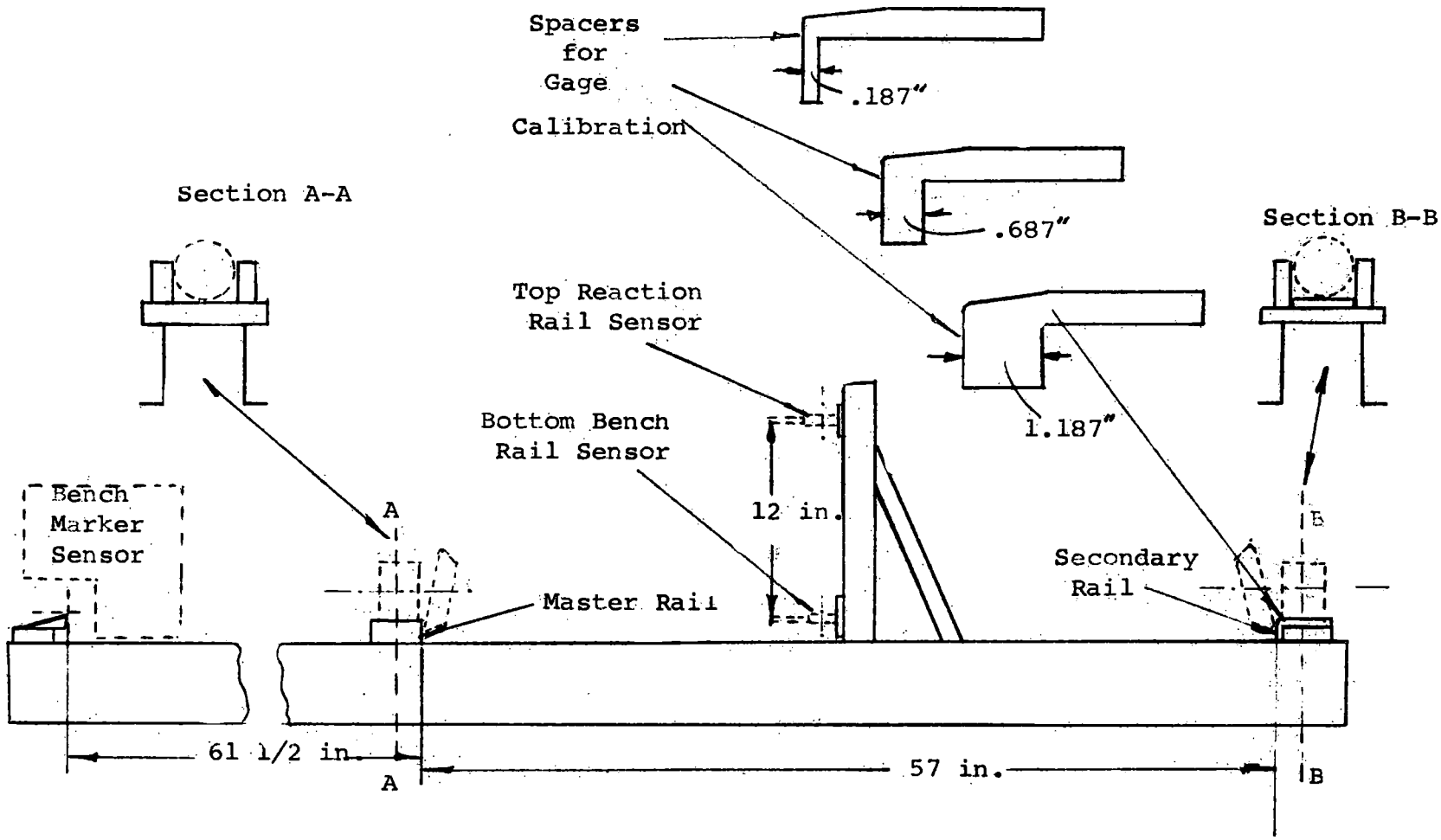

Figur3 3-17. Calibration Jig

built to position and retract the measuring frame. The schematic of the hydraulic system is shown in Figure 3-18. The actuators are used as follows:

a) Two cylinders to lower and lift the measuring frame.

b) One cylinder B to extend and retract the gage sensor.

c) One cylinder to retract the LIM reaction rail sensors.

In addition, a positioning and retraction system for the bench marker sensors is provided using an independent electrical system as shown in Figure 3-14.

3.6 Odometer and Tie Counter

As previously described, the odometer uses one of the wheels of the transfer vehicle. The mechanical arrangement of the odometer is shown in Figure 3-19. As shown in Figure 3-19, an optical encoder is used. It consists of two light sources, two photo transistors and a rotating disc with two sets of 44 windows each. The two photo transistors are used to provide the distance reading for both forward and backward travel of the transfer vehicle. This is accomplished by a 90° relative shift of the two photo transistor outputs which is generated by the staggered arrangement of the two sets of windows of the encoder wheel. The output of the two photo transistors are connected to an up and down counter.

The tie counter is a Micro Switch, Model 40FLI proximity switch. The presence of a metallic object affects the resonance of the switch circuit providing the output. The range of this proximity switch is 3/4 of an inch max. for a 1 inch diameter nut. The time resolution of the switch is approximately 4 milliseconds.

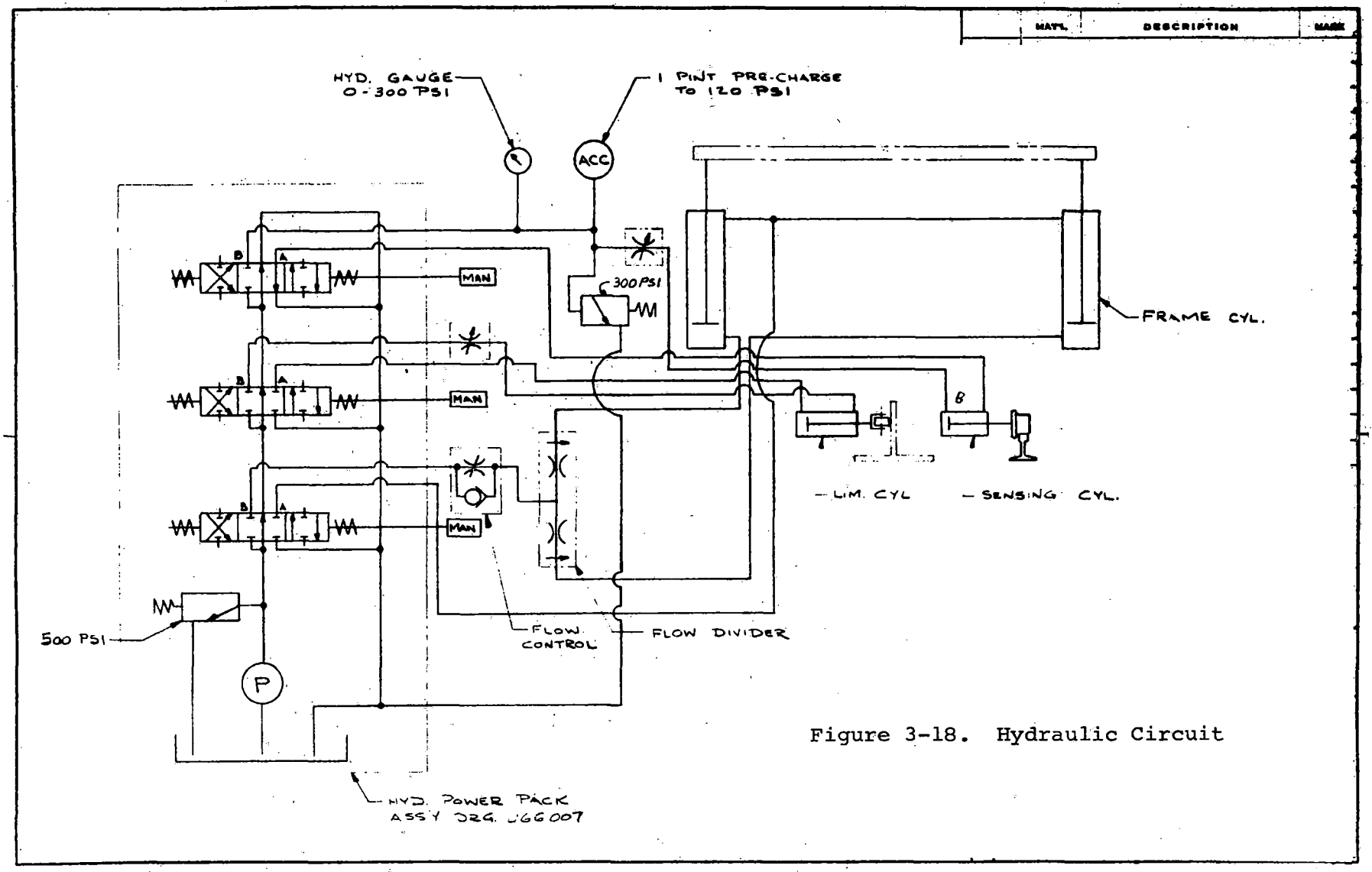

Figure 3-18. Hydraulic Circuit

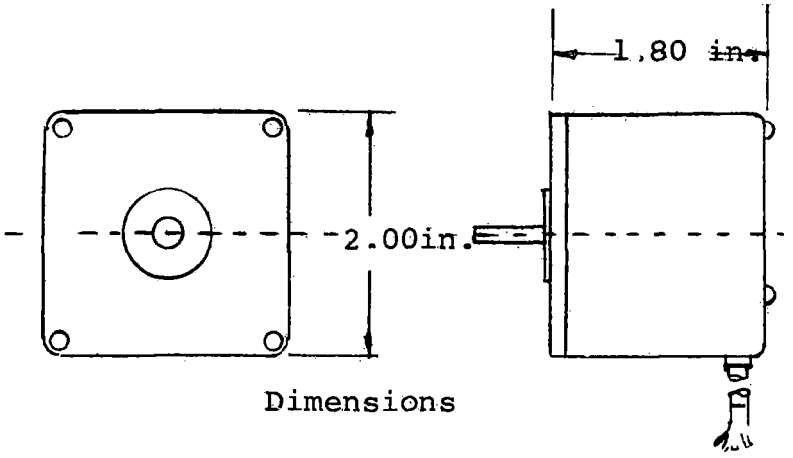

Dimensions

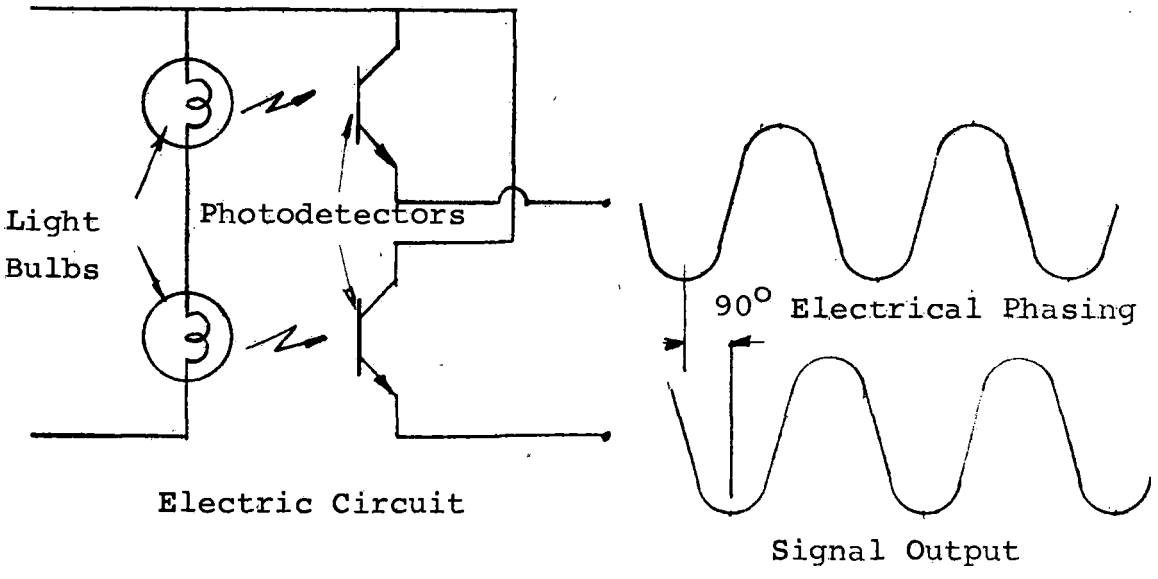

Electric Circuit

Signal Output

Figure 3-19. Odometer

3.7 Data Acquisition System (DAS)

The DAS has been designed to record in magnetic tape three types of measuring data; these are the sensor analog voltages, fixed data inputs and the distance data. These values are recorded in magnetic tape in the IBM 7 track format (BCD). The basic schematic of the DAS was described in Section 2.4.

The three functional sections of the system have been designed as follows:

Analog Voltages: The analog section of the DAS consists of an eight channel multiplexer, a sample and hold, a sign and a three digit BCD converter. The multiplexer switch in sequence one channel, allows the system to stabilize and then determine sign and convert the analog value into a digital signal, storing the information in the memory. After this operation, the multiplexer switches to the next channel and the cycle is repeated. The system input impedance is basically determined by the sample and hold amplifier, which has an input impedance of 100 MΩ. The multiplexer in front of the sample and hold is a semiconductor switch which does not affect the signal under measurement. Following the sample and hold is a converter which discriminates magnitude and sign. This is required because the analog digital converter only converts positive potentials; thus,as shown in Figure 3-20, a sign converter is used which converts negative input signals. The sign converter also provides a sign output indication to identify the sign of the input signal. The transfer accuracy of the analog voltage section components are:

Component	Transfer Accuracy
MM-8 multiplexer	± .01%
SHM-1 sample and hold	± .02% full scale
ADC-L converter	± .02% full scale ± 1/2 LSB

Fixed Data Inputs: The fixed data channels are used for the measured inputs corresponding to information which identifies each particular measurement. These channels are controlled by thumb wheel switches.

Distance Data: Two counters are provided in the system; one is the odometer and the other is the tie counter. Both counters accumulate in a decimal BCD mode and both counters are reversible to measure the distance in both directions. Consequently, counts may be both added and subtracted. The tie counter has three digits and the odometer counter has four digits. Increasing numbers correspond to a travel in the forward direction and decreasing numbers correspond to a reverse motion. With an initial setting of zero a forward motion generates increasing numbers up to 999 and 9999 for tie counters and odometer counts, respectively. A reverse motion with the initial zero setting will generate decreasing numbers from 999 and 9999, respectively.

Memory Storage: A 512 character memory is provided to store ten complete scans of data prior to the magnetic tape recording. This memory storage technique provides a more efficient magnetic tape utilization.

Magnetic Tape: The recording device of the DAS is a 7 track IBM compatible tape transport. The output format is the 7 track format with even parity. A view of the control panel and DAS is shown in Figure 3-20.

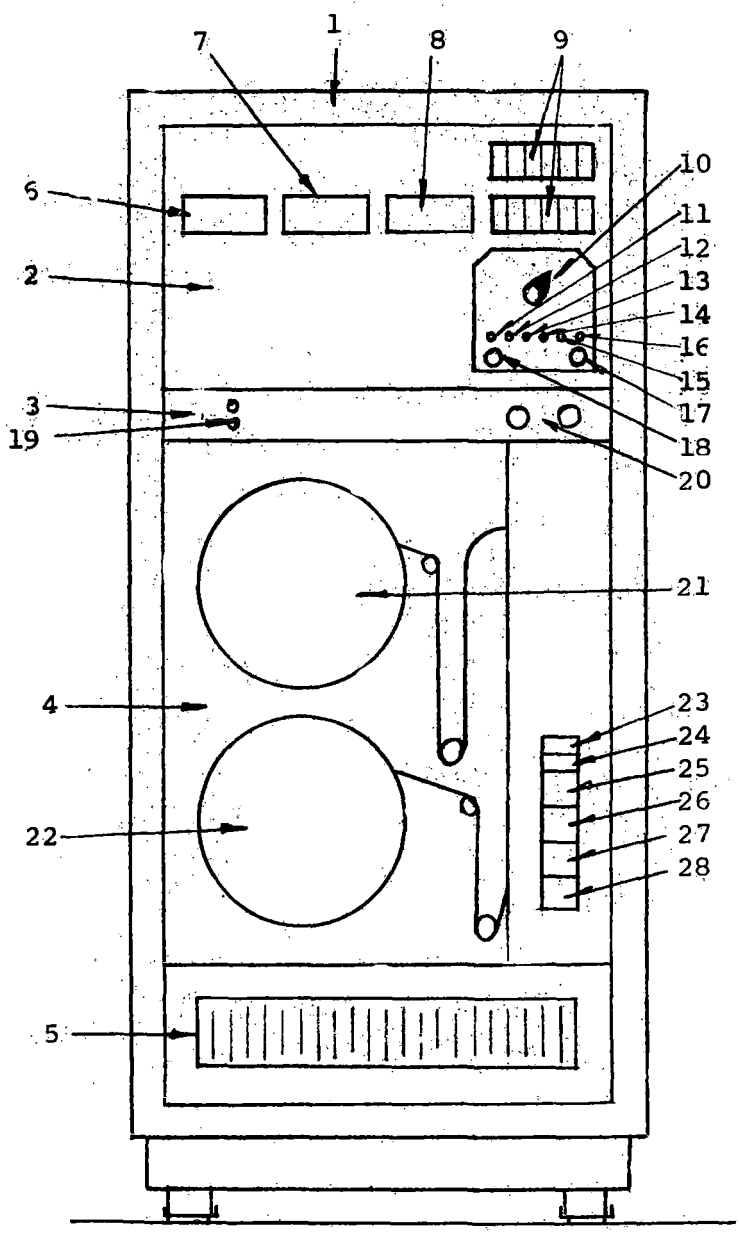

1. DAS Rack
2. Electronic interface
3. Reference power supply controls
4. Magnetic tape recorder
5. Blower
6. Tie counter display
7. Odometer display
8. Analog channel display
9. Manual data entry and display
10. Channel selector switch
11. Beginning of tape button
12. Inch-tie trigger selector
13. End of file button
14. Display light test
15. Tie reset
16. Inch reset
17. Entire display reset
18. DAS power supply
19. Reference supply coarse adjustment
20. Reference supply fine adjustment
21. Takeup reel
22. Load reel
23. Recorder power switch
24. File protector switch
25. Load-Unload switch
26. Reset switch
27. Rewind switch
28. Remote switch

Figure 3-20. Data Acquisition Panel.

4. TRANSFER VEHICLE AND LASER VEHICLE

This section presents a general description of the transfer vehicle (TV) which contains the measuring system and the small laser support vehicle (LSV) which houses the laser transmitter and its power supply.

4.1 Transfer Vehicle

The transfer vehicle is an adaptation of the Whiting Corporation "Trackmobile" especially modified to accomodate the GASL designed measuring system described in the previous section.

The vehicle consists of a 13 feet long and 8 feet 6 inch wide platform riding on four, 14 inches diameter wheels having cylindrical riding surfaces. The height of the platform above the top of the rails has been selected to clear the top of the LIM reaction rail. For the wheel diameter used, the LIM rail required independently mounted wheels. The independently mounted rear wheels of the vehicle are each powered by a chain drive from a common drive shaft. A cross section of the vehicle configuration is shown in Figure 4-1. The transfer vehicle has a rigid suspension.

The weight of the vehicle is 26,300 lbs including a removable ballast of 16,000 lbs in the form of steel plates which can be placed in front and rear of the transfer vehicle in receptacles.

A cut-out has been provided at the mid wheel base location to accomodate the measuring frame as shown in Figure 4-2. The measuring frame at its lowered measuring position is shown by the dotted lines. The mechanical linkage between measuring frame and transfer vehicle is provided by three 24 inch long turnbuckles. Two of the turnbuckles are located 12 in. above the rail head approximately 60 inches apart. The third turnbuckle is located at the center of the measuring frame 32 inches above the rail head. This arrangement permits the three turnbuckles to be initially adjusted to permit the proper orientation of the measuring frame at its measuring position. These three turnbuckles are connected to both the transfer vehicle and the measuring frame by means of horizontal hinge pins for the retraction and lowering operation.

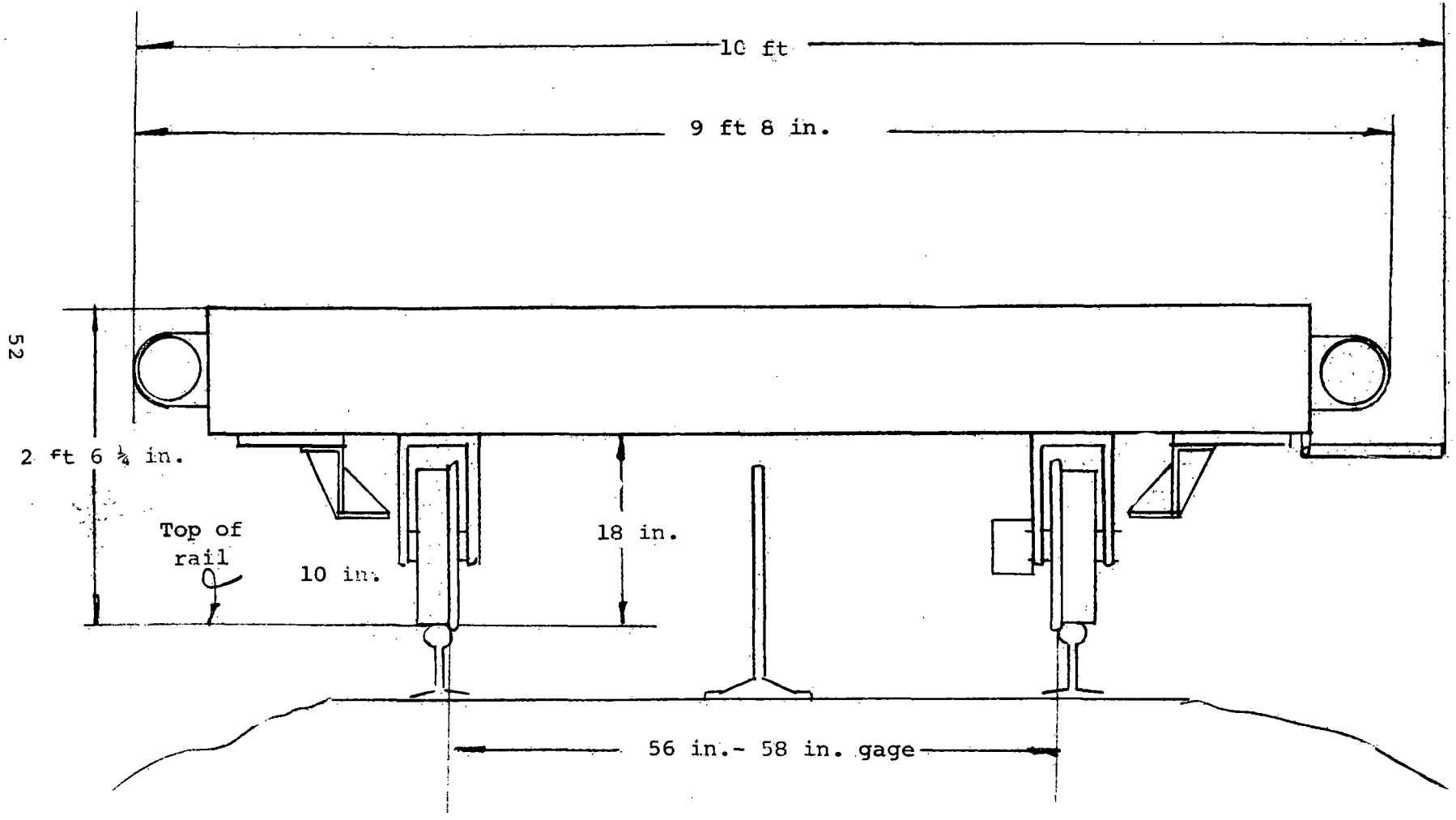

Figure 4-1. Transfer Vehicle Cross Section

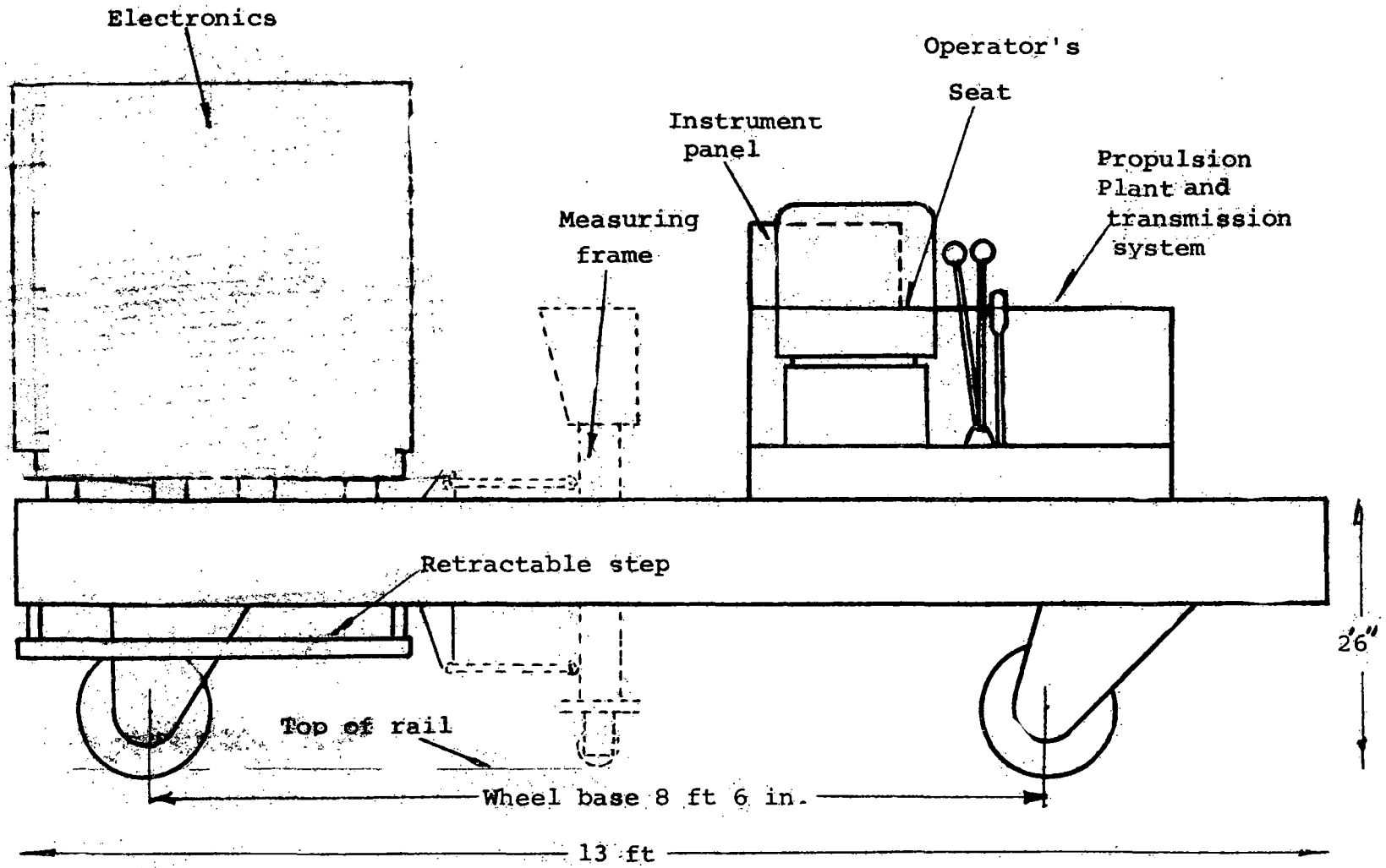

Figure 4-2. Side View of the Transfer Vehicle

Figure 4-2 also indicates the position of the DAS and control panel cabinets by the dotted lines as well as the location of the propulsion plant of the transfer vehicle.

The propulsion plant is a four cylinder 55 HP Willys engine. The transmission is a standard four-speed forward and reverse unit which provided the directional control. The transfer vehicle has a mechanical braking system which consists of a belt and 18 in. diameter drum mounted on the transmission shaft.

The hydraulic system used to raise and lower the measuring frame is also mounted on the transfer vehicle. The vehicle is designed for a crew of two; the driver of the transfer vehicle and the operator of the measurement system. The vehicle is provided with white and red traveling lights at each end for identifying direction of travel and a search light. Two photographs of the transfer vehicle are given in Figure 4-3.

4.2 Laser Support Vehicle

The laser support vehicle is a Nolan Co. "Track Dolly" which has been modified to clear the LIM reaction rail. This vehicle has three wheels. Lateral guidance is provided by the two double flanged wheels which ride on the master rail. The third wheel is unflanged. The vehicle is manually operated, has a friction braking system and a rail locking device. A center mast has been mounted on the vehicle to support the laser transmitter and a telescope. The laser transmitter is a Hughes Model 3076 HP with a 3m watt power output at 6328 Å wavelength. A collimator was added at the laser output. The collimator consusts of one divergent lens on the laser side, having a focal length of -12 mm and a diameter of 10 mm followed by a convergent lens having a focal length of 122 mm and a diameter of 24 mm. The collimator transforms the original laser beam of 1.2 mm into a 12 mm diameter beam at distances up to 200 ft.

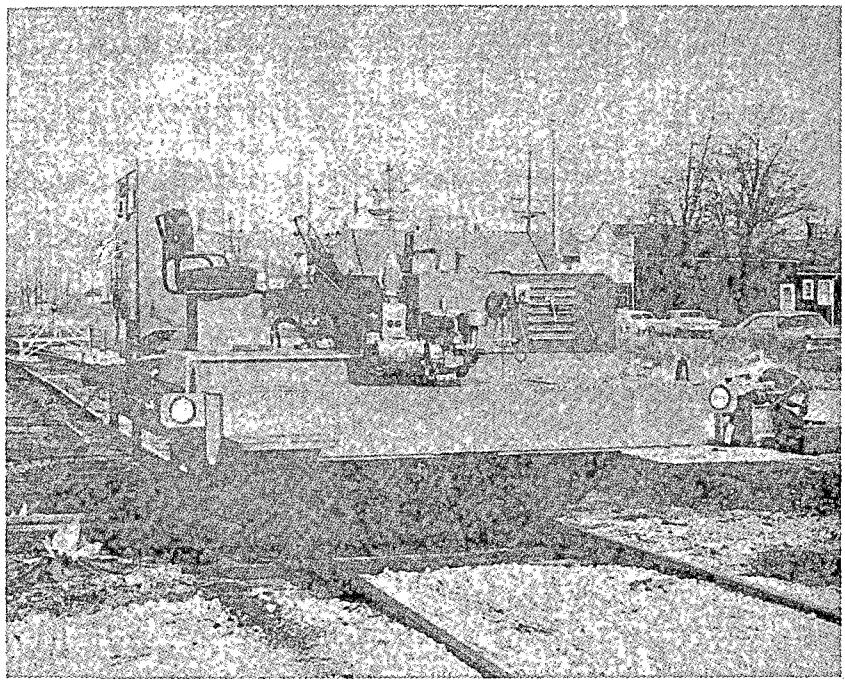

Rear View

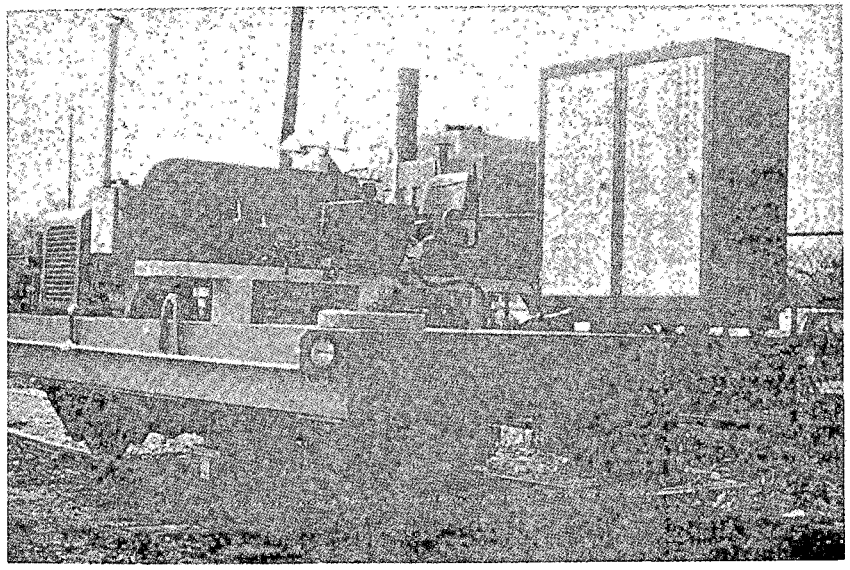

Front View

Figure 4-3. Transfer Vehicle

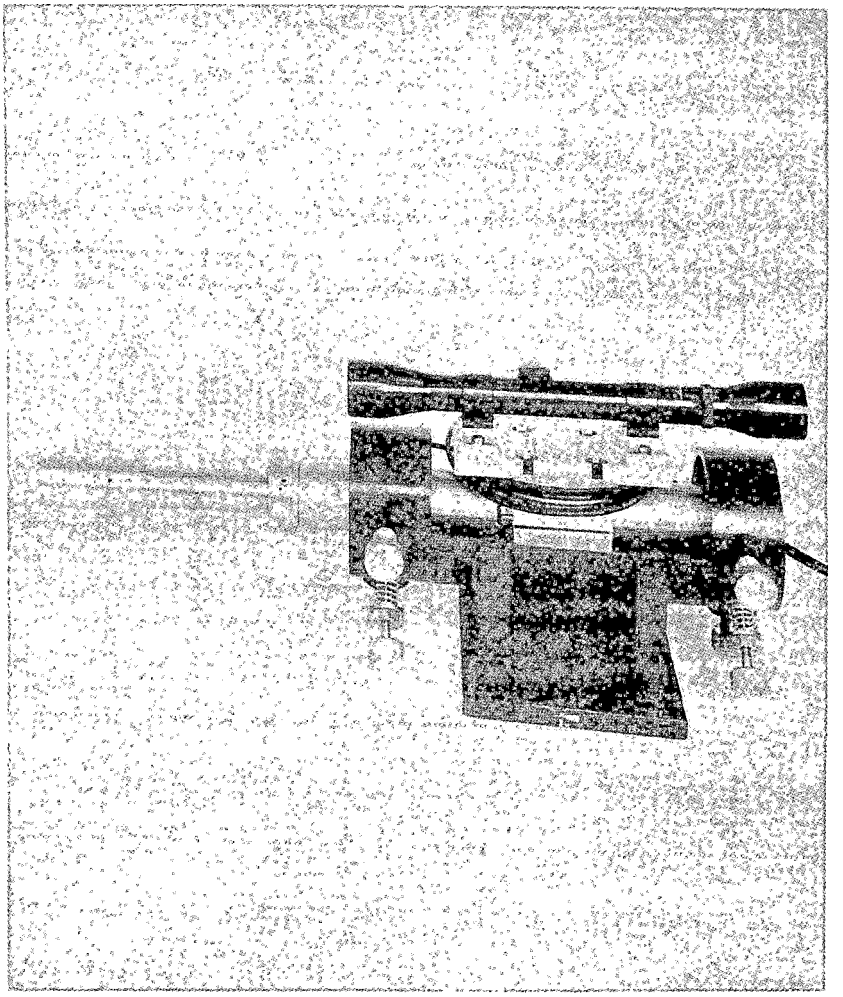

Figure 4-4. View of the Laser System

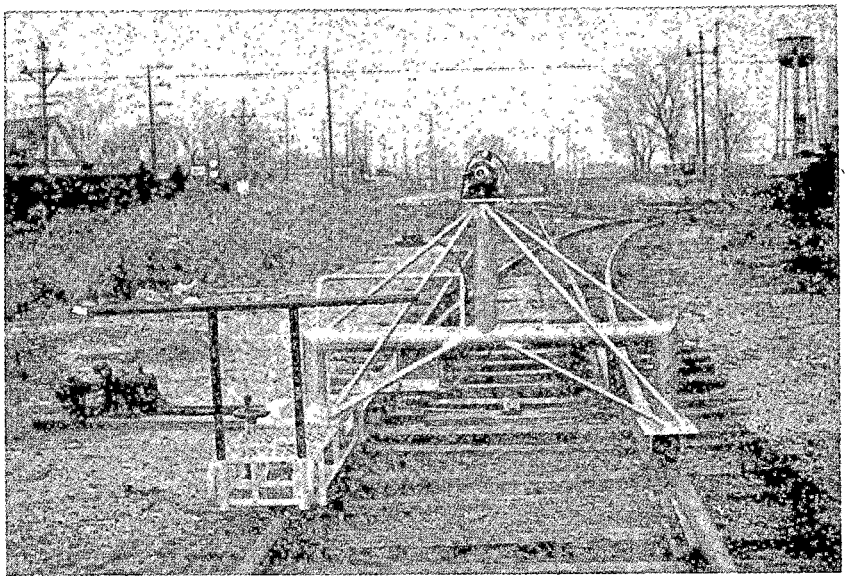

Figure 4-5. Laser Support Vehicle

A 3X telescopic sight boresighted with the laser beam is provided to assist in aiming the laser beam toward the laser tracker.

Figure 4-4 shows the components of the laser beam transmitter. As shown, the telescopic sight is rigidly attached to the support of the laser transmitter. The final aiming of the laser beam in both vertical and horizontal plane is produced by means of the adjusting screws shown in Figure 4-4. The laser transmitter power supply is powered by a 12 volt battery housed on a receptacle of the vehicle.

A photograph of the laser vehicle is shown in Figuer 4-5.

5. CALIBRATION AND VALIDATION PROGRAM

The entire measuring system including the measuring frame were designed and constructed at the GASL facilities in Westbury, New York. The transfer vehicle was built by the Whiting Corporation located in Harvey, Illinois. A series of factory acceptance tests of the measuring system components were conducted at GASL. At the completion of the GASL components factory acceptance tests, these components were shipped to Harvey, Illinois. The initial assembly of the TGSD was performed at the Whiting Corp. facilities where subsequently factory acceptance of the complete system was performed. Upon completion of the factory acceptance test of the complete system, the TGSD was shipped to Reading, Pennsylvania, for the validation testing program and finally the TGSD was shipped to Pueblo, Colorado, for the demonstration, testing program and initial LIM track survey.

5.1 GASL Factory Acceptance Test

The factory acceptance tests conducted at GASL included the calibration of the measurement system components as well as a presentation of the analysis of the overall performance of the TGSD. This study is presented in the form of an error analysis which is included in Appendix III.

The GASL factory acceptance tests were conducted on the following components:

Laser System
Electronic Level
Mechanical Sensors

5.1.1 Laser System. The laser system calibration was conducted with the laser source positioned 10 feet away from the laser tracker which was rigidly clamped to the bed of a precision milling machine. The laser tracker was connected to the DAS thus permitting the end-to-end system check. The milling machine bed, which was used to simulate the motion of the transfer vehicle, was moved to five different positions in the vertical and horizontal direction as shown in Figure 5-1. The

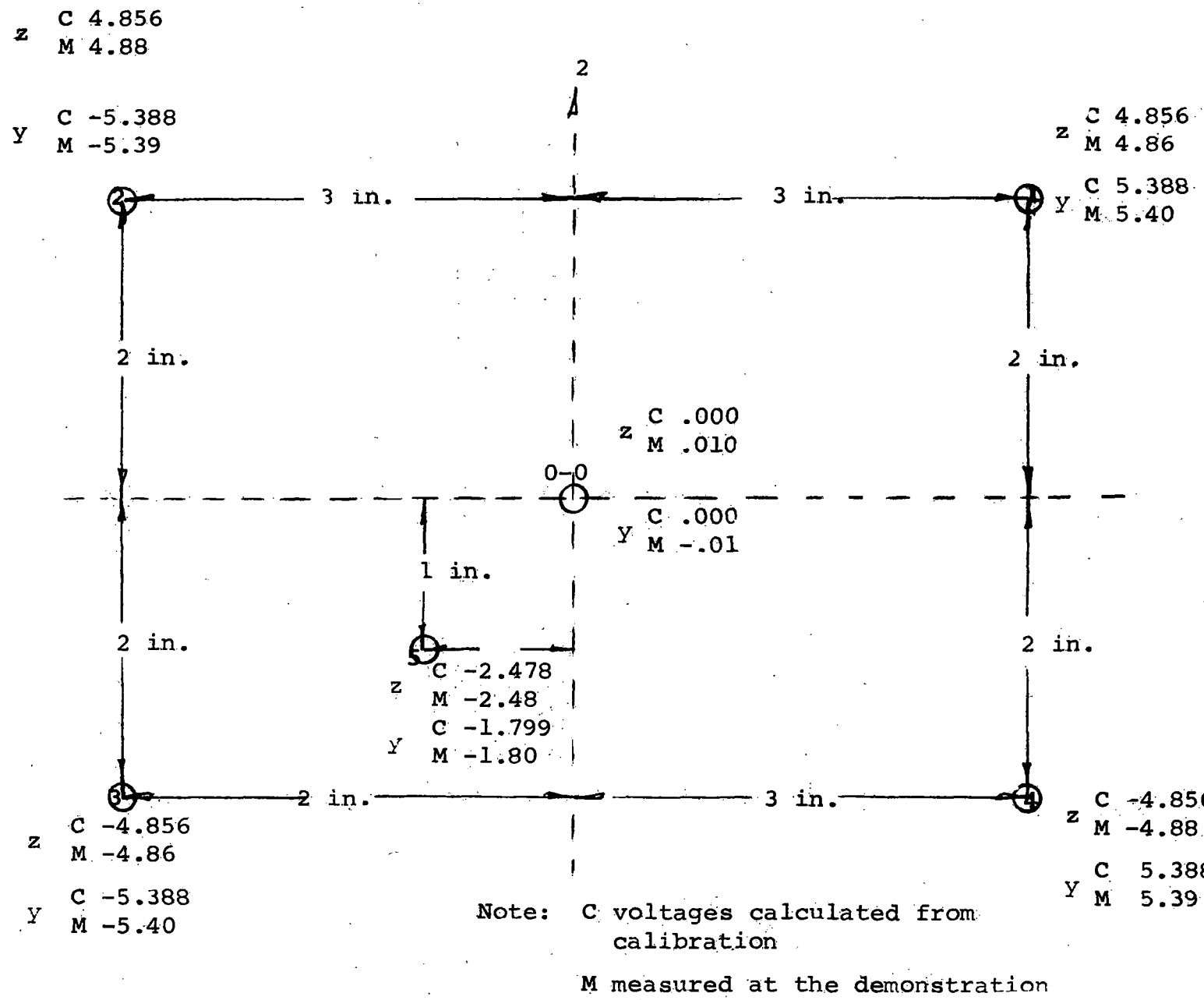

Figure 5-1. Factory Acceptance Test of Laser Tracker

circled point (0-0) represents the zero location of the instrument and all other measurements are referred to this origin.

The result of the measurements were part of the more comprehensive calibration procedure discussed previously in Section 3.2. The overall error in the entire range covered by Figure 5-1 is approximately .012 inches from the calibration curve.

The GASL factory acceptance test of the laser tracker was conducted with the laser source located 170 feet away from the laser tracker which was again connected to the DAS. The laser source was held stationary and the random motions of the laser beam due to scintillation was monitored at approximately one minute duration intervals. A complete discussion of the effects of laser beam bending and scintillation previously performed by GASL is presented in Reference 1. In addition, a special series of tests on beam bending and beam scintillation used in the design of the present system, were conducted by GASL at the Keuffel and Esser plant at Whippany, New Jersey. These results are presented in Appendix II.

5.1.2 Electronic Level. The GASL factory acceptance tests for the electronic level, which constitutes the cross level sensor, was performed by mounting the level on a precision indexing head and by monitoring the output with the DAS. Three precision bubble levels permanently attached to the electronic level box provided reference angles of 0°, $+5^{\circ}$, and -2°. The electronic level was rotated to the null position for each bubble level and the value at the DAS display output was recorded and compared with the calibration curve. The measured data was within $\pm$ 20 arc seconds from the calibration curve.

5.1.3 Mechanical Sensors. The factory acceptance tests for the two mechanical sensors of the LIM reaction rail were performed by mounting the sensors with the transducers fully extended position against a rigid plane surface and the electric output was connected to the DAS. Then, two precision spacer blocks were inserted between the rigid plane and sensor head to simulate three measuring positions:

Position (inches)	Equivalent LIM Gage
0	29 1/2
1 1/2	28
3	26 1/2

The result of the measurements were found to be within .015 inches from the calibration curve.

The factory acceptance tests for the gage wheel sensor was performed by mounting the gage wheel against a rigid surface with the transducer output connected to the DAS. By inserting the precision spacer blocks between the reference surface and the gage wheel, measurements were taken at positions which simulated rail gage of 56 in., 56 1/2 in. and 57 in. The results of those measurements were found to be within .006 from the calibration curve.

The factory acceptance tests of the bench marker sensors was performed by mounting the bench marker sensors against blocks simulating the bench markers and the output was connected to the DAS. The two transducers were moved to three calibrated positions over a total range of two inches. The voltages from the display of the DAS were recorded for each position. The results of these measurements were .006 from the calibration.

5.2 Whiting Factory Acceptance Test

The factory acceptance of the complete TGSD, performed at Whiting Corp. in Harvey, Illinois, was divided into two parts:

1) Operational Test of the Transfer Vehicle

2) Functional Test of Track Geometry Measuring System and DAS

5.2.1 Operational Test. The operational test of the transfer vehicle included both stationary and operating checks. The transfer vehicle was placed on a section of track and its geometric dimensions, controls,propulsion, braking and hydraulic controls were checked and were found to be acceptable. The operating checks were performed with the transfer vehicle running

over a 150 ft section of track and vehicle controls were checked at low speed and found to be acceptable.

5.2.2 Functional Test. The functional test of the TGSD at Whiting Corp. included:

- Stationary check and range of all sensors.
- Operating demonstration of DAS.
- Demonstration of laser system.

Satisfactory performance was demonstrated for all these tests.

5.3 Validation Test at Reading Facility

The purpose of these tests was to validate the accuracy of the TGSD. These validation tests were conducted on a specially prepared track inside the Reading Freight Car shop at Reading, Pennsylvania. The portion of the track used was 760 feet long and reference points along this track were surveyed using first order techniques. The results of the measurements obtained with the TGSD were compared against these measured reference points.

Eleven bench markers were located along the track at 76 feet intervals, as shown in Figure 5-2. A sketch of the track arrangement is given in Figure 5-3. As shown, the rails were embedded in concrete. Therefore, in order to simulate the tie counter, studs were inserted in the pavement as shown. The distance between studs was 19 in. which corresponds to the distance between ties.

The validation program included the demonstration of all mechanical and electrical functions of the TGSD. The program included:

- Demonstration of the TGSD
- Calibration of the Measuring System
- Determination of the TGSD Error
- Test Track Validation Survey

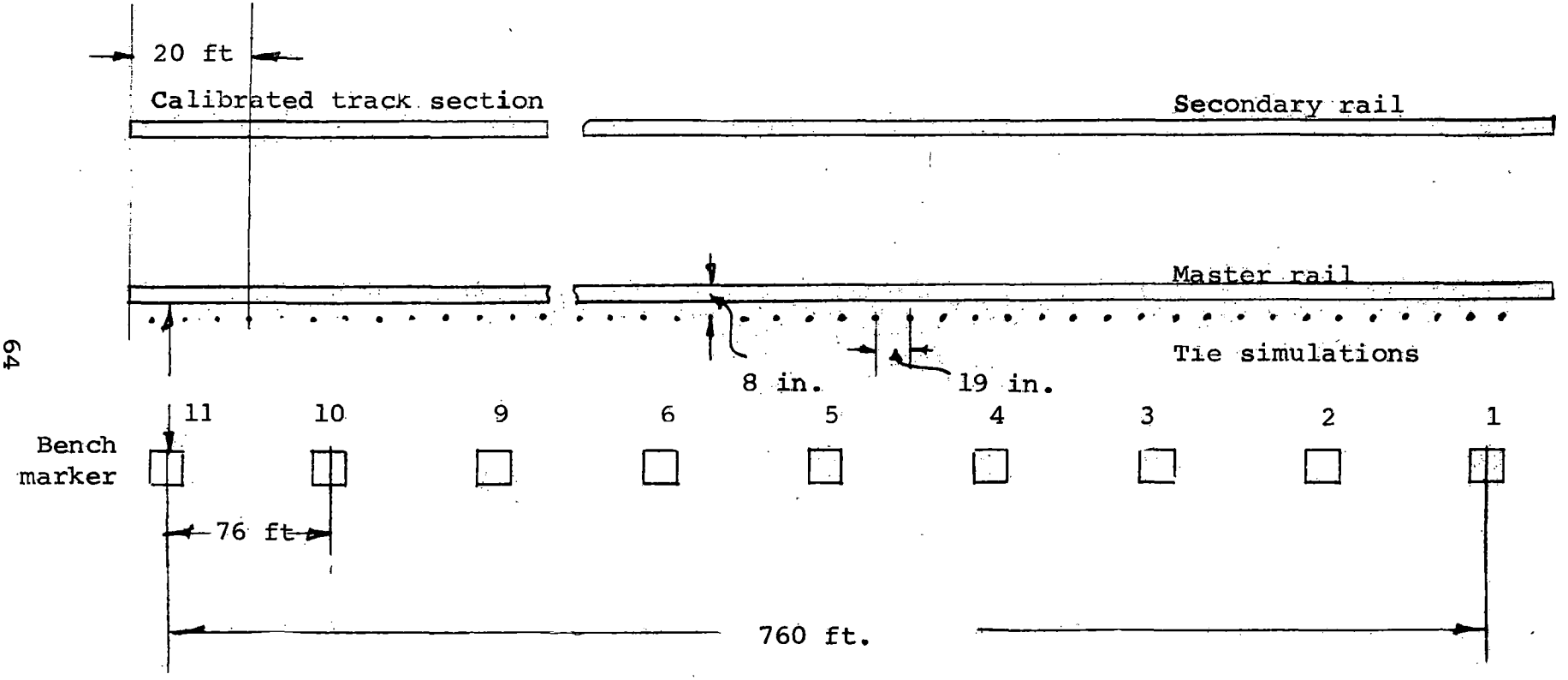

Figure 5-2. Reading Test Track

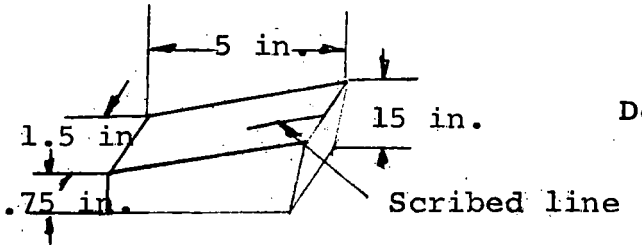

Detail of bench marker head

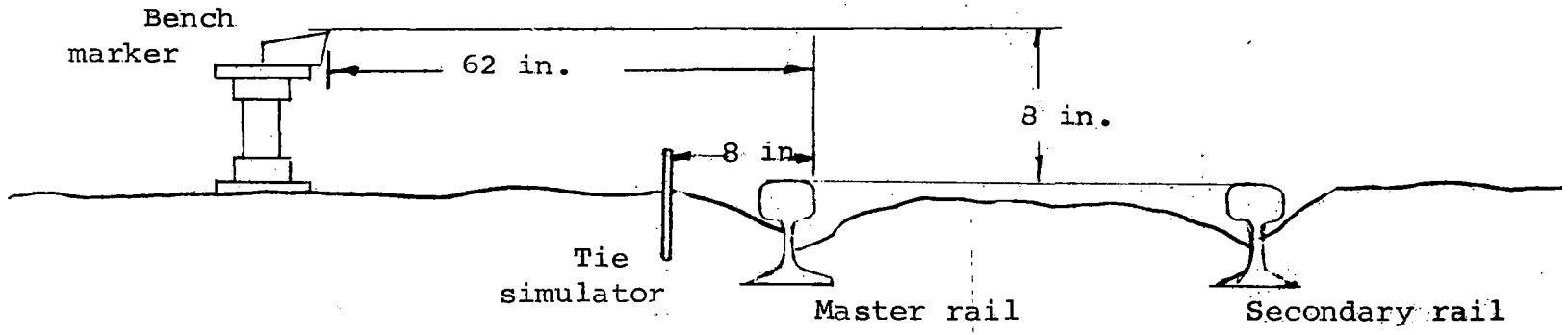

Figure 5-3. Reading Test Track Cross Section

The results of the validation program showed that the TGSD satisfied all of the requirements. The results of the validation program are presented in Tables 5.1, 5.2 and 5.3. The results presented in these tables were prepared by ENSCO, Inc. for F.R.A. using the data provided by the magnetic tapes of the TGSD. Table 5.1 shows the laser beam scintillation test. Table 5.2 shows the accuracy check of the measurement of gage, cross level, alignment and profile. The repeatability check data are presented in Table 5.3. On Table 5.3,one observes that the results of the repeatability tests are well within the range of the proposes specification.

The track loading test performed at the Reading facility showed no effect on the recorded data due to the proximity of the transfer vehicle to the laser support vehicle up to a minimum separation distance of 10 feet.

5.4 Demonstration and Operation of the TGSD at the DOT Test Site in Pueblo, Colorado

Upon completion of the validation tests at Reading, Pennsylvania, the TGSD was shipped to the Department of Transportation Test Site at Pueblo, Colorado. The DOT Test Site activity included the following:

a) Demonstration of the TGSD under actual operating conditions.

b) Initial survey of the LIM test track.

c) Training DOT personnel on proper use of the TGSD.

5.4.1 Demonstration Program and Survey of the Test Track. The demonstration program conducted at Pueblo, Colorado, included various functions of the TGSD which could not be performed at the two previous sites.

TABLE 5-1

LASER BEAM SCINTILLATION TEST

READING, PENNSYLVANIA

JUNE 9, 1972

Range	Peak to Peak Deviation Δy	Δz
25 ft	<.01 V; .006 in.	< .01 V; .004 in.
40 ft	<.01 V; .006 in.	.02 V; .008 in.
64 ft	<.01 V; .006 in.	< .01 V; .008 in.
100 ft	<.01 V; .006 in.	.02 V; .008 in.
160 ft	.03 V; .018 in.	.04 V; .016 in.

TABLE 5-2

ACCURACY CHECK

	TSD Contract Specifications	Surveyor Error	Test Results		
			20' Calibrated Area		760' Test Track
Gage g	± .031"	± .02"	± .05"		± .08"
Crosslevel θ	± .031	± .01	± .025"		± .025"
			Master Rail	Secondary Rail	
Alignment $\bar{y}$	± .016"	± .02"	± .015"		
Profile $\bar{z}$	± .016"	± .01"	± .01"		

TABLE 5-3

REPEATABILITY CHECK

		GASL Proposed Specifications	Test Results	
			Repeatability Tests*	Survey Runs**
Gage	g	± .005"	± .001"	± .02 90% of Data
Crosslevel	θ	± .0055"	± .005	± .01 (Resolution of System)
Tracker	$\hat{y}$	± .013"	± .006	xx
Tracker	$\hat{z}$	± .015"	± .004	xx
Benchmark	Y	± .005"	xx	± .003
Benchmark	Z	± .005"	xx	± .003
Alignment	$\bar{y}$	± .022"	± .02	xx
Profile	$\bar{z}$	± .024"	± .01	xx

* Repeatability test consisted of 10 runs over the 20-ft calibration area with minimum laser operating distance.

** Survey runs consist of data from 152-ft sequences over the entire 760-ft track.

Since no bench markers were available at the LIM test track at Pueblo, Colorado, the TGSD was operated in Mode II using overlapping measurements, or in Mode III, measuring only gages and cross-level.

The functions demonstrated included the following:

a) Transfer vehicle maximum speed

b) Production rate

c) LIM reaction rail gage measurement

d) Odometer operation

e) Tie counter operation

f) Track loading tests under actual test site conditions

g) Laser beam scintillation effects under actual site conditions

a) Transfer Vehicle Maximum Speed - The maximum speed of the transfer vehicle with the measuring frame in the retracted position was determined over the tangent section of the test track on an uphill 1% slope. The maximum recorded TV speed fully loaded with ballast was approximately 18 mph.

b) Production Rate - The production rate was estbalished from a single uphill pass of the entire length of the available test track (approximately 6.2 mi.) including both tangent and curved sections under Mode II operation. This production rate was approximately 1.5 mph.

c) LIM Reaction Rail Gage Measurement - The LIM reaction rail gage sensor box was installed and the nominal zero of the two transducers was set with the calibration jig. The LIM rail gage sensors were then operated and fully demonstrated.

d) Odometer Operation - The distance measured with the odometer, checked on the tangent portion of the test track was found to be within .06% of the independently measured track length. This value is well within the specified accuracy of .1%.

e) Tie Counter - The tie counter which is used to trigger the data acquisition system operated satisfactorily over the entire length of the test track which included approximately 22,000 bolts.

f) Track Loading Test - The measurement of the track loading effects were repeated using the same technique used at the Reading Test Site. No effect was detected up to a minimum separation distance of 10 feet between laser support vehicle and transfer vehicle.

g) Laser Beam Scintillation Effects - The laser beam scintillation effects were measured at distances between the laser transmitter to the laser tracker from 25 feet to 250 feet. The results of these measurements show that the maximum operating range should not exceed 175 feet.

5.4.2 Initial Survey of LIM Test Track. Finally, the TGSD was used to perform the following initial surveys of the test track runs:

a) Mode II survey of the High Speed Test Section portion of the track from tie 1708+30 to 1748+50, corresponding to a distance of approximately 4000 ft.

b) Mode II survey of the entire LIM test track.

c) Mode III survey of the entire test track.

Typical results obtained by processing the measured data for Mode II and Mode III operation are presented in Figure 5-4.

INPUT DATA TAPE 1611

8 3 72 PUEBLO

MO	DY	YR	RUN	SEQ	TIE	INCH	CHAN 1 g	CHAN 2 g_1	CHAN 3 g_2	CHAN 4 y	CHAN 5 z	CHAN 6 θ	CHAN 7 $-V_R$	CHAN 8 $+V_R$
			NOFREC=			1								
08	03	72	001	001	001	0015	56.660	27.726	27.897	33.694	51.700	.144	-996	995
08	03	72	001	001	002	0034	56.654	27.706	27.892	33.694	51.700	.145	-996	995
08	03	72	001	001	003	0055	56.644	27.701	27.900	33.694	51.700	.146	-996	995
08	03	72	001	001	004	0074	56.640	27.698	27.900	33.694	51.700	.146	-996	996
08	03	72	001	001	005	0094	56.641	27.691	27.895	33.694	51.700	.146	-996	996
08	03	72	001	001	006	0112	56.654	27.683	27.882	33.694	51.700	.146	-996	996
08	03	72	001	001	007	0134	56.612	27.721	27.922	33.694	51.700	.146	-996	996
08	03	72	001	001	008	0153	56.613	27.718	27.915	33.694	51.700	.146	-996	996
08	03	72	001	001	009	0173	56.616	27.708	27.897	33.694	51.700	.146	-996	996
08	03	72	001	001	010	0192	56.635	27.678	27.865	33.694	51.700	.144	-996	995
			NOFREC=			2								
08	03	72	001	001	011	0211	56.641	27.668	27.845	33.694	51.700	.146	-996	995
08	03	72	001	001	012	0230	56.642	27.663	27.845	33.694	51.700	.146	-996	996
08	03	72	001	001	013	0250	56.641	27.673	27.845	33.694	51.700	.147	-996	996
08	03	72	001	001	014	0272	56.653	27.686	27.855	33.694	51.700	.146	-996	995
08	03	72	001	001	015	0290	56.682	27.696	27.867	33.694	51.700	.146	-996	996
08	03	72	001	001	016	0310	56.688	27.728	27.905	33.694	51.700	.147	-996	996
08	03	72	001	001	017	0330	56.701	27.723	27.902	33.694	51.700	.146	-996	996
08	03	72	001	001	018	0349	56.734	27.701	27.880	33.694	51.700	.146	-996	996
08	03	72	001	001	019	0368	56.776	27.666	27.852	33.694	51.700	.145	-996	996
08	03	72	001	001	020	0388	56.799	27.638	27.830	33.694	51.700	.146	-996	995
			NOFREC=			3								
08	03	72	001	001	021	0407	56.799	27.631	27.820	33.694	51.700	.147	-996	995
08	03	72	001	001	022	0426	56.778	27.641	27.817	33.694	51.700	.146	-996	996
08	03	72	001	001	023	0444	56.770	27.651	27.827	33.694	51.700	.145	-996	996
08	03	72	001	001	024	0466	56.772	27.678	27.865	33.694	51.700	.146	-996	996
08	03	72	001	001	025	0484	56.763	27.721	27.902	33.694	51.700	.146	-996	996
08	03	72	001	001	026	0503	56.729	27.741	27.915	33.694	51.700	.145	-996	995
08	03	72	001	001	027	0523	56.718	27.773	27.935	33.694	51.700	.146	-996	995
08	03	72	001	001	028	0542	56.745	27.773	27.922	33.694	51.700	.145	-996	996
08	03	72	001	001	029	0562	56.770	27.773	27.910	33.694	51.700	.146	-996	996
08	03	72	001	001	030	0582	56.770	27.773	27.892	33.694	51.700	.147	-996	996
			NOFREC=			4								
08	03	72	001	001	031	0601	56.745	27.798	27.917	33.694	51.700	.146	-996	996
08	03	72	001	001	032	0621	56.720	27.803	27.927	33.694	51.700	.144	-996	996
08	03	72	001	001	033	0640	56.730	27.820	27.955	33.694	51.700	.145	-996	995
08	03	72	001	001	034	0659	56.730	27.838	27.975	33.694	51.700	.147	-996	995
08	03	72	001	001	035	0679	56.748	27.833	27.970	33.694	51.700	.146	-996	996
08	03	72	001	001	036	0699	56.750	27.835	27.957	33.694	51.700	.146	-996	995
08	03	72	001	001	037	0719	56.760	27.835	27.940	33.694	51.700	.146	-996	996
08	03	72	001	001	038	0738	56.744	27.838	27.932	33.694	51.700	.147	-996	996
08	03	72	001	001	039	0757	56.748	27.833	27.925	33.694	51.700	.146	-996	995
08	03	72	001	001	040	0776	56.751	27.833	27.925	33.694	51.700	.147	-996	996
			NOFREC=			5								

Figure 5-4. Typical Printout of a Track Measurement

5.4.3 Personnel Training. The final activity performed by GASL was the training of DOT personnel on the proper use of the TGSD. A series of lectures were given to the trainees to instruct them on the principle of operation of the TGSD. Finally, the trainees were instructed in the operation and maintenance of the TGSD including actual operational time during track measuring.

APPENDIX I

DEFORMATION OF THE TRACK UNDER LOAD AND INFLUENCE OF THE PROFILE MEASUREMENT

The present method of track surveying requires that the laser beam does not move during the measurement run, as the Transfer Vehicle (TV) approaches the Laser Support Vehicle (LSV) clamped to the rails. In practice this ideal condition can be relaxed as long as the displacement of the laser beam generates a displacement of the intercept point on the TV tracker that remains within the allowed error of the measurements. The laser beam moves because of the deformation of the track due to the presence of the transfer vehicle.

The track, which is equivalent to a long elastic beam of uniform cross section and elastic properties, receives a concentrated load at the axles of the vehicle and a distributed load over several ties along the track due to the ground reaction. The actual profile of the deformed track is determined by the following conditions of equilibrium of the track-ground system:

1) The reaction of the ground on each tie and the penetration of the tie into the ground satisfy some force-penetration law (that can be determined experimentally) characteristic of the tie-ground interaction.

2) The sum of the vertical ground reactions on <u>all</u> the ties balances the total weight of the track plus the vehicle.

An intuitive description of the phenomenon is the following:

Consider first a track initially horizontal (unloaded) and a 1-axle load applied on it, Figure I-1. Upon application of the load, the ties near the load point will penetrate a little more into the ground and receive a stronger reaction from it. However, a distributed bending moment appears now on the rails which generates a positive curvature (center of curvature above the track) and is symmetric with respect to the loading point. The penetration of the ties into the ground becomes therefore smaller and smaller, and, at some distance on each side of the axle, two symmetric points exist where the penetration is zero (first node).

At these node points the rail's slope is not horizontal but turned upward (in the direction away from the axle point); the effect of this is to lift the following part of the track further away above the unloaded position. As a consequence the track's own weight (with or without the reaction of the ground) tends to bend back the rails toward and beyond the horizontal direction. The curvature changes sign and a second pair of points is reached (2nd node) where the track is again at the initial level and its slope is turned downward, and so on.

A wavy curve is generated which is symmetric with respect to the load point and has a maximum (absolute value) deviation from the initial position at each peak that decreases rapidly with the distance from the load point. Each peak appears, naturally, between two consecutive nodes and the deviation occurs alternatively upward and downward with respect to the initial unloaded position. The distance between two consecutive nodes is constant in the case of 1-node load, but not constant

for a general load configuration. However, at a great distance from the vehicle, the deformation tends always to a sinusoid of constant wavelength and amplitude decaying exponentially.

If the load is applied with two axles the profile behavior changes substantially in the segment of track between the axles and near the load points, but far away from the vehicle it tends to the same profile generated by a 1-axle load applied to the mid point between the axles. If the ground force-penetration law for each tie is linear (Hook's law) the deformation is simply obtained by superposition of the two profiles.

A second important point is that, if the TV moves slowly the track deformed profile also moves following the TV at the same speed. As a consequence a segment of the rail fixed, say, to a particular tie will move and turn in the vertical plane as shown by the fixed TV configuration at the same changing distance from the loading point.

The laser source clamped at that particular segment of rail will perform the same displacement z and rotation $\frac{dz}{dx}$.

The displacement of the laser beam intercept point with the tracker plane on the TV results from the following terms:

1)	displacement of the measuring frame	$z(o)$
2)	displacement of the LV	$z(x)$
3)	displacement due to rotation of the laser beam	$-x \frac{dz}{dx}$

Thus, the total displacement of the intercept point $\Delta\bar{z}$ becomes

$$\Delta\bar{z} = z - z_o - x\frac{dz}{dz}$$

During the measurement, the quantity z_o remains constant (assuming uniform ground elastic modulus) and the amount of deviation $\bar{z}$ that changes with the distance z is given by

$$\bar{z} = z - x \frac{dz}{dz}$$

One must determine the minimum distance x_{min} such as for $x > x_{min}$ is $\bar{z} < \Delta\bar{z}_{all}$ where $\Delta\bar{z}_{all}$ is much smaller than the allowable error (say .003 inches which is 20% of the allowable error).

The problem can be solved by reducing it to the classic one of a continuous beam over elastic foundation with uniform beam cross-section, elastic properties and ground elastic modulus (References I-1 and I-2).*

The basic problem considers <u>one</u> concentrated load only; however, due to its linearity, the more general case of two or more loads can be obtained by super-position. Obviously the two rails are considered as two beams in parallel and the load equally subdivided between them.

The basic differential equation governing the vertical displacement z at the distance x from the load point is

$$\frac{d^4 z}{dx^4} + \frac{k}{EI} z = 0$$

with k/EI constant (the parameters k, E and I are defined below).

The most general solution is given by the sum of four terms involving four basic functions, ψ_1, ψ_2, ψ_3, ψ_4, and four constants, A_1, A_2, A_3, A_4, determined from the boundary conditions.

*I-1: Timoshenko, S. and Woinosky-Krieger, S., <u>Theory of Plates and Shells</u>, McGraw Hill Book Co., 2nd Ed., 1959.

I-2: Faupel, J. H., Engineering Design, John Wiley & Sons, 1964, p. 192.

$$x = A_1\psi_1(\beta x) + A_2\psi_2(\beta x) + A_3\psi_3(\beta x) + A_4\psi_4(\beta x)$$

where

$$\psi_1 = e^{\beta x}\cos \beta x$$

$$\psi_2 = e^{\beta x}\sin \beta x$$

$$\psi_3 = e^{-\beta x}\cos \beta x$$

$$\psi_4 = e^{-\beta x}\sin \beta x$$

The parameter β is given by

$$\beta = \sqrt[4]{\frac{k}{4EI}}$$

where

k is the foundation stiffness, namely the vertical distributed load [lb/in.] which generates a vertical displacement of 1 in.; k is measured in $lb/in.^2$

I is the moment of inertia of the rail's pair ($in.^4$) around the horizontal axis of inertia, and

E the modulus of Young of the rail material ($lb/in.^2$).

The parameter β has the dimension in^{-1}. $1/\beta = x^*$ is a characteristic length of the deformation and $2\pi/\beta$ is the wavelength of the deformation profile. z decays exponentially with the distance x.

The characteristic length x* can be expressed as a function of the rail height h:

$$x^* = h \sqrt[4]{\frac{E}{k} \left(\frac{I}{h^4}\right)}$$

It is interesting that the ratio $(I/h)^4$ does not change if a family of rails of different weight is considered in which the contours of each cross-section are similar. For the cases of interest, in which the load can be represented by a sequence of forces F_n, applied at points x_n of the track (measured from some origin fixed with the vehicle), the displacement z, the slope dz/dx, the bending moment M and the shear force Q are obtained by superposition of the one-force F_n values.

Only 4 basic functions φ_1, φ_2, φ_3, φ_4, are involved in the calculation, namely

$$\varphi_1 = e^{-\beta x} (\sin \beta x + \cos \beta x) = \sqrt{2}\, e^{-\beta x} \sin\left(\beta x + \frac{\pi}{4}\right)$$

$$\varphi_2 = e^{-\beta x} (\cos \beta x - \sin \beta x) = \sqrt{2}\, e^{-\beta x} \cos\left(\beta x + \frac{\pi}{4}\right)$$

$$\varphi_3 = e^{-\beta x} \cos \beta x$$

$$\varphi_4 = e^{-\beta x} \sin \beta x$$

The resulting values of z, dz/dx, M and Q are

$$z = \frac{1}{8\beta^3 EI} \sum_{1}^{n} F_n \, \varphi_1[\beta(x-x_n)]$$

$$\frac{dz}{dx} = -\frac{1}{4\beta^2 EI} \sum_{1}^{n} F_n \, \varphi_4[\beta(x-x_n)]$$

$$M = \frac{1}{4\beta} \sum_{1}^{n} F_n \, \varphi_2[\beta(x-x_n)]$$

$$Q = -\frac{F}{2} \sum_{1}^{n} F_n \, \varphi_3[\beta(x-x_n)]$$

In the case of a concentrated load F, applied at z = 0 of a beam of infinite length, the displacement z, the bending moment M and the shear force Q are given by

$$z = \frac{F \, \varphi_1(\beta x)}{8\beta^3 EI} \qquad M = \frac{F \, \varphi_2(\beta x)}{4\beta} \qquad Q = -\frac{F \, \varphi_3(\beta x)}{2}$$

which can be written again as

$$\frac{z}{z^*} = \varphi_1\left(\frac{x}{x^*}\right) \qquad \frac{M}{M^*} = \varphi_2\left(\frac{x}{x^*}\right) \qquad \frac{Q}{Q^*} = \varphi_3\left(\frac{x}{x^*}\right)$$

where

$$z^* = \frac{F}{8\beta^3 EI} \qquad M^* = \frac{F}{4\beta} \qquad Q^* = -\frac{F}{2}$$

The slope dz/dx becomes

$$\frac{dz}{dx} = \frac{z^*}{x^*}(\varphi_2 - \varphi_1) = -\frac{z^*}{x^*}\, 2\varphi_4 \left(\frac{x}{x^*}\right)$$

and the displacement $\bar{z}$ of the intercept point at $x = 0$ becomes:

$$\frac{\bar{z}}{z^*} = \frac{z - x\frac{dz}{dx}}{z^*} = \varphi_1 - \frac{x}{x^*}(\varphi_2 - \varphi_1) = \varphi_1 + 2\,\frac{x}{x^*}\,\varphi_4 .$$

For the case of two concentrated loads $\frac{F}{2}$ applied at $x = -a$ and $x = +a$, one has

$$\frac{z}{z^*} = \frac{1}{2}\left[\varphi_1\left(\frac{x+a}{x^*}\right) + \varphi_1\left(\frac{x-a}{x^*}\right)\right]$$

$$\frac{M}{M^*} = \frac{1}{2}\left[\varphi_2\left(\frac{x+a}{x^*}\right) + \varphi_2\left(\frac{x-a}{x^*}\right)\right]$$

$$\frac{Q}{Q^*} = \frac{1}{2}\left[\varphi_3\left(\frac{x+a}{x^*}\right) + \varphi_3\left(\frac{x-a}{x^*}\right)\right]$$

$$\frac{\frac{dz}{dx}}{z^*/x^*} = \frac{1}{2}\left[\varphi_2\left(\frac{x+a}{x^*}\right) + \varphi_2\left(\frac{x-a}{x^*}\right)\right] - \frac{1}{2}\left[\varphi_1\left(\frac{x+a}{x^*}\right) + \varphi_1\left(\frac{x-a}{x^*}\right)\right]$$

$$\frac{\bar{z}}{z^*} = \frac{1}{2}\left(1 + \frac{x}{x^*}\right)\left[\varphi_1\left(\frac{x+a}{x^*}\right) + \varphi_1\left(\frac{x-a}{x^*}\right)\right] - \frac{1}{2}\,\frac{x}{x^*}\left[\varphi_2\left(\frac{x+a}{x^*}\right) + \varphi_2\left(\frac{x-a}{x^*}\right)\right]$$

In Figures I-2 and I-3 the curves of z and $\bar{z}$ are plotted for the following two cases of interest:

1) Track formed of 2 rails of 119 lb/yard, with $I = 65$ in.^{4}, $E = 30 \times 10^6$ psi and $K = 1000$ lb/in.^{2}. (This value is estimated assuming that a running load of 1200 lb/ft over the track provides a penetration of the ties into the ground of .1 in.) A concentrated load of 25,000 lb is considered over 1 axle only.

2) Same track and ground properties with two 12,500 lb forces on each axle and 7.5 ft distance between axles.

The characteristic length x* becomes

$$x^* = \frac{1}{\beta} = 60 \text{ in.}$$

and, since the rail's height is 6 in., the ratio x*/h becomes

$$x^*/h = 10.$$

This ratio is only slightly affected by the change of ground stiffness k, due to the exponent 1/4 in the expression defining β, and as said before, does not change with the rail weight as long as the cross-section of the rail remains similar to the present one.

Figures I-2 and I-3 show that for both configurations, if the allowed displacement is z = .003 in., the minimum distance x_{min} is about 30 ft. Substantially higher displacements are shown at distances of the order of 20-25 ft. where the term -xdt/dx due to the laser beam rotation is substantially more important than the one due to the track deformation z itself.

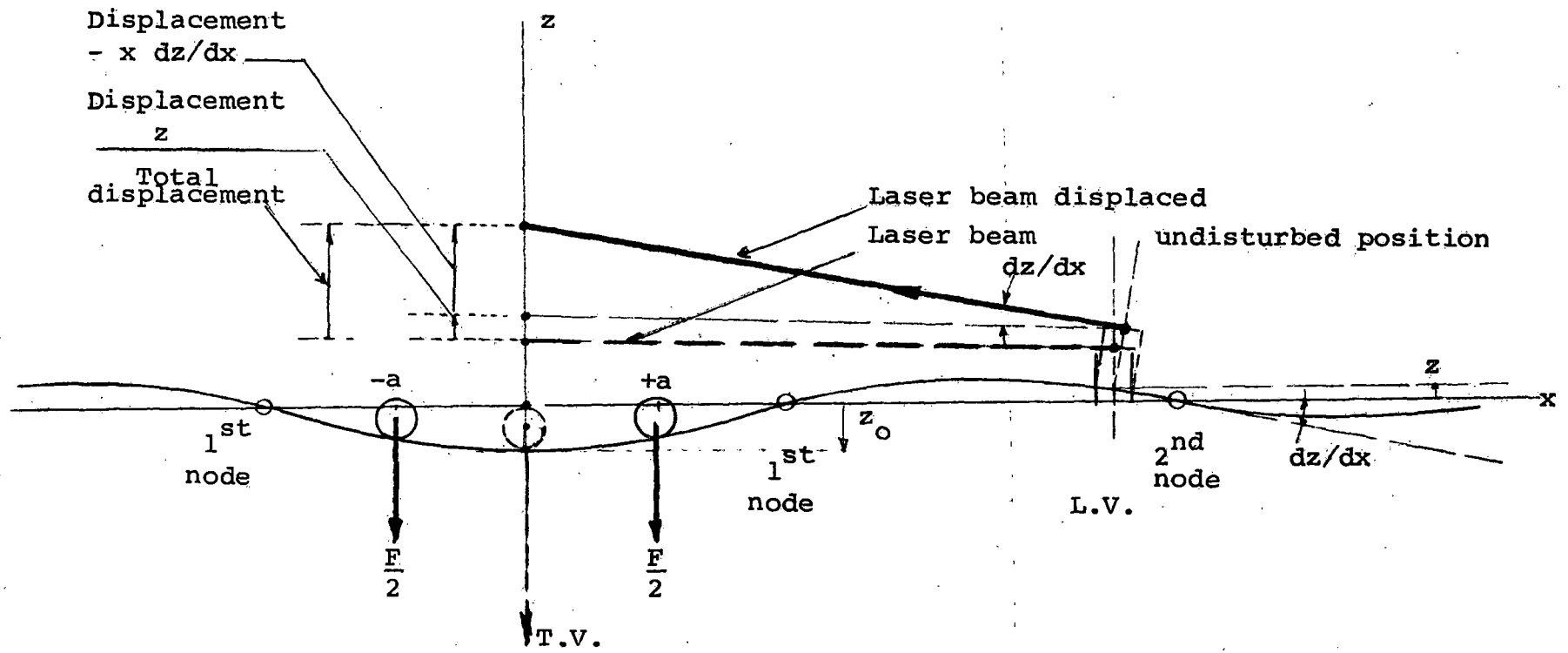

Figure I-1. Rail Track Profile and Laser Beam Displacement Due to T.V. Load

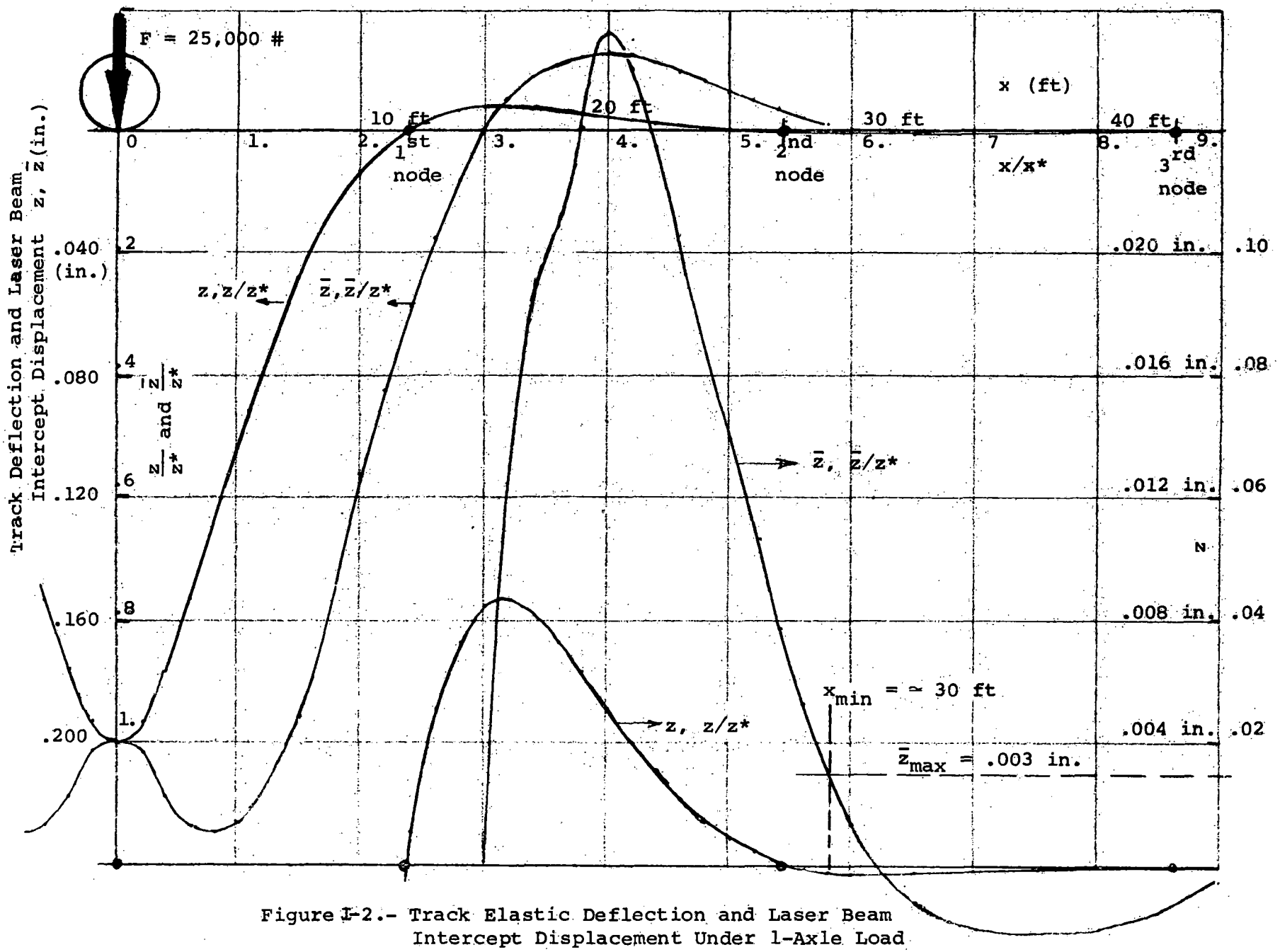

Figure I-2.- Track Elastic Deflection and Laser Beam Intercept Displacement Under 1-Axle Load

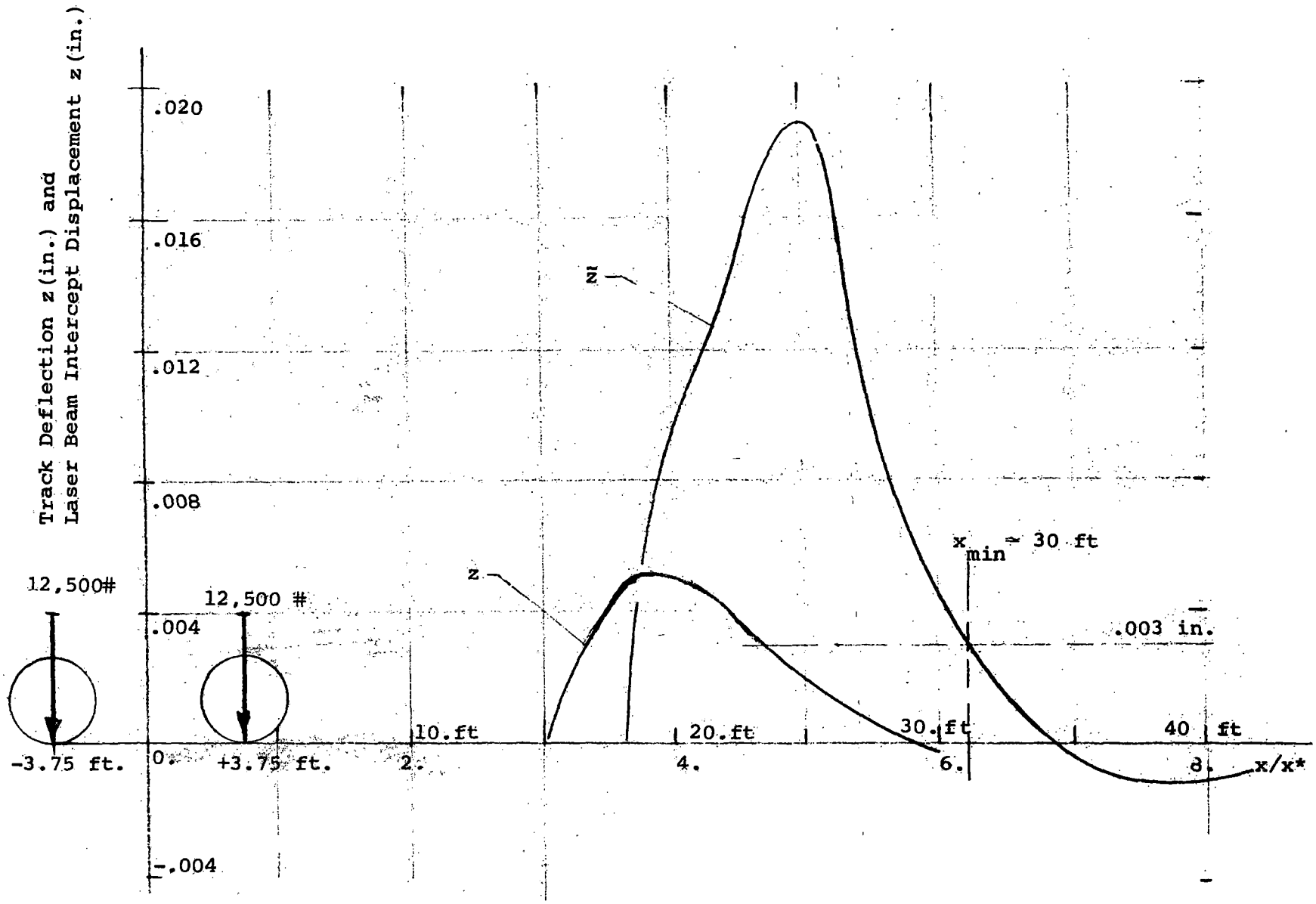

Figure I-3. Track Deflection and Laser Beam Intercept Displacement Under 2-Axle Load.

APPENDIX II

EXPERIMENTAL DETERMINATION OF LASER BEAM FLUCTUATIONS

The position of the laser beam reference with respect to the track under measurement was selected considering the following effects:

- Errors on the determination of alignment and profile for both rails as a result of the trigonometric transformation
- Beam bending due to thermal gradients along the vertical direction
- Laser beam fluctuation

The limited resolution of the electronic level introduces errors in the determination of rails to laser beam relative positions. Since these errors are proportional to the rail to laser beam distance it is advisable to mount the laser transmitter and laser tracker in close proximity to the track surface. However, density gradients on the air due to the air-ground temperature differences introduce curvatures in the path of the laser beam invalidating the assumption of the straightness of the reference line. Thermal gradients and consequently beam bending effects decrease with the height above ground. The third effect is the laser beam fluctuation which is due to the turbulent convective motion of the air in the vertical direction. The thermal inhomogeneities of the air distorts the light path in all directions. The frequency of this effect presents a wide spectrum extending from a fraction of a cycle per second to slightly above ten cycles per second. From GASL measurements and the available information on the subject, it can be seen that, for conditions

similar to the ones encountered at the Pueblo Test Track, beam bending is a dominant effect near the ground. For distances of the order of one to three feet, beam bending and fluctuation effects are similar and above those heights the laser beam fluctuations are more pronounced and remain constant with the altitude.

As a result of these considerations a four feet vertical height of the laser beam was adopted. Since substantially lower thermal gradients exist at night with less beam bending and scintillation, these times of the day were selected for the operation of the TGSD and a program was undertaken to determine the maximum range satisfying the contract requirement.

The program includes the measurement of fluctuations with a laser alignment system at night and under conditions similar to those expected during the track survey at the Pueblo Test Track.

The laser used was a Keuffel and Esser transmitter No. 712605; a detector target and readout unit No. 712600. The transmitter beam diameter is 12 mm; power output is .5 mW with an amplitude modulation of 10 KHz. The radiation wavelength is 632.8 n.m. The detector target diameter is one inch and divided in four sectors. The test was performed during the night early hours, at the manufacturer's plant at Whippany, New Jersey. It was a cloudless, fall night, with air temperatures in the forties and wind velocity below five miles per hour. The ground surface was a black top road running parallel to a two story building at approximately fifty feet distance.

The laser transmitter and receiver were located at distances of 56, 108, 165, 210 and 300 feet. By monitoring the output of the readout unit at each distance for intervals of approximately one minute, it was clear that fluctuations of the order of $\pm$ .010 inches were associated with 165 ft. range and data was recorded for two and a half hours at this distance. Typical results extending from 6:30 P.M. to approximately 8:00 P.M. are shown in Figure II.1. For simplicity, straight lines are used between points measured at one minute intervals. Between these points fluctuations of the order of two to four cycles per second and amplitudes up to .005 inch were observed.

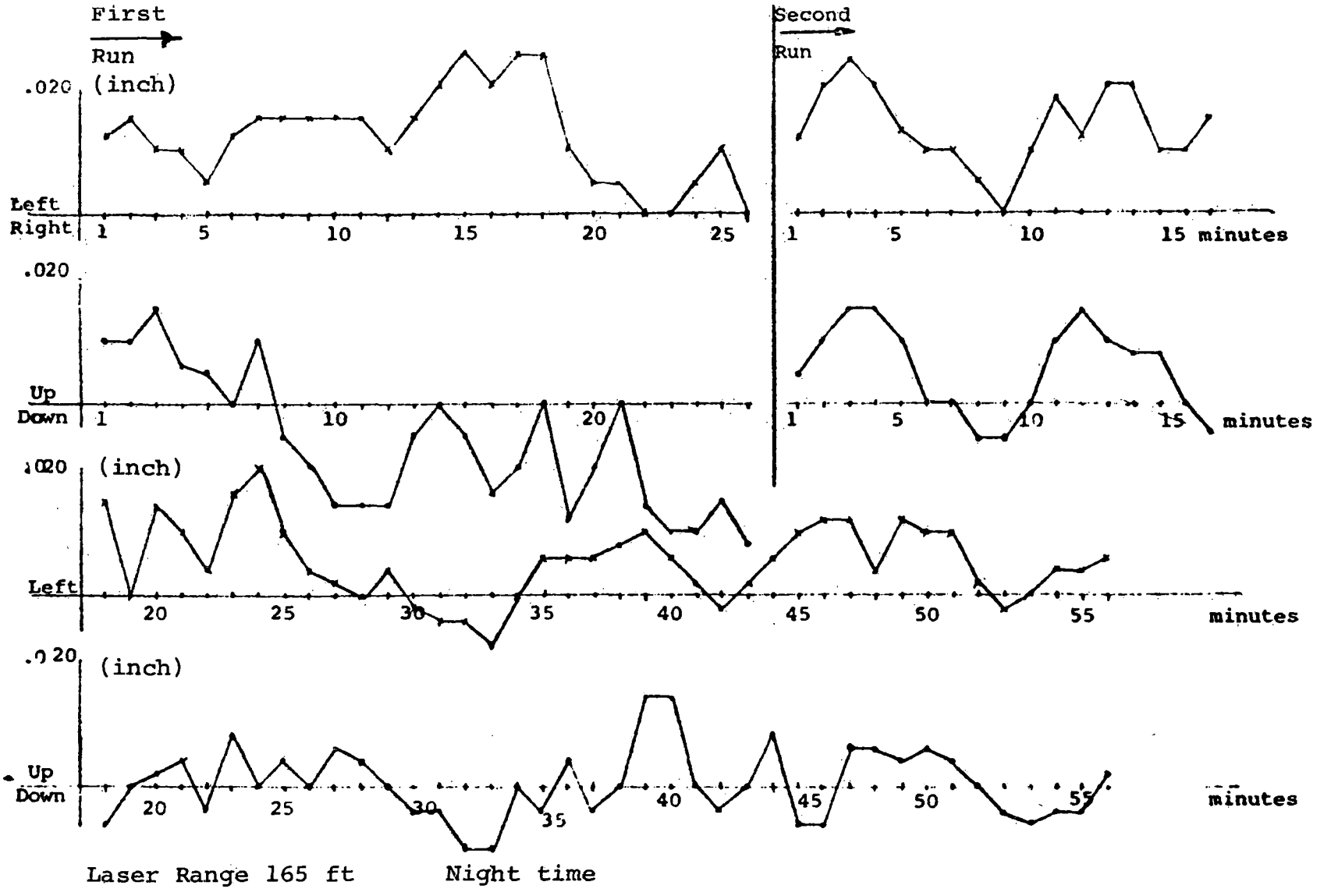

Figure II-1. Laser Beam Fluctuation (Figure 3-5 of Ref. 1)

APPENDIX III

ERROR ANALYSIS

This appendix is devoted to the computation of the error in the position of master rail, secondary rail and LIM reaction rail induced by the individual errors of the measurement performed with the sensors described in the report.

To perform the error analysis it is convenient to define first a fixed absolute frame of reference $\bar{x}$, $\bar{y}$, $\bar{z}$.

The absolute coordinates of the master rail $R_1 = (\bar{x}_{R1} \bar{y}_{R1} \bar{z}_{R1})$ are obtained, as said in Section 2.2, from the known absolute coordinates of two bench markers $\bar{x}_{Bm}$, $\bar{y}_{Bm}$, $\bar{z}_{Bm}$ and $\bar{x}_{Bm+1}$, $\bar{y}_{Bm+1}$, $\bar{z}_{Bm+1}$, respectively,[1] and from the following quantities measured at each position of the TV between the two bench markers in the frame of reference x, y, z of the track vehicle, as shown in Figure III-1.

1) x_m, y_m, z_m — coordinates of bench marker m taken with changed sign[2]

2) x_{m+1}, y_{m+1}, z_{m+1} — coordinates of bench marker m+1 taken with changed sign[2]

3) $y_{\ell m}$, $z_{\ell m}$, θ_m — coordinates of the laser beam intercept point $P_{\ell,m}$ and cross level at bench marker m

4) $y_{\ell m+1}$, $z_{\ell m+1}$, θ_{m+1} — same at bench marker m+1

5) y_ℓ, z_ℓ, θ — same at a position between two bench markers

6) $s-s_m$ — distance measured by the odometer along the master rail from bench marker m

---

(1) Without loss of generality, the absolute system of coordinates is set with the origin at bench marker m ($x_{Bm}=y_{Bm}=z_{Bm}=0$) and rotated about $\bar{z}$ until the bench marker m+1 lays in the plane $\bar{x}$ $\bar{z}$ ($\therefore \bar{y}_{Bm+1}=0$).

(2) x_m and x_{m+1} are not measured but their error is below 1/8 in. due to the positioning system. The resulting error is of higher order (Eq. III-9).

To obtain the absolute coordinates of the secondary rail and of the LIM reaction rail an additional set of measured quantities is required, i.e., the gage measurements obtained in Section 1-2.

7)	$g_m\ g_{m,1}\ g_{m,2}$	at station m
	$g_{m+1}\ g_{m+1,1}\ g_{m+1,2}$	at station m + 1
	$g\ g_1\ g_2$	at each position s between the bench markers

A vector representing the absolute position of any point of the track system is identified by a vector from the origin of the system $\bar{x}$, $\bar{y}$, $\bar{z}$, to the point. In particular $\vec{\ell}$ is the vector representing a point on the laser beam.

The absolute coordinates $\bar{x}_{R1}$, $\bar{y}_{R1}$, $\bar{z}_{R1}$ of the master rail R_1 are obtained from the measurement quantities 1 to 5, as explained in Section 2.2, in three steps; (Figure III-2).

1. The absolute position of the laser beam is obtained from the absolute coordinates of the two intercept points $P_{\ell,m}$, $P_{\ell,m+1}$. The coordinates of $P_{\ell,m}$ $P_{\ell,m+1}$ are determined by groups 1 to 4 of the measured quantities. The distance of a point P_ℓ along the laser beam from $P_{\ell,m}$ is given by

$$\left| \vec{\ell} - \vec{\ell}_m \right|$$

In particular, the distance between intercept points $P_{\ell,m}$, and $P_{\ell,m+1}$ is given by

$$\left| \vec{\ell}_{m+1} - \vec{\ell}_m \right|$$

2. An interpolation factor K along the laser beam is defined as the ratio between $\left| \vec{\ell} - \vec{\ell}_m \right|$ and $\left| \vec{\ell}_{m+1} - \vec{\ell}_m \right|$.

Because the laser beam is a straight line, one has

$$K = \frac{\vec{\ell} - \vec{\ell}_m}{\vec{\ell}_{m+1} - \vec{\ell}_m} = \frac{\bar{x}_\ell - \bar{x}_{\ell m}}{\bar{x}_{\ell m+1} - \bar{x}_{\ell m}} = \frac{\bar{y}_\ell - \bar{y}_{\ell m}}{\bar{y}_{\ell m+1} - \bar{y}_{\ell m}} = \frac{\bar{z}_\ell - z_{\ell m}}{\bar{z}_{\ell m+1} - \bar{z}_{\ell m}} \qquad \text{(III-1)}$$

K is a function of the coordinate s measured by the odometer.

Once the value of K is determined, the absolute coordinates of the intercept point P_ℓ of the laser beam with the plane of the measuring frame are obtained by means of Eq. (III-1).

3. Once the position of the laser beam point P_ℓ has been determined, the absolute coordinates of the master rail R_1 are obtained by using the measured quantities 5.

The absolute coordinates of both secondary rail and reaction rail are obtained from the coordinates of the master rail and the measured quantities of group 7.

In this approach the key point is the determination of the interpolation factor K. If the master rail were a straight line one would have

$$K = \frac{s - s_m}{s_{m+1} - s_m} \qquad \text{(III-2)}$$

Then the measurement of the odometer would be sufficient to determine the value of K. In the actual track configuration the distance of a point of the laser beam P_ℓ to $P_{\ell,m}$ is related to the distance $s - s_m$, measured by the odometer, through the equation

$$\left|\vec{\ell} - \vec{\ell}_m\right| = \int_{s_m}^{s} \hat{\vec{\ell}} \cdot \vec{ds} + \hat{\vec{\ell}} \cdot \Delta\,(\vec{\ell} - \vec{\tau})\Big|_{s_m}^{s} \qquad \text{(III-3)}$$

where $\hat{\vec{\ell}}$ is given by $(\vec{\ell}_{M+1} - \vec{\ell}_m)\Big/\left|\vec{\ell}_{m+1} - \vec{\ell}_m\right|$ and $\vec{\tau}$ is the vector which defines the position of a point of the master rail in the absolute frame of reference. In Eq. (III-3) $\Delta(\vec{\ell} - \vec{\tau})\Big|_{s_m}^{s}$ indicates the vector shown in Fig. III-2(b), which is the difference between $\vec{\ell} - \vec{\tau}$ at the position defined by s and the value $\vec{\ell}_m - \vec{\tau}_m$ at $s = s_m$.

The value of $\left|\vec{\ell} - \vec{\ell}_m\right|$ differs from $s - s_m$ because the master rail is not a straight line parallel to the laser beam (Fig. III-2(c). With a radius of curvature of the order of 12,000 ft., the effect of the curvature is Eq. (III-3), is of the order of 10^{-4}. By neglecting the curvature effect Eq. (III-3) reduces to

$$\left|\vec{\ell} - \vec{\ell}_m\right| = \frac{s - s_m}{\cos \bar{\psi}} \qquad \text{(III-4)}$$

where $\bar{\psi}$ is the average angle between the laser beam and the tangent to the master rail in the section $s - s_m$. The maximum value of $\bar{\psi}$ to be found in an actual measuring condition is given by the linear dimensions of the laser tracker and the distance between two bench markers. Thus the maximum value of $\bar{\psi}$ is of the order of .01. As a consequence the value of $\cos \bar{\psi}$ in Eq. (III-4) differs from unity by a quantity smaller than 10^{-4}.

Any error due to curvature and departure from parallelism of the same order of $\bar{\psi}$ can be neglected in a first order error analysis. For this reason $\left|\bar{\ell} - \bar{\ell}_m\right|$ is identified with $s - s_m$ in the approach described in this appendix and Eq. (III-2) is used to compute the value of the interpolation factor K.

To proceed with the error analysis a transformation of coordinates is required from the frame of reference attached to the measuring frame to the absolute reference system.

The transformation is given by the following equation (see Fig. III-3, in terms of the rotation matrix $|A|$

$$\vec{\bar{R}} = |A| \ \vec{R} \qquad \text{(III-5)}$$

where the absolute coordinates of $\vec{\bar{R}}$ are given as function of the coordinates (x, y, z) of $\vec{R}$ by

$$\left.\begin{aligned}
\bar{x} &= x \cos\gamma \cos\varphi + y(-\cos\theta \sin\varphi - \sin\theta \sin\gamma \cos\varphi) + \\
&\quad + z \quad (\sin\theta \sin\varphi - \cos\theta \sin\gamma \cos\varphi \\
\bar{y} &= x \cos\gamma \sin\varphi + y\ (\cos\theta \cos\varphi - \sin\theta \sin\gamma \sin\varphi) + \\
&\quad + z\ (-\sin\theta \cos\varphi - \cos\theta \sin\gamma \sin\varphi) \\
\bar{z} &= x \sin\gamma \quad + y \sin\theta \cos\gamma \quad + z \cos\theta \cos\gamma
\end{aligned}\right\} \text{(III-6)}$$

The coefficients in Eq. (III-6), are expressed in terms of three angles θ, γ, φ which are

θ cross-level. With a rotation θ about the axis x, the frame of reference x, y, z transforms to a new system x′, y′, z′ as shown in Figure III-6 where x′ = x and y′ is found in a horizontal plane.

γ grade angle. With a rotation γ about the axis y′, the frame of reference x′, y′, z′ transforms to the system x″, y″, z″ where y″ = y′ and z″ is vertical.

φ azimouth angle. With a rotation φ the system x″,y″,z″ transforms to the fixed absolute frame of reference $\bar{x}$, $\bar{y}$, $\bar{z}$.

Thus, the rail points are determined by the group of parameters 1),2),3),4),and the interpolation factor K, with the following set of equations:

$$\left.\begin{aligned} \bar{x}_{R1} &= \bar{x}_{R1}^{(o)} + \Delta \bar{x}_{R1} \\ \bar{y}_{R1} &= \bar{y}_{R1}^{(o)} + \Delta \bar{y}_{R1} \\ \bar{z}_{R1} &= \bar{z}_{R1}^{(o)} + \Delta \bar{z}_{R1} \end{aligned}\right\} \quad \text{(III-7)}$$

In Eq. (III-7) the equations on the right hand side are:

$$\begin{cases} x_{Rl}^{(o)} = (1-K)\, x_{Bm} + \\ \qquad + K\, x_{Bm+1} \\ y_{Rl}^{(o)} = (1-K) \left[y_{Bm} + (y_m + y_{\ell m}) \cos\theta_m - (z_m + z_{\ell m}) \sin\theta_m \right] + \\ \qquad +K \left[y_{Bm+1} + (y_{m+1} + y_{\ell m+1}) \cos\theta_{m+1} - (z_{m+1} + z_{\ell m+1}) \sin\theta_{m+1} \right] - \\ \qquad - \left[y \cos\theta - z \sin\theta \right] \\ z_{Rl}^{(o)} = (1-K) \left[z_{Bm} + (y_m + y_{\ell_m}) \sin\theta_m + (z_m + z_{\ell m}) \cos\theta_m \right] + \\ \qquad K \left[z_{Bm+1} + (y_{m+1} + y_{\ell m+1}) \sin\theta_{m+1} + (z_{m+1} + z_{\ell m+1}) \cos\theta_{m+1} \right] - \\ \qquad - \left[y \sin\theta + z \cos\theta \right] \end{cases} \qquad \text{(III-8)}$$

The terms $x_{Rl}^{(o)}$, $y_{Rl}^{(o)}$, $z_{Rl}^{(o)}$ represent the coordinates calculated by assuming

$$\begin{cases} \gamma = \varphi = \gamma_m = \varphi_m = \gamma_{m+1} = \varphi_{m+1} = 0 \\ x_m = x_{m+1} = 0 \end{cases}$$

The terms $\Delta\bar{x}_{Rl}$, $\Delta\bar{y}_{Rl}$, $\Delta\bar{z}_{Rl}$ are given by

The terms given by Eq.(III-9), represent a high order contribution to the calculation of the coordinates $\bar{x}_{R1}$, $\bar{y}_{R1}$, $\bar{z}_{R1}$. Consequently they should be retained in the error analysis only if high order error terms have to be included.

By differenciating Eq. (III-7), one obtains:

$$
\begin{aligned}
\Delta\bar{x}_{R1} = {} & (1-K)\, x_m \cos\gamma_m \cos\varphi_m + (y_m + y_{\ell m})(-\cos\theta_m \sin\gamma_m - \sin\theta_m \sin\varphi_m \cos\varphi_m) + (z_m + z_{\ell m})(\sin\theta_m \sin\varphi_m - \cos\theta_m \sin\gamma_m \cos\varphi_m)\Big] + \\
& + K\, x_{m+1} \cos\gamma_{m+1} \cos\varphi_{m+1} + (y_{m+1} + y_{\ell m+1})(-\cos\theta_{m+1} \sin\varphi_{m+1} - \sin\theta_{m+1} \sin\gamma_{m+1} \cos\varphi_{m+1}) + (z_{m+1} + z_{\ell m+1})(\sin\theta_{m+1} \sin\varphi_{m+1} - \cos\theta_{m+1} \sin\gamma_{m+1} \cos\varphi_{m+1})\Big] + \\
& y\,(-\cos\theta \sin\varphi - \sin\theta \sin\gamma \cos\varphi) + z\,(\sin\theta \sin\varphi - \cos\theta \sin\gamma \cos\varphi)
\end{aligned}
$$

$$
\begin{aligned}
\Delta\bar{y}_{R1} = {} & (1-K)\, x_m \cos\gamma_m \sin\varphi_m + (y_m + y_{\ell m})(\cos\theta_m (\cos\varphi_m - 1) - \sin\theta_m \sin\gamma_m \sin\varphi) + (z_m + z_{\ell m})(-\sin\theta_m (\cos\varphi_m - 1) - \cos\theta_m \sin\gamma_m \sin\varphi_m)\Big] + \\
& + K\, x_{m+1} \cos\gamma_{m+1} \sin\varphi_{m+1} + (y_{m+1} + y_{\ell m+1})[\cos\theta_{m+1} (\cos\varphi_{m+1} - 1) - \sin\theta_{m+1} \sin\gamma_{m+1} \sin\varphi_{m+1}] + (z_{m+1} + z_{\ell m+1})[-\sin\theta_{m+1} (\cos\varphi_{m+1} - 1) - \cos\theta_{m+1} \sin\gamma_{m+1} \sin\varphi_{m+1}]\Big] + \\
& - y\,(\cos\theta (\cos\varphi - 1) - \sin\theta \sin\gamma \sin\varphi) + z\,(-\sin\theta (\cos\varphi - 1) - \cos\theta \sin\gamma \sin\varphi)
\end{aligned}
$$

$$
\begin{aligned}
\Delta\bar{z}_{R1} = {} & (1-K)\, x_m \sin\gamma_m + (y_m + y_{\ell m}) \sin\theta_m (\cos\gamma_m - 1) + (z_m + z_{\ell m}) \cos\theta_m (\cos\gamma_m - 1)\Big] + \\
& + K\, x_{m+1} \sin\gamma_{m+1} + (y_{m+1} + y_{\ell m+1}) \sin\theta_{m+1} (\cos\gamma_{m+1} - 1) + (z_{m+1} + z_{\ell m+1}) \cos\theta_{m+1} (\cos\gamma_{m+1} - 1)\Big] + \\
& y \sin\theta (\cos\gamma - 1) + z \cos\theta (\cos\gamma - 1)
\end{aligned}
\qquad \text{(III-9)}
$$

$$\delta\bar{x}_{Rl} = \delta K \left(\bar{x}_{Bm+1} - \bar{x}_{Bm}\right.$$

$$\begin{aligned}
\delta\bar{y}_{Rl} = {} & (1-K)\left[(\delta y_m + \delta y_{\ell m})\cos\theta_m - (\delta z_m + \delta z_{\ell m})\sin\theta_m + \delta\theta_m\{-(y_m+y_{\ell m})\sin\theta_m-(z_m+z_{\ell m})\cos\theta_m\}\right] + \\
& + K\left[(\delta y_{m+1}+\delta y_{\ell m+1})\cos\theta_{m+1} - (\delta z_{m+1}+\delta z_{\ell m+1})\sin\theta_{m+1}+\delta\theta_{m+1}\{-(y_{m+1}+y_{\ell m+1})\sin\theta_{m+1}-(z_{m+1}+z_{\ell m+1})\cos\theta_{\ell m+1}\}\right] - \\
& - \left[\delta y\cos\theta - \delta z\sin\theta + \delta\theta(-y\sin\theta - z\cos\theta)\right] + \\
& + \delta K\left[\left\{\bar{y}_{Bm+1}+(y_{m+1}+y_{\ell m+1})\cos\theta_{m+1}-(z_{m+1}+z_{\ell m+1})\sin\theta_{m+1}\right\}-\left\{\bar{y}_{Bm}+(y_m+y_{\ell m})\cos\theta_m-(z_m+z_{\ell m})\sin\theta\right\}\right]
\end{aligned}$$

$$\begin{aligned}
\delta\bar{z}_{Rl} = {} & (1-K)\left[(\delta y_m + \delta y_{\ell m})\sin\theta_m + (\delta z_m+\delta z_{\ell m})\cos\theta_m + \delta\theta_m\{(y_m+y_{\ell m})\cos\theta_m p(z_m+z_{\ell m})\sin\theta_m\}\right] + \\
& + K\left[(\delta y_{m+1}+\delta y_{\ell m+1})\sin\theta_{m+1} + (\delta z_{m+1}+\delta z_{\ell m+1})\cos\theta_{m+1}+\delta\theta_{m+1}\{(y_{m+1}+y_{\ell m+1})\cos\theta_{m+1}-(z_{m+1}+z_{\ell m+1})\sin\theta_{m+1}\}\right] - \\
& - \left[\delta y\sin\theta + \delta z\cos\theta + \delta\theta(y\cos\theta - z\sin\theta)\right] + \\
& + \delta K\left[\left\{\bar{z}_{Bm+1}+(y_{m+1}+y_{\ell m+1})\sin\theta_{m+1}+(z_{m+1}+z_{\ell m+1})\cos\theta_{m+1}\right\}-\left\{\bar{z}_{Bm}+(y_m+y_{\ell m})\sin\theta_m+(z_m+z_{\ell m})\cos\theta_m\right\}\right]
\end{aligned}$$

(III-10)

$\delta\bar{x}_{R1}$, $\delta\bar{y}_{R1}$, $\delta\bar{z}_{R1}$ are the errors in the absolute coordinates of the master rail.

The computation of these errors can be simplified by observing that the contribution due to measurements performed at the bench markers m and m+1 change linearly from m to m+1 as indicated by the interpolating factors (1-K) and K. The maximum error in Eq.(III-10), is given by the largest error encountered at a bench marker.

Thus K can be assumed to be zero and the errors δy_m , $\delta y_{\ell m}$, δz_m , $\delta z_{\ell m}$, $\delta\theta_m$ are the ones to be considered.

The errors δy , δz , $\delta\theta$, are assumed to be equal to the errors $\delta y_{\ell m}$, $\delta z_{\ell m}$, $\delta\theta_m$ respectively.

The expected RMS errors of the sensor outputs are obtained from the calibration Table III-1 and their values are:

$\delta K = 1"/1800"$	$= \pm .00055$	(in./in.)
δy_n	$= \pm .001$	(in./in.)
δz_m	$= \pm .001$	(in./in.)
$\delta y = \delta y_{\ell m}$	$= \pm .002$	(in./in.)
$\delta z = \delta z_{\ell m}$	$= \pm .003$	(in./in.)
$\delta\theta = \delta\theta_m$	$= \pm .0001$	(rad)

Additional errors δz and δy of $\pm$ .008 (in) are also considered in the location of the laser intercept point due to laser beam fluctuation. The coefficients in Equation III-10, are computed from the Table III-1 and from the characteristic of the measuring system and in the worse case they are

$$\cos \theta = 1$$

$$\sin \theta = \theta = .175$$

$$\bar{x}_{\ell m+1} - \bar{x}_{\ell_m} = 1800 \text{ in.}$$

$$\bar{y}_{\ell m+1} - \bar{y}_{\ell m} = 5 \text{ in.}$$

$$\bar{z}_{\ell m+1} - \bar{z}_{\ell m} = 4 \text{ in.}$$

$$(y_m \theta_m + z_m) = 68 \text{ in.}$$

$$(y_m + z\theta_m) = 104 \text{ in.}$$

$$y\theta + z = 61 \text{ in.}$$

$$y + z\theta = 39 \text{ in.}$$

Using the values indicated above the individual contribution to the errors and the total RMS error is calculated for $\bar{x}$, $\bar{y}$ and $\bar{z}$ in the Table III-2. The value of $\theta = \pm 10^\circ$ and the approximation $\cos \theta \sim 1$ is used in the estimate.

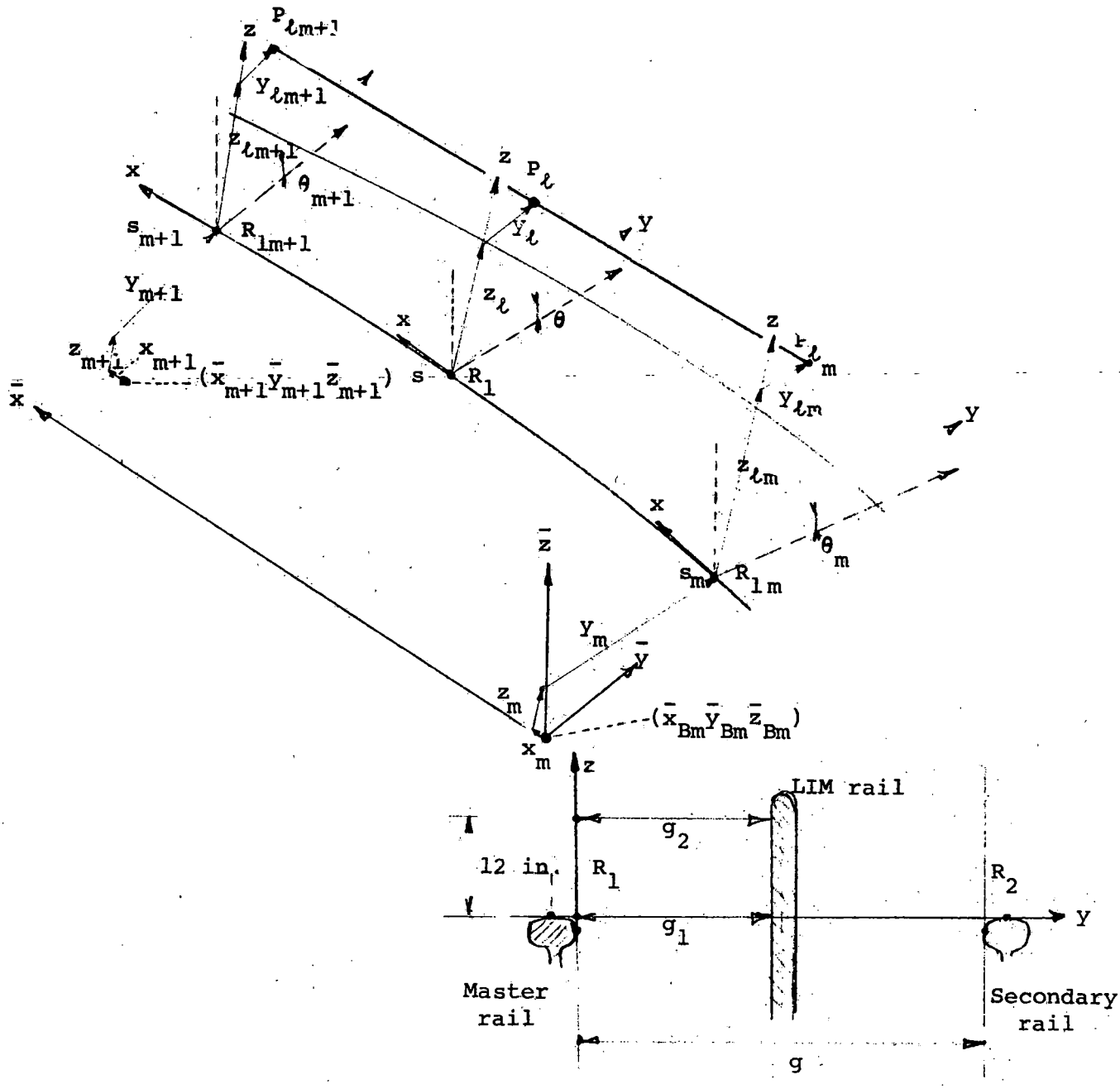

Figure III-1. Frames of Reference of the Measuring System.

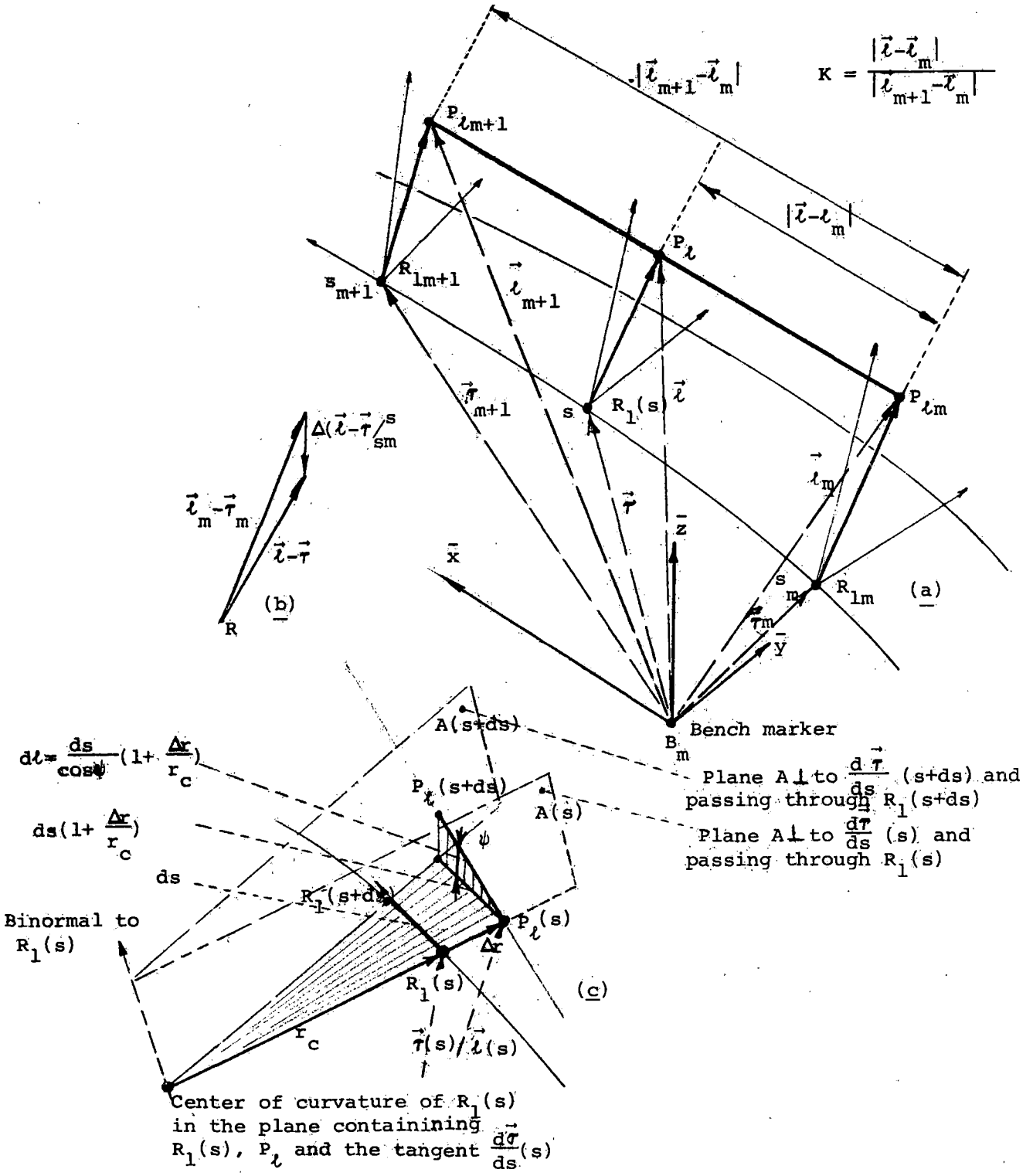

Figure III-2, Definition of the Vector Quantities Defined in the Error Analysis.

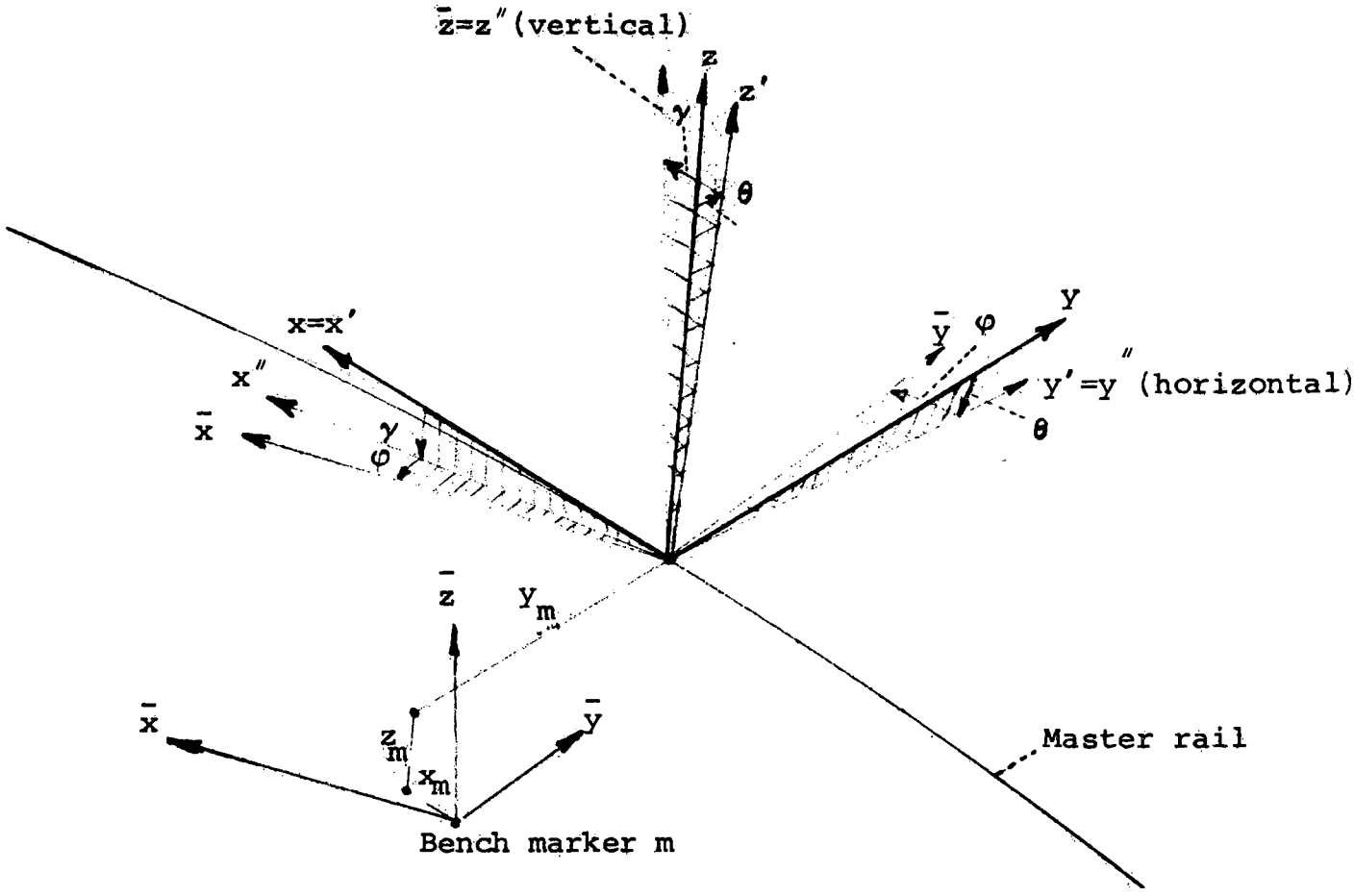

Angles of rotation are taken with positive sign

- θ cross level
- γ master rail grade
- φ master rail azimuth relative to $\bar{x}$

Figure III-3. Transformation of Coordinates from the System of Reference of the Measuring Frame to the System of Reference of the Bench Markers.

TABLE III-1

CALIBRATION OF ANALOG CHANNELS

PARAMETER	SYMBOL	RECORDER CHANNEL	ZERO OUTPUT	SENSOR RANGE	SENSOR CONSTANT	NONLINEARITY	SCATTERING	DAS RESOLUTION (10 mv)
GAGE	g	1	56.48"	$\pm$ 1"	+8.40 $\frac{\text{VOLT}}{\text{INCH}}$	$\pm 4\times10^{-3}$ Inch	$\pm 1\times10^{-3}$ Inch	$\pm .6\times10^{-3}$ Inch
LIM GAGE (TOP)	g_1	2	28.00"	$\pm$ 2"	-4.008 $\frac{\text{VOLT}}{\text{INCH}}$	$\pm 6\times10^{-3}$ Inch	$\pm 2\times10^{-3}$ Inch	$\pm 1.2\times10^{-3}$ Inch
LIM GAGE (BOTTOM)	g_2	3	28.79"	$\pm$ 2"	-4.00 $\frac{\text{VOLT}}{\text{INCH}}$	$\pm 2\times10^{-3}$ Inch	$\pm 1\times10^{-3}$ Inch	$\pm 1.2\times10^{-3}$ Inch
TRACKER y	y	4	28.49"	$\pm$ 5"	-1.796 $\frac{\text{VOLT}}{\text{INCH}}$	$\pm 5\times10^{-3}$ Inch	$\pm 3\times10^{-3}$ Inch	$\pm 2.8\times10^{-3}$ Inch
TRACKER z	z	5	47.81"	$\pm$ 4"	+2.428 $\frac{\text{VOLT}}{\text{INCH}}$	$\pm 2\times10^{-3}$ Inch	$\pm 1\times10^{-3}$ Inch	$\pm 2.0\times10^{-3}$ Inch
CROSS LEVEL	θ	6	0.00°	$\pm$10"	- .854 $\frac{\text{VOLT}}{\text{INCH}}$	$\pm 50\times10^{-3}$ Degrees	$\pm 6\times10^{-3}$ Degr.	$\pm 5.8\times10^{-3}$ Degrees
BENCH MARKER z	z_m	7	-0.09"	$\pm$ 1"	-8.544 $\frac{\text{VOLT}}{\text{INCH}}$	$\pm 3\times10^{-3}$ Inch	$\pm 1\times10^{-3}$ Inch	$\pm .6\times10^{-3}$ Inch
BENCH MARKER y	y_m	8	-16.36"	$\pm$ 1"	-8.560 $\frac{\text{VOLT}}{\text{INCH}}$	$\pm 2\times10^{-3}$ Inch	$\pm 1\times10^{-3}$ Inch	$\pm .6\times10^{-3}$ Inch
REFERENCE VOLTAGE (NEGATIVE)	$-V_R$	7	0.00 V	-9.99 V	Adjusted to -9.95 Volt			$\pm 5.0\times10^{-3}$ Volt
REFERENCE VOLTAGE (POSITIVE)	$+V_R$	8	0.00 V	-9.99 V	Adjusted to +9.95 Volt			$\pm 5.0\times10^{-3}$ Volt

TABLE III-2

$\delta\bar{x}$ $\delta K \cdot (\bar{x}_{\ell m+1} - \bar{x}_{\ell m}) = 1.000$ in. $= \delta\bar{x}_{RMS}$

$\delta\bar{y}$

$\delta y_{\ell m}$	=	.010,0
$\delta z_m \theta_m$	=	.000,2
$\delta z_{\ell m} \theta_m$	=	.001,9
δy_m	=	.001,0
$\delta\theta_m (y_m \theta_m + z_m)$	=	.006,8
δy	=	.002,0
$\delta z\theta$	=	.000,5
$\delta\theta(y\theta+z)$	=	.006,1
$\delta K(\bar{y}_{\ell m+1} - \bar{y}_{\ell m})$	=	.002,8

$\delta\bar{y}_{RMS} = .014$ (in.)

$\delta\bar{z}$

$\delta y_m \theta_m$	=	.000,2
$\delta y_{\ell m} \theta_m$	=	.001,8
δz_m	=	.001,0
$\delta z_{\ell m}$	=	.011,1
$\delta\theta_m (y_m + z_m\theta_m)$	=	.010,4
$\delta y\theta$	=	.000,4
δz	=	.003,0
$\delta\theta(y + z\theta)$	=	.003,9
$\delta K\ (z_{\ell m+1} - z_{\ell m})$	=	.002,2

$\delta\bar{z}_{RMS} = .016$ (in.)

APPENDIX IV

STATEMENT OF WORK

A. General

The Contractor shall furnish the necessary qualified personnel, facilities, materials, equipment, and services as may be required, to perform the required effort for development, fabrication, and demonstration of a Special Track Geometry Survey Device which will measure the track geometry of a high precision railroad test track located at the High Speed Ground Test Center near Pueblo, Colorado and to record the measurements for automatic data processing. The Device shall be developed in accordance with the following technical specifications including delivery and test site demonstration.

B. Performance Specifications

The performance requirements for the Survey Device are as follows:

1. Track Geometry Measurements:

   a. General

      The Device shall measure and record the data necessary to determine the actual track geometry to within the tolerances specified in Table 1. The Device must measure absolute rail position directly or make the chord measurements necessary to derive the absolute rail position. If chord measurements are used, the contractor shall provide or define the technique required to derive the absolute rail position from the recorded data. The points at which the measurements are to be taken on each rail shall be as shown in Figures 2 and 3.

   b. Profile and Alignment

      Data recorded by the Device shall describe the profile and alignment of the inside rail over the entire length of track to the accuracy specified. The profile and alignment of the outer rail may be directly measured in the same manner or it may be derived from the inside rail measurements, the gage and crosslevel through data processing. However, all resulting measurements shall be made to the accuracy specified.

   c. Gage and Crosslevel

      The gage and crosslevel of the track shall be measured and recorded (at coincident intervals with the profile and alignment measurements) to the tolerances specified.

d. Distance along the Track

The location on the track where each measurement is taken shall be known and recorded along with the geometry measurements. The location of each tie shall be recorded and the tenth tie and hundreth tie shall be specially identified. The distance along the track of each geometry measurement and tie location shall be traceable to a survey monument. The device shall be capable of automatically recording track geometry data at each tie (tie centers are 19"). The accuracy of the distance measurement shall be at least 0.1%.

e. LIM Reaction Rail Position

The position of the reaction rail shall be measured from the reference rail. Two measurements of position shall be made, one in line with the top of the conventional rails and the other 12" above, as shown in Figure 3.

2. Tolerance and Range Requirements

In order to measure and record data which can be processed accurately enough to comply with the LIM track specifications, the accuracy requirements of the Track Survey Device shall be as shown in Table 1. These requirements indicate the recorded measurement tolerances for specific chord lengths approximate to that shown. The tolerances indicated in Table 1 shall apply to the entire system, including the measurements recorded by the device and the data processing. It must be possible to obtain accurate data to the tolerances specified in Table 1 for the chord lengths shown.

3. Data Output Requirements

The Survey Device shall record the required measurement data on seven track, IBM compatible, magnetic tape. Information identifying data and time of the run, test conditions and the type of measurement shall be recorded.

A process of procedure for determining the track geometry parameters from the recorded data and verifying the accuracy of the resultant values shall be provided by the contractor.

The recorded data form and format that will be required for data processing shall be specified in consultation with and approved by the Government or designated Government contractors in the first design review.

TABLE 1

Tolerance and Range Requirements
For Midchord offsets for Indicated Chord Lengths

Measured Parameter	Range	Tolerance in ± inches for the indicated Chord-Lengths *			
		10'	31'	100'	700'
Profile (for each rail)	±2" + X	1/64	1/32	3/64	1/12
Alignment (for each rail)	±2" + Y	1/64	1/32	3/64	1/12
Crosslevel (and Superelevation)	±10"		1/32		
Gage - For conventional rails)	55 1/2" to 57 1/2"		1/32		
Position for Reaction Rail	26" to 30"		1/32		

Where X - is the offset resulting from vertical curvature. The smallest vertical curve is 2600 foot radius. The length of the spirial is 2000 feet for an 8" superelevation.

Where Y - is the midchord offset based on the reference chord that the Contractor will use for his system on a 2-1/2 mile radiua curve.

* Chord length measurements may be made to the nearest tie.

If the absolute rail position is obtained with reference to a fixed offset reference line of markers or instrument devices as opposed to a moving chord reference line, the tolerance requirements shall be that of Table 2.

TABLE 2

Tolerance Requirements for Absolute Rail Measurements

Measured Parameter	Tolerance in + inches
Profile (for each rail)	1/64
Alignment (for each rail)	1/64
Crosslevel (and Superelevation)	1/32
Gage - For conventional rails and reaction rail	1/32

NOTE: The Range being the same as in Table 1.

The track geometry measurements shall have at least a 90 percent confidence factor of being within the tolerances specified. If the accuracy requirements cannot be met by a single pass over the track under test, then several passes shall be specified in order to arrive at a statistical value which is within tolerances.

4. Survey Monument Referencing

A procedure shall be defined and specified for referencing the measurements or for determination of the position of the reference point used by the device with respect to a fixed survey monument. The contractor is not responsible for performing the measurement of the reference point to the survey monument.

5. Validation

The contractor shall be responsible for defining and detailing the procedure for validating and calibrating the measurements made by the device as well as defining the configuration of the monuments for the calibration test track section.

C. Operating Requirements

1. Production Rate (Speed of Tests)

The average production rate of the device shall be at least 3 miles per hour and shall include all passes necessary to meet the accuracy requirements.

2. Operating Personnel

The device shall be designed for operation by technician type personnel with a reasonable amount of special training. The operation of the device and resulting measurements shall be as automatic as possible and relatively insensitive to human error.

3. Set-up and Calibration

After the device has been placed on the track, the equipment shall be ready for track measuring within one hour. The device shall be capable of being easily calibrated by the Government within the one hour set-up period. Once calibrated, the device shall maintain its calibration throughout a period of eight (8) hours.

4. Power

Device shall be self-propelled and provide its own electrical power.

5. Speed

When not measuring, the device shall travel at least 20 miles per hour on a 1-1/2% grade and negotiate 5% grades at some slower speed.

6. Environment

The Device need not be operated during inclement weather. The device shall operate as required in the vicinity of Pueblo, Colorado, except that it need not meet the requirements during days when the extreme of temperature is above 100° F, or below 0° F, or during days on which the difference between high and low temperature is greater than 40° F.

7. Interface

The device shall operate on the LIM track with the reaction rail in place. The device shall have a clearance above the reaction rail of 15-1/2" measured from top of running rails.

8 Track Loading

The device shall load the track at the points of measurement with 25,000 lbs. distributed over about 10 feet of track. It will be considered advantageous if the load can be incrementally varied from 10,000 to 30,000 lbs. at the points of measurement. If ballast material is used, it is advantageous to use an inexpensive material, (e.g., sand, water, etc.) which is easily removable. The Contractor shall initially provide the ballast material.

9. Storage

The device shall be weather-proofed, suitable for year-around outside storage at ambient air temperatures of -30° F to 105° F. Certain precision parts or electronic equipment may be removed for inside storage if necessary.

10. Lifting

The device shall be provided with lifting hooks or other means suitable for placing the device on and removing it from the LIM track by an overhead 20 ton crane at the Test Center.